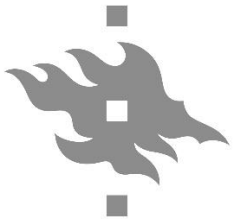

Master's thesis

Petrology and Economic Geology

Geological 3D modelling of Aijala-Metsämonttu Cu-Zn-Au-Ag-Pb deposits

Joonas Sandström

12/2021

Supervisors:
Petri Peltonen
Janne Hokka

Master's Programme in Geology and Geophysics

Faculty of science

HELSINGIN YLIOPISTO
HELSINGFORS UNIVERSITET
UNIVERSITY OF HELSINKI
MATEMAATTIS-LUONNONTIETEELLINEN TIEDEKUNTA
MATEMATISK-NATURVETENSKAPLIGA FAKULTETEN
FACULTY OF SCIENCE

Tiedekunta – Fakultet – Faculty	Koulutusohjelma – Utbildningsprogram – Degree programme
Faculty of Science	Master's Programme in Geology and Geophysics

Opintosuunta – Studieinrikting – Study track

Petrology and Economic Geology

Tekijä – Författare – Author

Joonas Sandström

Työn nimi – Arbetets titel – Title

Geological 3D modelling of Aijala-Metsämonttu Cu-Zn-Au-Ag-Pb deposits

Työn laji – Arbetets art – Level	Aika – Datum – Month and year	Sivumäärä – Sidoantal – Number of pages
Master's thesis	12/2021	66 + 6 Appendices

Tiivistelmä – Referat – Abstract

Aijala-Metsämonttu volcanogenic massive sulphide ore deposit belongs to Orijärvi regional volcanogenic massive sulphide mineralisation, localised within the schist zone southwestern Finland. Aijala-Orijärvi zone is an island-arc structure formed during the Paleoproterozoic (1895-1891 Ma). The mining operation in Aijala took place in 1949–1958 and Metsämonttu in 1952–1958 and 1964–1974. The Aijala and Metsämonttu deposits were 1 km apart. The main ore types were massive vein-like pyrite, sphalerite, pyrrhotite, chalcopyrite, and galena.

The purpose of this thesis was to produce modern geological 3D models of the Aijala and Metsämonttu volcanogenic massive sulphide ore deposits and numerical grade models of the utilised minerals (copper, lead, zinc, silver, and gold) using historical material and to interpret the occurrences and emplacements of precious metals and base metals. In addition, compare the accuracy of the 3D models with digitised historical material. Geological 3D and numerical grade models were created using implicit modelling. Historical data used in this thesis consist of 266 drill holes from Aijala and 274 drill holes from Metsämonttu. Also, 61 mine tunnel maps and 47 cross-sections were used to create the geological models.

The Aijala-Metsämonttu volcanogenic massive sulphide ore deposits are in the same stratigraphic zone between the footwall quartz-feldspar-porphyry and hanging wall amphibolite. Sulphide lenses of both deposits are vertically on the south side of the footwall and hanging wall contact. The main host rocks to sulphide ores are skarn and cordierite-gneiss. Several local faults intersect the deposits. The most significant faults displaced overlying blocks to the south in Aijala and to the north in Metsämonttu.

The Aijala-Metsämonttu deposit belongs to the Zn-Pb-Cu group. The occurrence style and concentrations of metals vary between deposits. Copper ore is present in Aijala but absent in Metsämonttu, whilst zinc-lead ore is present in Metsämonttu but absent in Aijala. Precious metals occur in both deposits with a companion of base metals. The Metsämonttu deposit is rich in precious metals compared to the Aijala deposit, and the presence of high content of precious metals correlates with the incidence of lead ore. Precious metals concentrations increase from east to west and deeper in Metsämonttu.

Avainsanat – Nyckelord – Keywords

VMS, Volcanogenic massive sulphide ore deposit, 3D model, Geology

Säilytyspaikka – Förvaringställe – Where deposited

HELDA – Digital repository of the University of Helsinki

Muita tietoja – Övriga uppgifter – Additional information

HELSINGIN YLIOPISTO
HELSINGFORS UNIVERSITET
UNIVERSITY OF HELSINKI
MATEMAATTIS-LUONNONTIETEELLINEN TIEDEKUNTA
MATEMATISK-NATURVETENSKAPLIGA FAKULTETEN
FACULTY OF SCIENCE

Tiedekunta – Fakultet – Faculty	Koulutusohjelma – Utbildningsprogram – Degree programme
Matemaattis-luonnontieteellinen tdk.	Geologian ja geofysiikan maisteriohjelma

Opintosuunta – Studieinrikting – Study track

Petrologia ja taloudellinen geologia

Tekijä – Författare – Author

Joonas Sandström

Työn nimi – Arbetets titel – Title

Geological 3D modelling of Aijala-Metsämonttu Cu-Zn-Au-Ag-Pb deposits

Työn laji – Arbetets art – Level	Aika – Datum – Month and year	Sivumäärä – Sidoantal – Number of pages
Maisterintutkielma	12/2021	66 + 6 Liitettä

Tiivistelmä – Referat – Abstract

Aijalan ja Metsämontun vulkanogeeniset massiiviset sulfidimalmiesiintymät sijaitsivat Lounais-Suomen liuskevyöhykkeellä ja kuuluivat Orijärven vulkanogeeniseen malmiprovinssiin. Aijala-Orijärvi vyöhyke on vulkaaninen saarikaari, joka muodostui Paleoproterotsooisella aikakaudella 1895–1891 Ma. Aijalan kaivos oli toiminnassa 1949–1958 ja Metsämontun kaivos 1952–1958 sekä 1964–1974. Aijalan ja Metsämontun sulfidimalmiesiintymien etäisyys toisistaan on 1 km. Päämalmimineraalit olivat rikkikiisu, sinkkivälke, magneettikiisu, kuparikiisu ja lyijyhohde, jotka esiintyivät juonityyppisinä.

Tämän maisterintutkielman tarkoituksena oli mallintaa historiallista aineistoa käyttäen, kolmiulotteisesti Aijalan ja Metsämontun geologinen ympäristö ja numeeriset vyöhykemallit hyödynnetyistä metalleista (kupari, lyijy, sinkki, hopea ja kulta). Mallien avulla tulkittiin jalometallien ja perusmetallien esiintymistä ja sijoittumista. Lisäksi selvitettiin 3D-mallien vastaavuutta historialliseen aineistoon. Geologiset ja numeeriset 3D-mallit tehtiin implisiittisellä mallinnuksella, käyttämällä Aijalasta 266:n kairasydämen aineistoa. Metsämontusta oli käytettävissä tiedot 274:stä kairasydämestä. 3D-mallien tekemiseen käytettiin myös 61 kaivostunnelikarttaa ja 47 poikkileikkauskuvaa.

Aijalan ja Metsämontun vulkanogeeniset massiiviset sulfidimalmiesiintymät ovat samassa stratigrafisessa horisontissa, jalkapuolen kvartsi-maasälpä-porfyyrin ja kattopuolen amfiboliitin välissä. Molempien esiintymien sulfidijuonet ovat samansuuntaisia ja pystysuoria, ja ne sijaitsevat jalkapuolen ja kattopuolen kontaktin eteläpuolella. Isäntäkivet sulfidimalmille ovat karsi kivet ja kordieriittigneissi. Esiintymiä leikkaavat useat paikalliset siirrokset, joista merkittävimpien yläpuoliset siirrot ovat etelään Aijalassa ja pohjoiseen Metsämontussa.

Metallimineraalien pitoisuusjakauman perusteella Aijala-Metsämonttu-esiintymä kuuluu Zn-Pb-Cu ryhmään. Esiintymien metallipitoisuudet ja metallien jakaumat eroavat toisistaan. Aijalassa tavataan kuparimalmi, mutta ei Metsämontussa, kun taas sinkki-lyijymalmia esiintyy vain Metsämontussa, mutta ei Aijalassa. Jalometallit esiintyvät perusmetallien seurassa molemmissa esiintymissä. Metsämontussa jalometallien pitoisuudet ovat korkeammat kuin Aijalassa, ja jalometallien korkeat pitoisuudet seuraavat lyijymalmia. Metsämontun esiintymässä jalometallien pitoisuudet kasvavat länteen päin ja syvemmälle.

Avainsanat – Nyckelord – Keywords

VMS, Vulkanogeeninen massiivinen sulfidiesiintymä, 3D-malli, geologia

Säilytyspaikka – Förvaringställe – Where deposited

HELDA – Helsingin yliopiston digitaalinen arkisto

Muita tietoja – Övriga uppgifter – Additional information

TABLE OF CONTENTS

1. INTRODUCTION

Ore deposits play an increasingly important role in the economy of Finland and the EU. The European Commission has listed 26 raw materials considered critical (Blengini et al. 2020), but all mined raw materials e.g. base metals, although not classified as critical, are important (Eynard et al. 2020). Ores containing sulphides have been mined to produce metals and sulphur in Finland since the 16th century, and between 1530 and 2001, 418 mines have been operating (Puustinen 2003).

The Aijala Cu-Zn deposit and the Metsämonttu Zn-Pb-Cu deposit are in the schist zone of Southwest Finland, and both deposits are in the same horizontal stratigraphic zone at the top of the quartz-feldspar-porphyry series (Latvalahti 1979). They belong to the Orijärvi regional volcanogenic massive sulphide (VMS) camp, formed ca. 1895–1891 Ma (Eilu et al. 2012). Quartz-feldspar-porphyry rocks are in origin rhyolite, dacite, and tuff, felsic meta-volcanic (Latvalahti 1979). The main ore minerals are massive vein-like pyrite, sphalerite, pyrrhotite, chalcopyrite, and galena in the Aijala and Metsämonttu deposits (GTK 2019a; GTK 2019b). Host rocks are thoroughly altered felsic and intermediate to mafic volcanic rocks and sedimentary units. The dominant metamorphic rocks are cordierite-mica, andalusite-cordierite-muscovite and cordierite-anthophyllite gneisses (Latvalahti 1979).

The Aijala and Metsämonttu mines have been closed for fifty years, and they are in Kisko, near the town of Salo in Southwest Finland (Fig. 1). Metamorphic facies in the Orijärvi area are well known through the fundamental studies of Eskola (1914). Most of the research in petrology and lithology in the Aijala and Metsämonttu areas dates from the 1970s and 1980s (Wennervirta and Papunen 1974; Parkkinen 1974a, b, c; Huhma and Latvalahti 1975; Parkkinen 1975a, b; Latvalahti 1979; Mäkelä 1989).

The purpose of this thesis is to use historical materials from the two mines (Aijala and Metsämonttu) and create geological 3D models of lithologies along with the numerical grade models of the selected elements (Cu, Pb, Zn, Ag, and Au) and interpret the occurrence and emplacement of precious metals within these base metals dominated deposits. The distribution of precious metals within the Aijala and Metsämonttu deposits has not been studied in detail before (Huhma and Latvalahti 1975; Parkkinen 1975a, b;

Latvalahti 1979; Mäkelä 1989). In addition, compare the accuracy of the 3D models with the digitised historical material.

The Aijala and Metsämonttu deposits have not been modelled before using geological 3D software because it was not possible at the time of the mining in 1949–1974. During the mining, lithological contacts and base and precious metals distribution were determined on the mine level maps and cross-sections, which include information on underground working, and rock types and assays from drill cores. Therefore, modern 3D models are helpful to interpret the geological environments with the commodities in the bedrock.

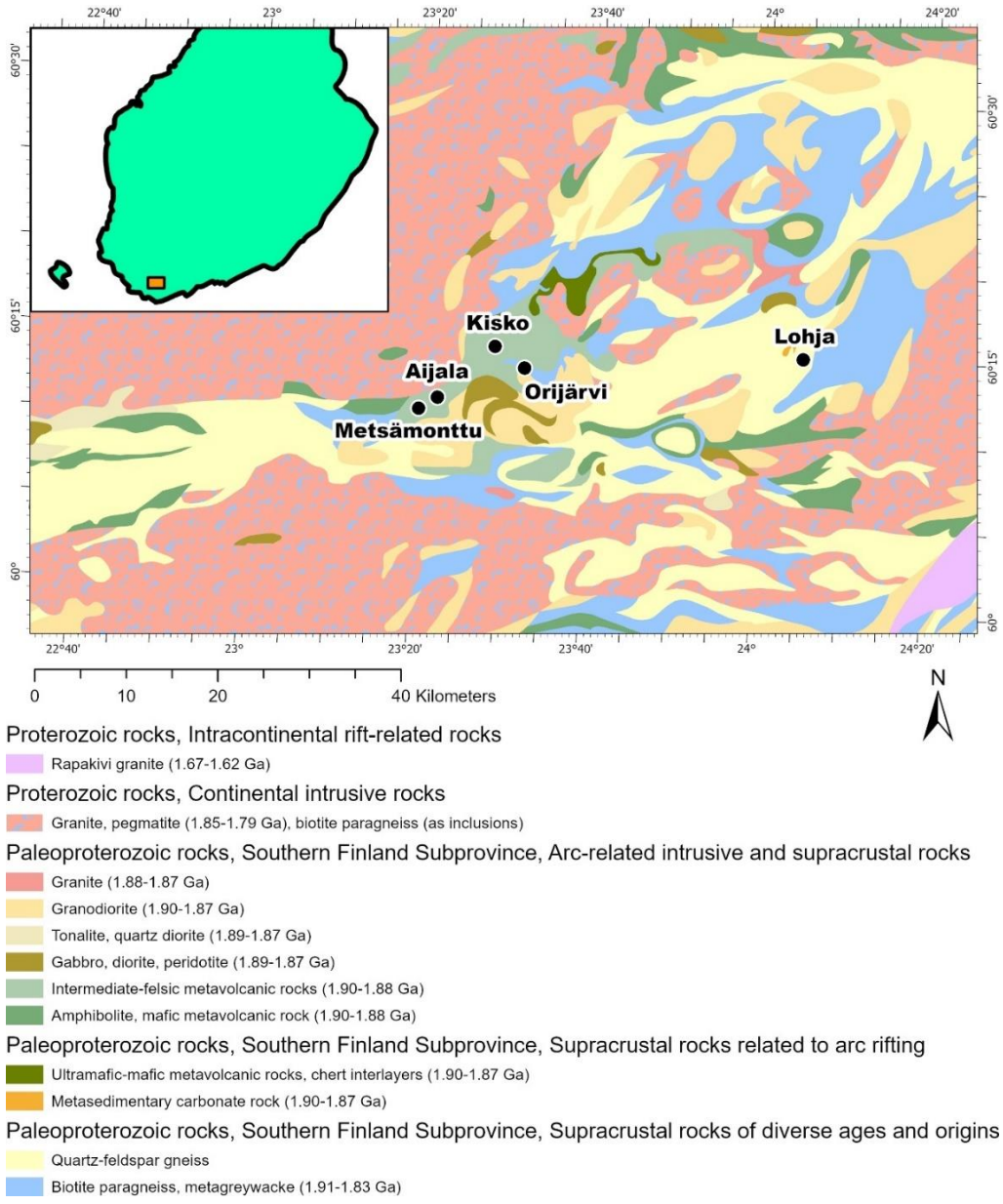

Figure 1. Lithological map of the Kisko area, showing the Aijala and Metsämonttu area. Modified after Geological Survey of Finland (abbr. GTK) (2021).

2. VOLCANOGENIC MASSIVE SULFIDE DEPOSITS AND ASSOCIATED MINERALISATIONS

VMS deposits are accumulations of base metal sulphides that occur stratiform or stratabound. VMS deposits form in submarine volcanic environments on or near the seafloor by hydrothermal convection. Typically, polymetallic massive lenticular sulphides are formed by precipitation from hot (250 to 350 ºC), chemically active hydrothermal solutions. This is caused by the concentrated discharge of metal-rich hydrothermal solutions originating from circulation through the seafloor (Hannington 2014).

VMS deposits are valuable sources of copper, lead, zinc, silver, and gold (Cu, Pb, Zn, Ag, and Au) and, to a lesser extent, cobalt, selenium, tin, manganese, bismuth, cadmium, tellurium, indium, germanium and gallium (Co, Se, Sn, Mn, Bi, Cd, Te, In, Ge and Ga). Some VMS deposits also contain minor amounts of antimony, arsenic, and mercury (Sb, As, and Hg) (Galley et al. 2007; Hannington 2014). VMS deposits consist of pyrite (FeS_2) and pyrrhotite ($Fe_{(1-x)}S$; X = 0 to 0.2) as the main iron sulphides, with varying amounts of the main sulphide ore minerals chalcopyrite ($CuFeS_2$), galena (PbS), and sphalerite ((Zn, Fe)S). Also, arsenopyrite (FeAsS) and bornite (Cu_5FeS_4) are typical sulphide minerals in VMS deposits (Hannington 2014).

VMS deposits have produced 6 % Cu, 13 % Pb, 27 % Zn, 9 % Ag, 2.6 % Au, and substantial amounts of other by-product metals worldwide (Singer 1995). Rough estimates of the total reserves (Cu + Pb + Zn) in VMS deposits are nearly 389 million tonnes (Mt), including already produced, current known resources and undiscovered reserves (Franklin et al. 2005). In Finland, undiscovered reserves of VMS deposits have been estimated to be 730,000 t Cu, 1.6 Mt Zn, 150,000 t Pb, 1,100 t Ag, and 16 t Au (Rasilainen et al. 2014).

VMS deposits have specific characteristics that depend on their geological settings. The original geological settings of old VMS deposits have been interpreted by comparing them to well-preserved young terranes hosting VMS deposits (e.g., Besshi, Cyprus, and Kuroko types) (Franklin et al. 2005). VMS deposits can be classified based on their host-

rocks, base metal content, and gold content (Large 1992; Barrie and Hannington 1999; Franklin et al. 2005).

The classification types of lithotectonic settings are distinct, though there are slight variations and overlapping for each. The compositional properties of the different types are unique. This lithotectonic classification system includes five types (Franklin et al. 2005), and the sixth type has been added afterwards (Galley et al. 2007).

In addition to lithotectonic setting, the base metal classification is also commonly used. It subdivides VMS deposits into two distinct groups (Cu-Zn and Zn-Pb-Cu) that mainly expresses the compositions of the underlying volcanic rocks (Fig. 2; Large 1992; Barrie and Hannington 1999). Volcanic rocks of the bimodal series host deposits of the Cu-Zn group. Mafic rocks dominate these, but felsic volcanic rocks usually occur in the vicinity of the deposits. The deposits of the Zn-Pb-Cu group form at caldera margins and are pyroclastic-dominated. They usually occur stratigraphically sequentially with >50 % of felsic volcanic rocks or almost equal amounts of felsic volcanic rocks and sedimentary strata (Franklin et al. 2005).

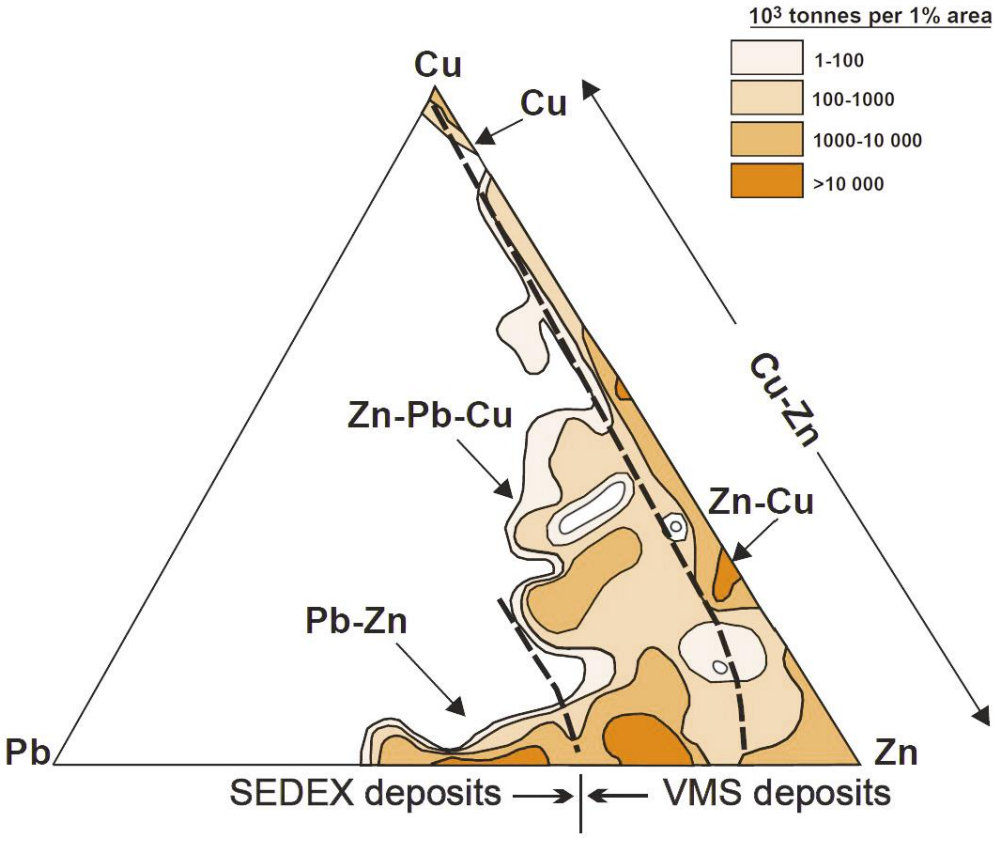

Figure 2. Base metal-based classification system for VMS deposits. Modified after Franklin (1996) and Galley et al. (2007).

3. REGIONAL GEOLOGY OF SOUTHWESTERN FINLAND

The region of southwestern Finland was formed as a result of several geological processes. The rocks in the region were deposited, deformed, and metamorphosed during the Svecofennian orogeny between ca. 1.93–1.77 Ga. The Svecofennian orogeny consists of five orogenic sequences that partially overlap: The Lapland-Kola orogeny (1.93–1.91 Ga), the Lapland-Savo orogeny (1.92–1.89 Ga), the Fennian orogeny (1.89–1.87 Ga), the Svecobaltic orogeny (1.84–1.80 Ga), and the Nordic orogeny (1.82–1.79 Ga) (Lahtinen et al. 2005). The Svecofennian orogenic evolution is divide into four major events: the microcontinent accretion stage (1.92–1.88 Ga), the large-scale continental extension stage (1.87–1.84 Ga), the continent-continent collision stage (1.87–1.79 Ga), and the orogenic gravitational collapse and stabilisation stage (1.79–1.77 Ga) (Lahtinen et al. 2005; Korja et al. 2006).

The supracrustal bedrock in the Kemiö-Orijärvi-Lohja belt comprises primarily metavolcanic rocks such as volcanic breccias, felsic and mafic tuffs, pillow lavas, and agglomerates, which are interlayered with epiclastic metasediments, pelites, and calcareous rocks (Colley and Westra 1987). In Aijala, supracrustal rocks are mostly mafic-intermediate- and felsic-volcanoclastic rocks. Mafic metavolcanic rocks occur one-third in volume compared to felsic metavolcanic rocks (Mäkelä 1989).

Within the Aijala and Orijärvi areas, supracrustal rocks can be divided into the upper, middle, and lower groups based on their lithology (Latvalahti 1979). The upper group consists of argillaceous sediments. The middle group consists of mafic volcanic rocks with intermediate metavolcanic rocks. The lower group consists of quartz-feldspar-porphyry lithologies and greywackes formed from volcanogenic rocks and epiclastic metasediments. This lower group also includes the interlayers of skarns, limestones, and iron formations (Latvalahti 1979; Simonen 1980). The Aijala and Metsämonttu ore deposits are hosted by the felsic metavolcanites sequence of the upper part of the lower group, near its contact with middle group mafic-intermediate metavolcanic rocks interbedded with epiclastic sedimentary rocks (Mäkelä 1989). Rocks of volcanic origin occur more commonly in the Aijala-Orijärvi area than in the east or west of the area (Väisänen 1988).

4. SULFIDE ORE DEPOSITS IN AIJALA AND METSÄMONTTU

Aijala and Metsämonttu ore deposits are hosted by the schist zone of southwestern Finland, formed mainly of the fine-grained quartz-feldspar-rich metamorphic rocks, and variations thereof. Calcareous schists and amphibolites also occur in this zone. The schist zone is surrounded by granodiorites and intrusive mafic rocks in the south and southeast, and by the Perniö granite in the north and west (Fig. 3; Wennervirta and Papunen 1974). The Orijärvi-Aijala zone is interpreted as an island-arc structure formed during a mid-Precambrian Eon (Latvalahti 1979).

The Aijala and Metsämonttu sulphide ores are situated near the WSW–ENE ridge of the anticline, where rock types are dominated by amphibolite and quartz-feldspar-porphyry rocks. The amplitude of the syncline on the south side is 2–4 km, and it contains quartz-granodiorites and trondhjemite-gneisses extensively (Parkkinen 1975a). The Aijala-Metsämonttu deposits were formed between felsic and intermediate to mafic metavolcanites in the same stratigraphic contact zone (Mäkelä 1989). Disseminated ore minerals occur in centimetre to metre thick bands, and in places widen into 10 metre thick massive lenticular orebodies. The main host rocks are skarn-carbonate and cordierite-gneiss (Parkkinen 1975a).

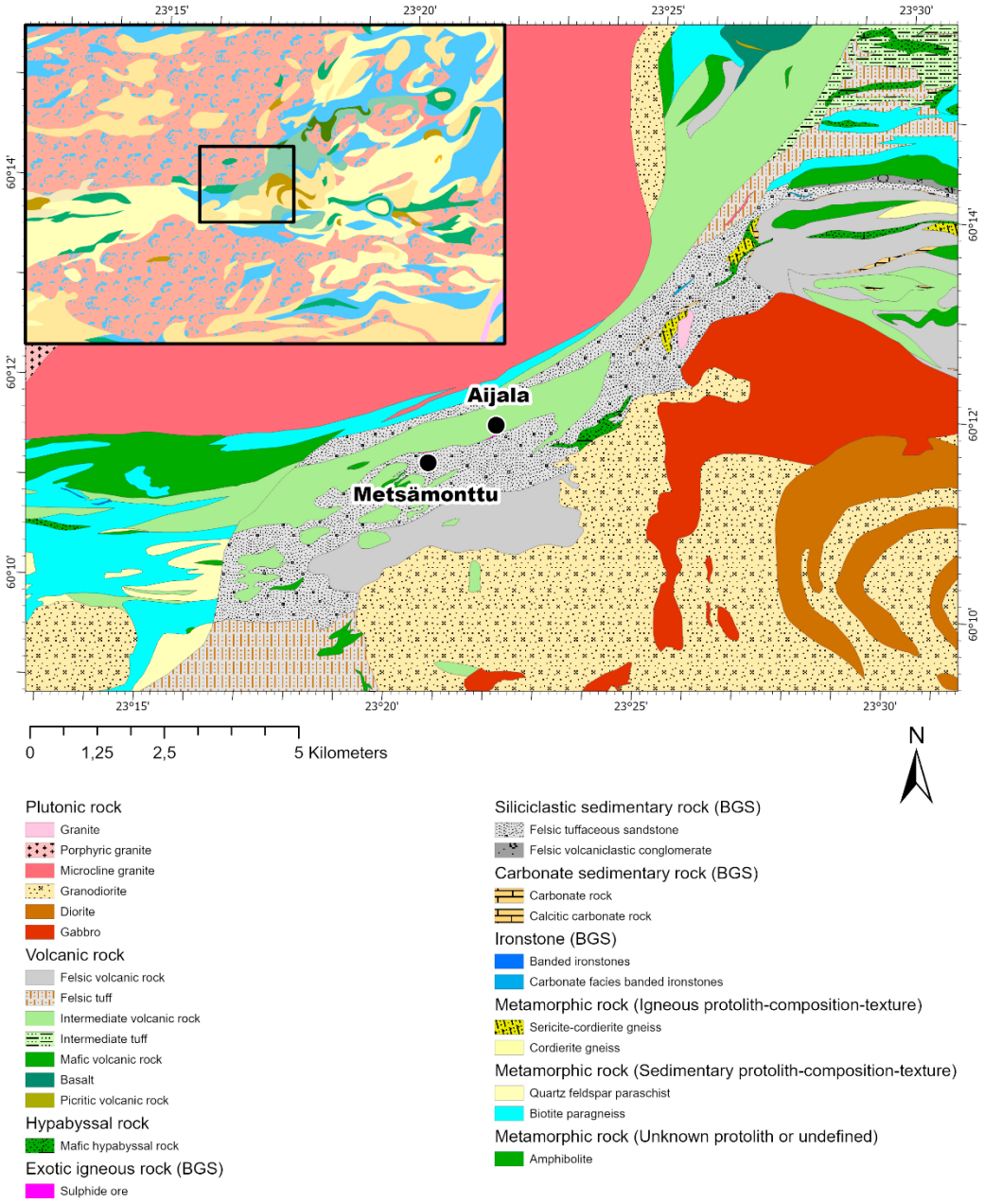

Figure 3. Geological map of Aijala and Metsämonttu. The small picture is a lithological association map from Fig. 2. Modified after GTK (2021).

Two theories have been proposed for the ore formation processes in the Aijala and Metsämonttu region. In the first theory, there are three ore formation phases. The first phase involves sedimentation and volcanism, followed by progressive regional metamorphism that forms primary iron sulphides. The second phase includes hydrothermal metamorphism processes during regional metamorphic regression, followed by the formation of Pb ores. Zn ores can be connected to the first and second phases. The third phase is the emplacement of Cu ores during shear movements. The

timing of the second and third phases can be almost simultaneous. In the second theory, all the ore types are of the same volcanogenic origin, but Pb and Cu ores are concentrated and separated at certain points (Parkkinen 1975a).

The alteration, the metal paragenesis, and the depositional environment indicate that the ores in Aijala and Metsämonttu are deposited from hydrothermal solutions. Hydrothermal activity continued for some time after the ores were deposited because alteration phenomena have been observed stratigraphically above the Aijala deposit (Mäkelä 1989).

Metal dispersion haloes of Cu, Pb, Zn, Hg, As and S, characterise ore zones in Aijala and Metsämonttu. Amphibolites tend to have high Cu and As values, although As values above background has also been found in the quartz-feldspar-porphyry rocks. Quartz-feldspar-porphyry lithology is characterised by background values exceeding Zn, Pb and S. The most precise ore indicators are Cu, Zn, Pb and As. Anomaly occurrences of the indicator elements are consistent because of the relatively simple geology of the Aijala area; the ores are situated in the straight contact zone between two main rock types, amphibolite and quartz-feldspar-porphyry. The ore deposits are surrounded by an endogenous halo, based on the overall geochemical picture of the area (Wennervirta and Papunen 1974).

4.1. Tectonic evolution and structures

The tectonic evolution of the Paleoproterozoic Uusimaa Belt, SW Finland, consists of the early deformation phases D1–D2 (~1.89–1.87 Ga) (Väisänen et al. 2002; Skyttä 2007) and the later D3 (~1835–1825 Ma), D4 (~1820 Ma), and D5 (<1820 Ma) deformation phases (Skyttä and Mänttäri 2008). The quartz-feldspar-porphyry zone of Aijala-Orijärvi area records two distinct folding phases F1 and F2 (Tuominen 1957; Mäkelä 1989; Ploegsma and Westra 1990).

Deformation phase F1 is partly predated regional metamorphism and includes the early subhorizontal thrust folding and a later second phase of crustal shortening (Ploegsma and Westra 1990). The metamorphic grade reached the highest degree during the F2 phase (Latvalahti 1979). F1 folding is isoclinal, with fold axes horizontal or plunging slightly towards the east. The characteristic features of younger folding F2 vary locally, although

it is also isoclinal and with the sub-vertical axis plunging towards the northwest at high angles (Latvalahti 1979; Mäkelä 1989).

Parkkinen (1975a) suggested that three schistosity sets control the boundaries of lithologies and disseminated ore zones. The oldest schistosity 005/70–90E, is the first generation of pervasive schistosity that altered the primary structures. It is coeval with the prograde metamorphism. The second schistosity, 330/90E, is one of the most important factors for the primary placement of ore. The third schistosity, 115/80–90S, intersects with the preceding schistosities, and its crenulation cleavage associated with the late shear events. Based on the structural sequence of Parkkinen (1975a), the ore minerals were originally situated parallel to the vertically oriented limb of F2 folds that formed due to N–S compression. The minor folds and the shears have determined the final location of the ore after the main folding event.

The Aijala-Orijärvi area is characterised by several fault zones (Latvalahti 1979), formed after the last deformation episode D5 due to separate incidents, presumably at 1.79–1.77 Ga, 1.64–1.55 Ga, and ~1.26 Ga (Lahtinen et al. 2005; Skyttä 2007). Both Aijala and Metsämonttu deposits record these faults, which only have local effects (Latvalahti 1979).

4.2. Metamorphism

Regional metamorphism in the Aijala-Orijärvi area developed mainly during D_1 before microcline granites emplaced (Latvalahti 1979) at the time when the accretion of island arcs and microcontinents to the Karelian microcontinent took place at 1.92–1.88 Ga (Ehlers et al. 1993; Korja et al. 2006; Lahtinen et al. 2009).

Diagnostic mineral assemblage in the Aijala-Orijärvi region are muscovite, quartz, and plagioclase (An_{20}) (Latvalahti 1979). Table 1 shows diagnostic metamorphic mineral assemblages in Metsämonttu. P-T conditions during regional metamorphism are close to the conditions of the following chemical reaction (Bucher and Grapes 2011).

$$KAl_3Si_3O_{10}(OH)_{10} + SiO_2 = KAlSi_3O_8 + Al_2SiO_5 + H_2O \quad (1)$$

Muscovite (Ms) quartz (Qtz) K-feldspar (Kfs) sillimanite (Sil)

Table 1. Diagnostic metamorphic mineral assemblages in Metsämonttu after Mäkelä (1989).

Rock type	Main minerals	Type of metamorphism	Drill core
Cordierite-mica gneiss	Quartz-muscovite-biotite-cordierite-staurolite-plagioclase ($An_{20–30}$)	Prograde	MM-244 / 66.5 m
– " –	Quartz-muscovite-cordierite-biotite-plagioclase ($An_{20–30}$)	– " –	MM-188 / 285.1 m
Muscovite schist	Quartz-andalusite-muscovite	– " –	MM-311 / 25.0 m
– " –	Muscovite-quartz	– " –	MM-310 / 60 m
Chlorite-mica gneiss	Plagioclase ($An_{0–10}$)-quartz-chlorite-microcline-epidote-garnet	Retrograde	MM-138 / 95.5 m
– " –	Plagioclase ($An_{0–10}$)-quartz-muscovite-biotite-epidote-chlorite	– " –	MM-222 / 66.8 m

Experimental results have shown that in the melt absent reaction, muscovite begins to break down and react with quartz at around 600 °C and low-P (< 300 MPa), producing K-feldspar and sillimanite. At over 300 MPa pressure, muscovite decomposes and produces sillimanite, K-feldspar, and leucogranite melts (Bucher and Grapes 2011).

Some of the of cordierite-sericite-mica-gneisses in the Orijärvi area, contain andalusite together with sillimanite. Latvalahti (1979) suggested that, the temperature has been above 480 °C and pressure lower than 370 MPa (Bucher and Grapes 2011; Wei et al. 2004). Within the Aijala-Orijärvi region, metamorphism took place under low-pressure amphibolite facies conditions (~650 ± 30 °C and ~300 MPa) (Latvalahti 1979).

4.3. Alteration

Altered rocks occur primarily in the footwalls of the Aijala and Metsämonttu deposits. They are continuous and lateral lithologies, their volume increases downwards, and the intensity of alteration varies widely. The rock types whose chemical composition has been chanced are now fine-grained silicic rocks, dolomitic limestones, chlorite-bearing diopside-tremolite-skarns, cordierite-biotite-gneisses, cordierite-anthophyllite rocks, and cordierite-bearing sericite/muscovite-schists and -gneisses (Mäkelä 1989).

Latvalahti (1979) suggested that the alteration zones associated with sulphide ores can be divided into two zones based on the chemical composition and areal distribution of the rock types: (1) the inner alteration zone includes hydrothermal alteration pipe and wall rocks of the lenticular orebodies, and (2) the outer alteration zone consists of blanket-type altered acidic rocks. Mäkelä (1989) have further discussed that the various altered rocks do not only represent different types alteration but were initially produced from rocks with a different chemical composition. A clear and sharp distinction in chemical composition on the contacts between different altered rock types supports that. Therefore, zoned intensive metasomatic alteration was not the only cause of sharp contrasts between the altered rock types.

In Aijala, the dominant altered rocks are cordierite-muscovite-gneisses, dolomitic limestones, and skarns. In Metsämonttu, they are muscovite-gneisses, cordierite-mica (biotite, muscovite, phlogopite) -gneisses, cordierite-anthophyllite-gneisses, dolomitic limestone, and skarns. Some of the gneisses containing fine-grained, quartz-feldspar-rich bands, with or without quartz-eye porphyries, resemble felsic metavolcanites. The gneisses containing cummingtonite-plagioclase ($An_{50–60}$) -rich bands can be interpreted to resemble mafic-intermediate metavolcanites (Mäkelä 1989)

4.4. Aijala Cu-Zn deposit

The mining operation in Aijala took place in 1949–1958 (Warma 1975; Heiskanen and Stenberg 1971). The total amount of ore mined from the Aijala VMS ore deposit was 0.83 Mt (GTK 2019a), and the average concentrations of the metals mined in Aijala were 1.6 wt.%

copper (Cu), 0.7 wt.% zinc (Zn), 14.2 wt.% sulphur (S), 14 g/t silver (Ag), and 0.7 g/t gold (Au) (Mäkelä 1989).

The Cu-Zn deposit in Aijala is a set of lenticular-shaped sulphide orebodies. Sulphide orebodies are vertically on the south side of the hanging wall amphibolite. A vertical shear zone controls ores in Aijala, and it cuts the ore zone at a small angle (Parkkinen 1975b). In Aijala, sulphides occur in skarn-carbonate rocks that were associated with schists (Varma 1954). Ore deposits in Aijala are situated on the north side of the iron sulphide zone (Parkkinen 1975b). Table 2 shows the amounts of metals produced from the Aijala deposit.

Table 2. Quantities of metals produced from the Aijala deposit. GTK (2019a).

Commodity	Total production (t)	Importance
Copper	13 320.61	Small deposit
Zinc	5 531.74	Occurrence
Silver	11.7	Occurrence
Lead	20	Occurrence
Gold	0.58	Occurrence
Sulphur	12 931	Occurrence

The largest dimensions of the ore-covered area in Aijala are 500 m in length, 80 m in width, and 600 m in depth. The dip of the orebodies is almost vertical, and the strike of the orebodies is 60°. The widths of the discrete sulphide zones range from centimetres to metres, with a maximum width of about 10 m. In the middle and northernmost parts of the deposit, the main ore, Cu ore, occurs as a 10-metre-thick lenticular orebody with massive ore pockets (up to 10 wt.% and 14 wt.% Cu), and from there, Cu ore continues as narrow disseminated zones to the western and eastern ends of the deposit. Iron sulphide ore occurs as a narrow zone on the south of the main ore. The ores can be divided into two groups: (1) Zn-bearing Cu ore, which is the main ore type, (2) iron sulphide ore, involving minor and localised Pb-bearing zones (up to 7.74 wt.% Pb). Iron sulphide and Cu ores in Aijala had equivalents in Metsämonttu. However, Metsämonttu-type Zn-Pb-Fe ore does not exist in Aijala (Parkkinen 1975b).

Iron sulphide associations represent the primary syngenetic ore formation in a specific stratigraphic horizon in Aijala. In contrast, the Zn-bearing Cu ore is epigenetic and was mobilised into the shear. The occurrence of these two ore types is similar in Aijala and Metsämonttu (Parkkinen 1975b).

A set of local thrust faults occur in Aijala. Two major faults cut the orebodies at a depth of 200–350 m (in the local mine coordinate system), dipping 35–70° towards the north, displacing the overlying block 100 m towards the south. Mobilisation of chalcopyrite and its concentration into pockets has been associated with the early stages of the genesis of the Aijala fault. South-dipping faults (45–75°) almost perpendicular to the main faults also occur in the Aijala (Parkkinen 1975b). Table 3 shows ore minerals identified from the Aijala deposit.

Table 3. Ore minerals identified from the Aijala deposit (Parkkinen 1975b).

Mineral	Formula	The mineral occurs as the main ore mineral
Pyrite	FeS_2	yes
Chalcopyrite	$CuFeS_2$	yes
Sphalerite	ZnS	yes
Pyrrhotite	$Fe_{1-x}S$ (x = 0 to 0.2)	yes
Galena	PbS	yes
Arsenopyrite	FeAss	yes
Marcasite	FeS_2	not
Mackinawite	$(Fe,Ni)_{1+x}S$ (x = 0 to 0.11)	not
Magnetite	$Fe^{2+}Fe^{3+}{}_2O_4$	not
Rutile	TiO_2	not
Silver	Ag	not

Chalcopyrite is most abundant sulphide mineral in the central part of the Aijala deposit. It exhibits remobilisation into the shear zones during tectonic activity, occurs as veins penetrating other ore generations and massive ore pockets and zones. Elsewhere within the deposit, chalcopyrite crystallised after tectonic activity, also occurring as an accessory phase in all other ore types (Parkkinen 1975b).

Sphalerite is a common accessory mineral but only rarely the most abundant ore mineral, being typically associated with chalcopyrite and sometimes with galena. Primarily sphalerite occurs as dissemination, but like chalcopyrite, it has been remobilisation into

the fractures. Galena is an uncommon ore mineral in Aijala. As the main ore mineral, galena occurs only within local veinlets or in small sulphide accumulations (Parkkinen 1975b).

4.5. Metsämonttu Zn-Pb-Cu deposit

The mining operation in Metsämonttu took place in 1952–1958 and 1964–1974 (Warma 1975; Heiskanen and Stenberg 1971). The total amount of ore mined from the Metsämonttu VMS ore deposit was 1.5 Mt (GTK 2019b), and the average concentrations in Metsämonttu were 0.3 wt.% Cu, 0.8 wt.% lead (Pb), 3.5 wt.% Zn, 13.2 wt.% S, 25 g/t Ag, 1.4 g/t Au (Mäkelä 1989).

The dimensions of the Metsämonttu sulphide deposits are 400 m in length, 70 m in width, and 700 m in depth. The orebodies strike is 70°, and the dip is almost vertical. The ores can be divided into two groups: (1) Zn-Pb-Fe ore, which is the main ore type, (2) Cu ore that continues intermittently from the eastern parts of the main ore to the northwest, towards Aijala. Zn-Pb-Fe ore does not continue to Aijala (Parkkinen 1975a). Ore deposits in Metsämonttu are situated on the south side of the iron sulphide zone (Parkkinen 1975b). Table 4 shows the amounts of metals produced from the Metsämonttu deposit.

Table 4. Quantities of metals produced from Metsämonttu. GTK (2019b).

Commodity	Total production (t)	Importance
Zinc	44 927.23	Small deposit
Gold	1.13	Small deposit
Lead	7 050.43	Small deposit
Copper	1 575.55	Occurrence
Silver	19.67	Occurrence
Sulphur	11 3014.7	Small deposit

The ore zone is bound on the north side by intermediate volcanic rocks. The western end of the ore formation naturally ended in a constriction. The eastern end of the ore formation is being intersected by the major Metsämonttu-Aijala shear zone. This Metsämonttu-

Aijala shear zone dips 65° towards NW, its width varies between 50–200 m, and it cuts ore zones at a small angle (Parkkinen 1975a).

The main overthrust fault in Metsämonttu is at a depth of 150–160 m (in the local mine coordinate system), dipping 10–20° towards the south, displacing the overlying block 300 m towards the north. Extensions of the sulphide lenses have been found at a depth of 220–230 m (in the local mine coordinate system). Also, a set of overthrust faults cut the lenticular orebodies from at least three different depths (220, 380, and 560 m in the local mine coordinate system). These three faults are dipping 10–20° towards the south with a minor displacement of the overlying blocks towards the north. These faults do not reach as far as Aijala because the older Metsämonttu-Aijala shear zone and its parallels cause stepwise displacements that compensate for the displacements of the younger faults in Metsämonttu. A set of fractures also cuts the ore deposits, dipping 45–70° towards NNW, with minor displacement (Parkkinen 1975a).

The sulphide ores in Metsämonttu are situated in a specific stratigraphic horizon, on the south side of the hanging wall amphibolite. The most important elements of ore formation are contacts between different rock types, a specific side contact between the main orebody and the cordierite-gneiss, schistosity, folding, and shear zones (Parkkinen 1975a). According to Varma (1954), the ore mineral paragenesis in Metsämonttu is: pyrite, pyrrhotite, sphalerite, galena, and chalcopyrite. Table 5 shows ore minerals identified from the Metsämonttu deposit.

Table 5. Ore minerals identified from the Metsämonttu deposit (Parkkinen 1975a).

Mineral	Formula	The mineral occurs as the main ore mineral
Pyrite	FeS_2	yes
Pyrrhotite	$Fe_{1-x}S$ (x = 0 to 0.2)	yes
Chalcopyrite	$CuFeS_2$	yes
Sphalerite	ZnS	yes
Galena	PbS	yes
Boulangerite	$Pb_5Sb_4S_{11}$	yes
Arsenopyrite	FeAss	yes
Marcasite	FeS_2	yes
Tennantite	$Cu_6(Cu_4C^{2+}_2)As_4S_{12}S$	yes
Tetrahedrite	$Cu_6(Cu_4C^{2+}_2)Sb_4S_{12}S$	yes
Andorite	$AgPbSb_3S_6$	yes
Geocronite	$Pb_{14}(Sb,As)_6S_{23}$	yes
Pyrargyrite	Ag_3SbS_3	not
Chalcocite	Cu_2S	not
Covellite	CuS	not
Mackinawite	$(Fe,Ni)_{1+x}S$ (x = 0 to 0.11)	not
Cubanite	$CuFe_2S_3$	not
Molybdenite	MoS_2	not
Thucholite		not
Magnetite	$Fe^{2+}Fe^{3+}_2O_4$	
Ilmenite	$Fe^{2+}TiO_3$	
Rutile	TiO_2	
Arsenic	As	not
Antimony	Sb	not
Bismuth	Bi	not
Gold	Au	not
Silver	Ag	not

Chalcopyrite is one of the main ore minerals in the Metsämonttu deposit. It occurs in both veins and pockets as almost monomineralic fractions or as a common accessory mineral in all ore types. Chalcopyrite represents the final stage of crystallisation occurring as interstitial to other minerals. Older generations of chalcopyrite are present as inclusions in sphalerite and primary pyrite. Also, chalcopyrite occurs as lamellar intergrowths with cubanite (Parkkinen 1975a).

Sphalerite is also one of the main ore minerals, being present either as the disseminated form that gradually transitioned to massive ores or as a typical accessory with iron

sulphides. Intergrowths between sphalerite and chalcopyrite are common, where sphalerite is predominant (Parkkinen 1975a).

Galena and boulangerite are common ore minerals, along with chalcopyrite and sphalerite. Galena occurs as a reticulated pattern of disseminated veinlets with grain sizes of a few millimetres. Disseminated coarse-grain boulangerite coexists with galena or, to a lesser extent, with arsenopyrite and chalcopyrite (Parkkinen 1975 a).

In the lower part of the Metsämonttu deposit (also called the Uusi Metsämonttu deposit), concentrations of S and Zn were highest in the middle, while the highest concentrations of Ag were found at the western and southern ends of the deposit. Also, Pb and Ag were concentrated to a lesser extent in the southern part of the formation. The concentration of Cu was highest in the SE block, decreasing towards the west. In contrast to Cu, the concentration of Pb decreases from west to east (Parkkinen 1975a).

4.6. Precious metals

The anomalous concentration of silver was 3–4 ppm in the lower parts of Metsämonttu. Silver and lead show strong mutual correlation, regardless of rock type. The highest silver concentrations were within the lead ores that were surrounded by carbonate rocks (Huhma and Latvalahti 1975).

In the lower parts of the Metsämonttu deposit, small interstitial gold grains (Ø 0.01–0.05 mm) occur together with sphalerite, galena and boulangerite. Gold grains are typically present with chalcopyrite in the cracks and also occur as thin films (Ø 0.002 mm) along grain boundaries. Gold is also associated with gangue minerals; it occurs especially along cleavages of tremolite grains. Native silver occurs with sphalerite as inclusions, thin films, and grains with a diameter of less than 0.01 mm. Occasionally silver is bound with gold forming electrum (Parkkinen 1975a).

5. MATERIALS AND METHODS

Historical drill core logs and assays were used for 3D modelling of the geology and sulphide ores of Aijala and Metsämonttu. The materials used were collected and produced during the mineral exploration and mining operations by Outokumpu Oy between 1945–1976. GTK has digitised historical materials and provided them for this thesis (Leväniemi et al. 2020). The original materials comprise the machine- and hand-typed drill core reports, geological profile maps, hand-drawn mine level maps with lithologies, and bedrock maps.

5.1. Historical drill core reports

GTK archive contains reports on 542 drill cores from the Aijala and Metsämonttu deposits. Using Excel, the data of the drill core reports were manually digitised partly on behalf of GTK personnel and partly on behalf of the author. After digitisation, the data were processed and validated by the author. Overlapping lithology intervals and assay intervals were corrected, and incorrect concentration values and invalid local coordinates, dips, and azimuths were corrected.

540 of the 542 drill cores have been used to create geological 3D models (Appendix 5). These 540 drill cores total length is 52074.00 metres. Drill cores MM-145 and MM-278 lack coordinate and elevation information, and they were not found in other materials. Of these 540 drill core reports, 477 reports include all the necessary information, 20 cores lack either location or direction information, and 43 cores lack two or more location or direction information. Missing information was recovered either from mine tunnel maps and cross-sections or subsequent reports.

The 540 used drill cores for 3D models include a total of 11,452 intervals of rock types. Table 6 shows the 11 main rock types that have been used in the historical mine reports between 1942 and 1972. They were simplified from the 245 original rock types in the drill core reports. The geological 3D models do not include rock types, for which no equivalent rock type is evident among the 11 main rock types. The 13^{th} class was created for such misfits.

Table 6. Rock types including overburden (soil) in Aijala and Metsämonttu. The first 12 are from the original reports. Quartz-porphyry is same than quartz-feldspar-porphyry mentioned earlier.

Count	Original rock type
1	Amphibolite
2	Quartz-porphyry
3	Mica-schist
4	Sericite-schist
5	Cordierite-schist
6	Skarn
7	Ore
8	Soil
9	Pegmatite
10	Quartz
11	Phyllite
12	Limestone
13	Other

Survey data is missing on 383 holes. Dip angle and azimuth values only from the beginning of the drill hole have been measured on these holes, and those values were used as the end values of the holes in the 3D models. A complete survey of directional measurements along the drill hole is available for 157 holes.

From the Aijala and Metsämonttu drill core samples, 12 different elements have been analysed: Cu, Pb, Zn, S, Fe, Au, Ag, Ni, Co, Hg, Se, and Sb. A variable number of samples (1–104) per drill core have been analysed from 378 drill cores between 1942 and 1975. Assays include a total of 5,599 intervals (mean length of samples is 2.435 in Aijala and 2.708 m in Metsämonttu) with varying numbers of measured elements. Cu, Pb, and Zn have been measured in almost all samples. Au has been measured about 15 % of all samples and Ag from about 67 % of all samples (Table 7). In the original reports, concentrations of elements have been reported either as a per cent or parts per million (ppm). Au and Ag have been reported in g/t or ppm.

Table 7. The elements analysed from the Aijala and Metsämonttu drill core samples. Not all elements have been analysed from same samples.

Element	Assay pcs	Drill cores
Cu	5261	345
Pb	4892	240
Zn	5291	334
S	4608	321
Fe	15	6
Au	852	158
Ag	3756	193
Co	3177	80
Hg	2494	66
Se	71	14
Ni	3179	80
Sb	340	7

5.2. Mine level maps and cross-sections

Hand-drawn mine level maps (38 maps of the Aijala mine and 23 maps of the Metsämonttu mine) and cross-sections (30 of the Aijala mine and 17 of the Metsämonttu mine) were used as an aid to improve the geological 3D models (Appendix 6). Mine level maps and cross-sections include information on mine grid coordinates, rock types, drill holes, structural details, and concentrations of elements (Fig. 4). In addition, cross-sections with only major shears and brittle faults were used to aid the modelling of structures (6 of the Aijala mine and 5 of the Metsämonttu mine). Mine level maps and cross-sections were imported into the modelling software.

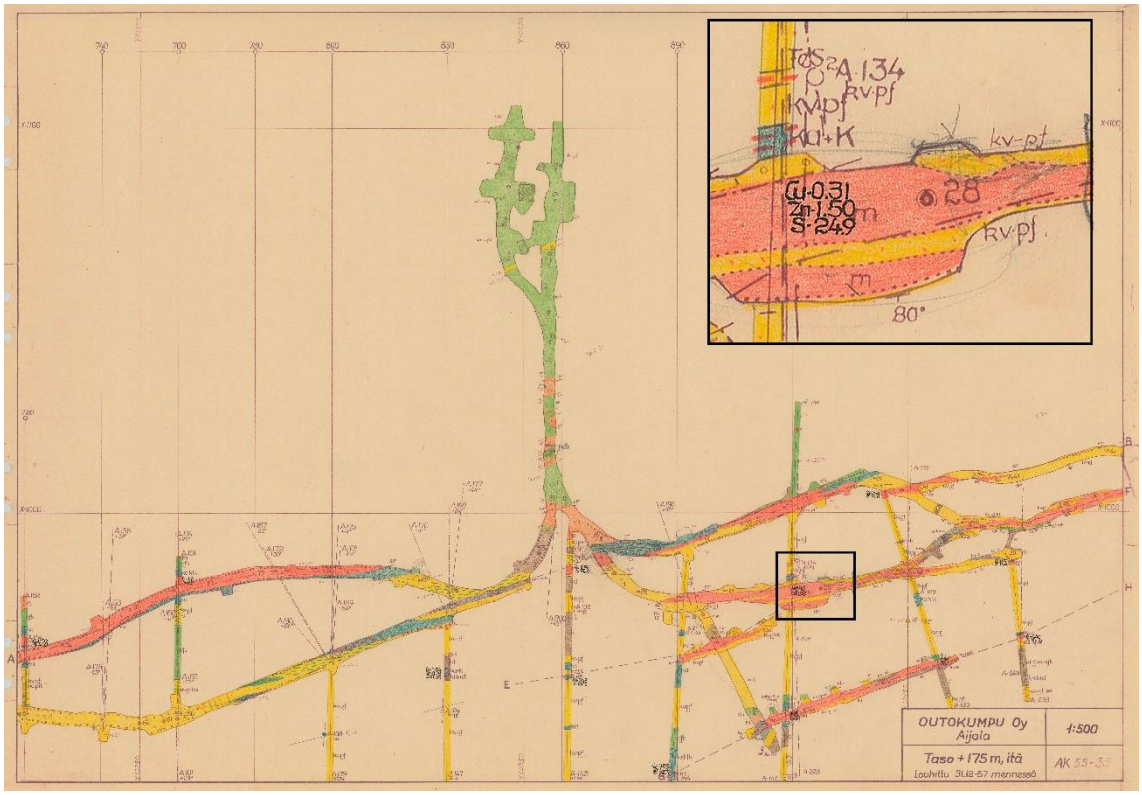

Figure 4. Original mine level map 1:500 of the east part of the Aijala deposit. Level +175 m in the local coordinate system. Modified after Outokumpu Oy (1957).

5.3. Mine grid coordinates

Coordinate conversions from local mine coordinates to ETRS-TM35FIN coordinate system has some uncertainties. Coordinates on the maps and drill core locations are in the local mine grid coordinate system. The mine coordinate grid is rectangular, and the coordinates are indicated in metres. The Helmert transformation formula from the local mine grid to the ETRS-TM35FIN has been done by GTK personnel (Appendix 3; Kuorikoski 2019) and was utilised in this study.

The georeferencing has been done using the coordinates of the boundary markings of the mine district (Mp0, 7K, 26k, and 27K). The verification was done on behalf of GTK personnel using boundary markers of the mine district (P77 and Mp12) and drill hole locations (A-061, A-063, A-069, A-072, A-073, and A-076) (Outokumpu 1975; Kuorikoski 2019).

5.4. Software and creating geological 3D models

Leapfrog Geo software is the program used for 3D modelling. Leapfrog Geo uses an advanced implicit modelling engine (Fast Radial Basis Functions (fRBF)), which makes it fast and flexible. An implicit modelling engine is an automated way to model surfaces directly from geological data. Dynamic updating allows the model to be updated quickly when new data is available. When creating a 3D model of the drill core data, all the necessary information must be included in the input files: coordinates, elevation, azimuth, dip, rock type, and, if necessary, numerical data, e.g., assays (Seequent Limited 2021). Geological and numerical 3D models are useful to determine structures, lithologies relationship, and the occurrences and emplacements of base metals and precious metals.

The digitised historical drill core data, which consists of the collar (coordinates and elevation), survey (depth, azimuth, and dip), rock types (beginning and end of intervals, and rock type), and assay (measured elemental concentrations) files, were imported into the Leapfrog. Also, all 61 hand-drawn mine level maps and 58 cross-sections were individually imported into the Leapfrog (Appendix 6). The local X and Y coordinates of the three points on each mine level map were converted to the ETRS-TM35FIN N and E coordinates using a Helmert converter. The elevation of each mine level map was then converted to correspond to the actual elevation. Two X and Y points with their elevations from each cross-section were converted to the ETRS-TM35FIN coordinate system.

The digital elevation model (DEM) 2x2 m and topographic map were downloaded from the National Land Survey of Finland (NLS) download services (NLS 2021). Georeferencing of the topographic map was done using ArcGIS before it was imported into the Leapfrog. The clipping boundary was delimited beyond the outermost ends of the drill cores. Topography (surface resolution 3) was made using DEM, and a clipping boundary was set to restrict the size of the topography. The elevations of the surface drilling were adjusted to correspond to the elevation of the topography in those where it differs by more than 1.5 metres.

The imported rock type data, including soil, consists of 12 classes in Aijala and Metsämonttu areas (Table 6). The 13th rock type class, "Other", was selected as ignore, it was not modelled with fRBF. The drill holes in Aijala and Metsämonttu boundary boxes

were selected using the stroke tool and assigned to their own drill hole groups. The drill holes were divided into Aijala and Metsämonttu groups based on the location to make it easier to keep the divided rock types in order. Separate query filters were created for both models based on the newly created drill hole groups.

The soil layers were created using the erosions tool in both models. Soil covers all surface area in Aijala and partly in Metsämonttu. Soil cover is thinner in Metsämonttu than in Aijala. Both mine areas have some outcrops, but the models do not present the correct situation because the drilling locations were not at those places. The soil thickness varies in drilling areas from 5 m to 15 m in Aijala and from 2 m to 8 m in Metsämonttu.

The split rock type groups were created for both deposits, and a query filter was selected to show drill holes according to the model to be worked. Ore, skarn, and pegmatite rock types between amphibolite on the north and quartz-porphyry on the south were split into discrete parts, one at a time. These discrete parts of the rock type units were selected using the stroke tool based on the mine level maps and cross-sections, and they were assigned to new rock type groups in both models, respectively. The discrete rock type groups were created for both models to make it easier to keep the divided lithologies in order (Appendix 4).

Ore lenses were created individually using the vein modelling tool. The shape and size of the ore lens models were finalised one by one, drawing the horizontal and vertical lines of the footwall and hanging wall using mine level maps and cross-sections, respectively. The slicer tool was used to slice the 3D models from the working plane. Due to the scarcity of mine level maps and cross-sections in the lower parts of the Metsämonttu mine, the ore lenses were drawn based on the sketch images found in the reports of Heiskanen and Stenberg (1971) and Warma (1975). The smaller ore units were modelled separately in both deposit models using the intrusion tool. These include the scattered data of the ore that were not included in the ore lenses in the Aijala and Metsämonttu models. The intrusion tool is the most suitable application for modelling small discrete units. The plane tool was used to draw planes in both deposit models separately, and the plane was set to the same dip angle (80°) and azimuth (330°) as the ore lenses. The smaller ore units in both models were set to follow the plane, and ellipsoid ratios of ore units were set to 3, 3, 1.

In both mines, ore lenses are parallel with several thin vein-like skarn units. As with the ore deposits, the modelling of the skarn veins was made using the vein modelling tool, and the intrusion tool was used to modelling the scattered data of skarn next to the veins. Due to limited rock type data in the lower parts of the mines, skarn units were continued deeper, to the lower limit of the boundary boxes, in the same manner as they occur above their location in the upper parts of the models. The shape and size of the skarn vein models were finalised one by one, the same as the ore lenses, insofar as there were mine level maps and cross-sections. As with the smaller ore units, the smaller skarn units were adjusted to the plane (dip 80°, azimuth 330°), and ellipsoid ratios were set at 3, 3, 1.

Pegmatite vein units were created in both deposit models using the vein tool, and the intrusion tool was used for scattered data of pegmatite to create small pegmatite units. Quartz rock type data occurs scattered around both deposits. Small quartz veins were created using the intrusion tool. Pegmatite and quartz units that were created using the intrusion tool were adjusted as before, using a plane (dip 80, azimuth 330, and ellipsoid ratios 3, 3, 1).

Mica-schist, sericite-schist, and cordierite-schist units were created in both deposit models using the intrusion tool. All the schists models were adjusted using plane (dip 80, azimuth 330, and ellipsoid ratios 3, 3, 1). Lithology boundaries were also adjusted using lines based on the maps and cross-sections.

Phyllite units were created only in the Aijala model using the intrusion tool. Phyllite occurs in thin units near the surface at the eastern end of the Aijala mining area. Metsämonttu rock type data contains only three data points of phyllite; they were not modelled due to scarcity of data. Limestone units occurred in several discrete small units and were created for both models with the intrusion tool. Phyllite and limestone models were adjusted using plane (dip 80, azimuth 330, and ellipsoid ratios 3, 3, 1).

Of the two significant lithologies, the hanging wall amphibolite was selected for modelling because its contacts are more easily detectable from the mine level maps and cross-sections than the footwall quartz-porphyry. Although amphibolite is a large continuous unit, its contacts with other lithologies are complex, especially against the hanging wall quartz-porphyry. The intrusion tool was used to create an amphibolite unit

because it is the most flexible and versatile for modifying lithology models. Boundary contacts with other lithologies were modified using lines based on the mine level maps and cross-sections.

Faults were created using lines and points in both models based on cross-sections of major shears and brittle faults. The Aijala model has two curvilinear faults dipping 50° towards the NNW and three faults perpendicular to the first two, dipping 50–70° towards the SE and SSE. The Metsämonttu-Aijala shear zone runs on the north side of the Aijala deposit, dipping 70° towards the NW. The Metsämonttu model has three curvilinear faults dipping 20° towards the S, and the Metsämonttu-Aijala shear zone runs on the south side of the Metsämonttu deposit, dipping 70° towards the NW.

The Aijala and Metsämonttu models were activated to obtain output volumes with the following chronology of units: soil, ore, skarn, pegmatite, quartz, cordierite-schist, sericite-schist, mica-schist, phyllite, limestone, and amphibolite. Quartz-porphyry was selected as background rock type to create a footwall and fill all the empty spaces. The Metsämonttu model does not include phyllite. Faults were not activated because the distribution of drill cores is uneven on the different sides of the faults, which would create empty gaps and cause the models to become distorted.

5.5. Creating numerical models

The utilised metals (Cu, Pb, Zn, S, Au, and Ag) were selected for the numerical grade models. The concentrations of Au and Ag are in ppm in the imported assay data because they have been measured in either ppm or g/t. The Cu, Pb, and Zn concentrations are in per cent or ppm in the original assay reports. The ppm concentrations of the base metals were converted to percentages in the assay data. The numeric composites were made for each selected mineral in both models and the soil unit was filtered out.

The fRBF interpolant models were created for each metal in both models. The metal from the composited table was selected as the numeric value. The query filter and the model boundary were set to the model in the making. The surface resolution was set to 10. After creating the numeric models, each model was processed individually. The spheroidal interpolant, alpha value 7, no drift, and base range 20 were set for all numeric models.

Total sills were set the same as the variances, and nuggets were set 20 % of the total sill values. Trend directions 330/80 and ellipsoid ratios 4, 4, 1 were set for all numeric models for correspond to the orebodies on the historical maps and cross-sections. Depending on the incidence frequency of values, intervals were created for each mineral in both models.

6. RESULTS

6.1. Geological 3D models of Aijala and Metsämonttu

Even though the distance between mines is only about 1.5 km, geological models of both mines were made with their own boundary boxes because of the scarcity of the drilling data between mines. Boundary boxes were placed for the Aijala (length 777 m, width 633 m, depth 595 m) and Metsämonttu (length 1,415 m, width 921 m, depth 771 m) deposits based on the extent of the drill holes with both mine areas. The ore lenses and smaller ore units are clearly visible on the mine maps and cross-sections. The Aijala deposit has five distinct ore lenses and two smaller ore units. The Metsämonttu mine has three ore lenses in the upper parts and five ore lenses in the lower parts (Uusi Metsämonttu). Several smaller ore units occur in the vicinity of the ore lenses in the upper parts of the Metsämonttu deposit.

Figures 5 shows the 540 drill cores (52,074.00 metres) and solid ore lenses within the boundary boxes. The underground workings from which the drillings are made run obliquely (WSW-ENE) relative to the boundary boxes. The geological 3D models are most accurate in the middle of the models; only a few drillings reached the outer edges. The 11 rock type classes are from the original reports.

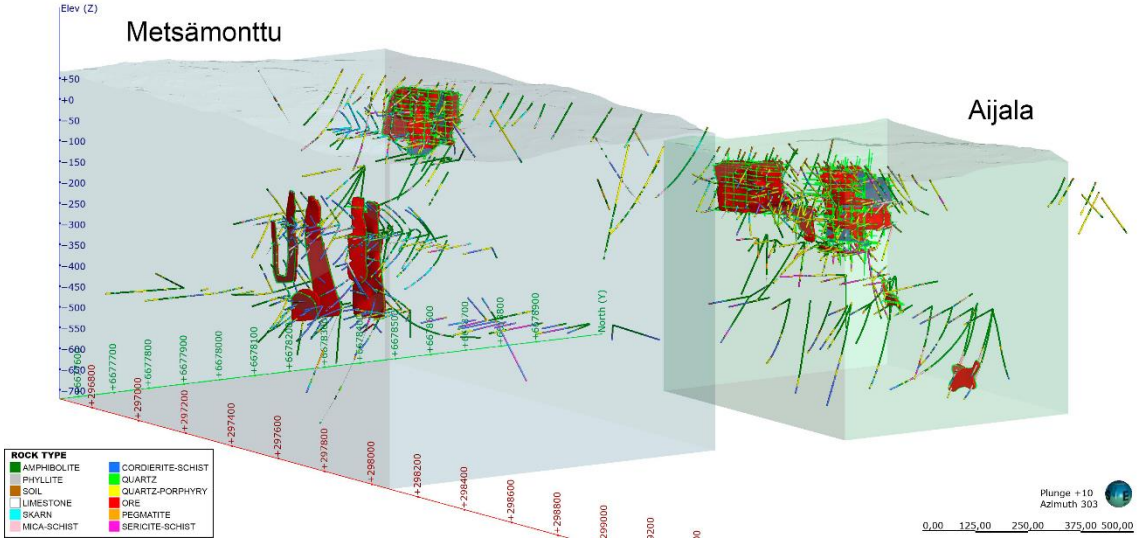

Figure 5. Boundary boxes, drill cores, ore lenses, and drawn outlines of orebodies in the Aijala and Metsämonttu models.

The major Metsämonttu-Aijala shear strikes SW-NE on the north side of the lenticular orebodies in Aijala and on the south side of the Metsämonttu orebodies not being in contact with sulphide orebodies. Both Aijala and Metsämonttu areas are characterised by faulting, which have had only local effect. (Fig. 6a and b).

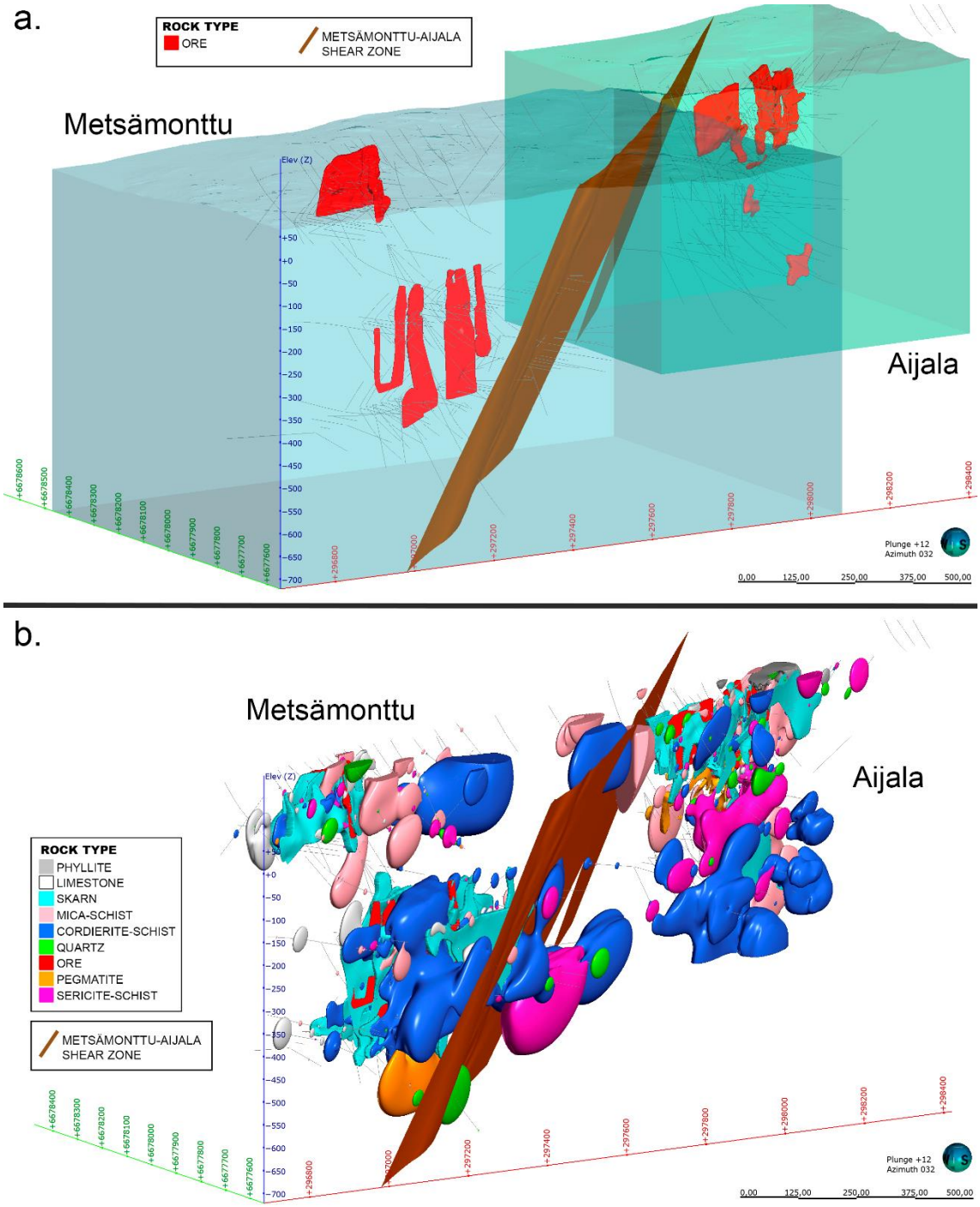

Figure 6. **a.**) Sulphide orebodies, drill core traces and the major Metsämonttu-Aijala shear zone. Ores of the Metsämonttu are on the north side of the shear zone, and ores at Aijala are on the south side of the shear zone. Looking towards NE. **b.**) The major Metsämonttu-Aijala shear zone and distribution of all lithologies except the footwall quartz-porphyry and the hanging wall amphibolite are indicated. Looking towards NE.

Figures 7a and b show the extent of footwall quartz-porphyry and the hanging wall amphibolite and altered rocks in between. Altered rocks are mainly enclosed by the footwall quartz-porphyry. Overburden is not included in the figures if it impairs visualisation. The soil thickness varies from 5 m to 15 m in Aijala and 2 m to 8 m in Metsämonttu.

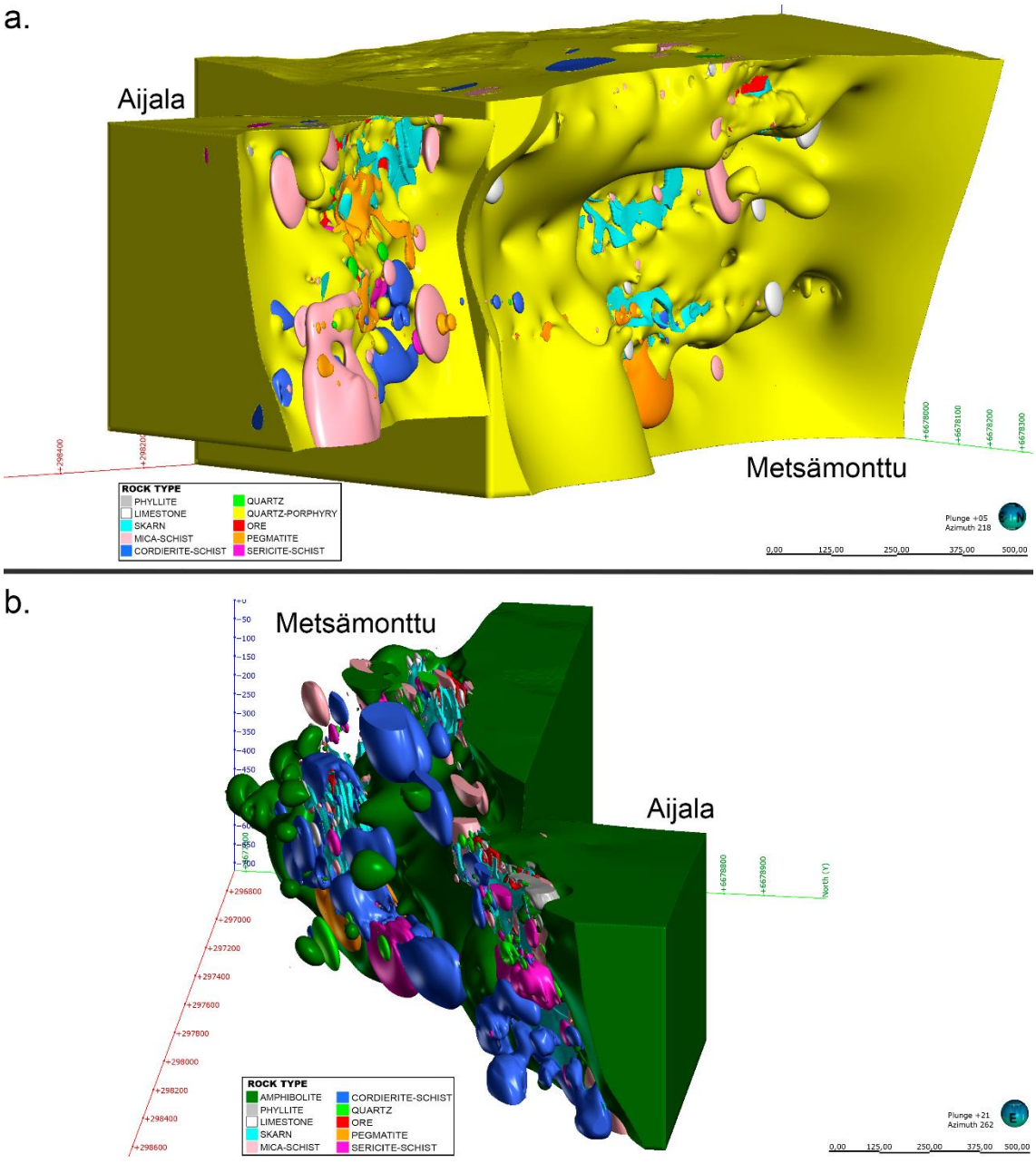

Figure 7. Geological 3D models for Aijala and Metsämonttu, emphasizing the distribution of altered rocks lithologies and sulphide lenses between the footwall quartz-porphyry and hanging wall amphibolite. Overburden is not included. Mica-schist occurs closer to amphibolite, while the occurrence of other lithologies is concentrated more to the south, within quartz-porphyry. **a.)** The footwall quartz-porphyry and all lithologies in between. Looking towards SW. **b.)** The hanging wall amphibolite and all lithologies in between. Looking towards W.

Figure 8 shows the distribution of the sulphide orebodies with the footwall and hanging wall. In the Metsämonttu deposit, orebodies are more extensive enclosed by the footwall quartz-porphyry than by the hanging wall amphibolite compared to the Aijala deposit.

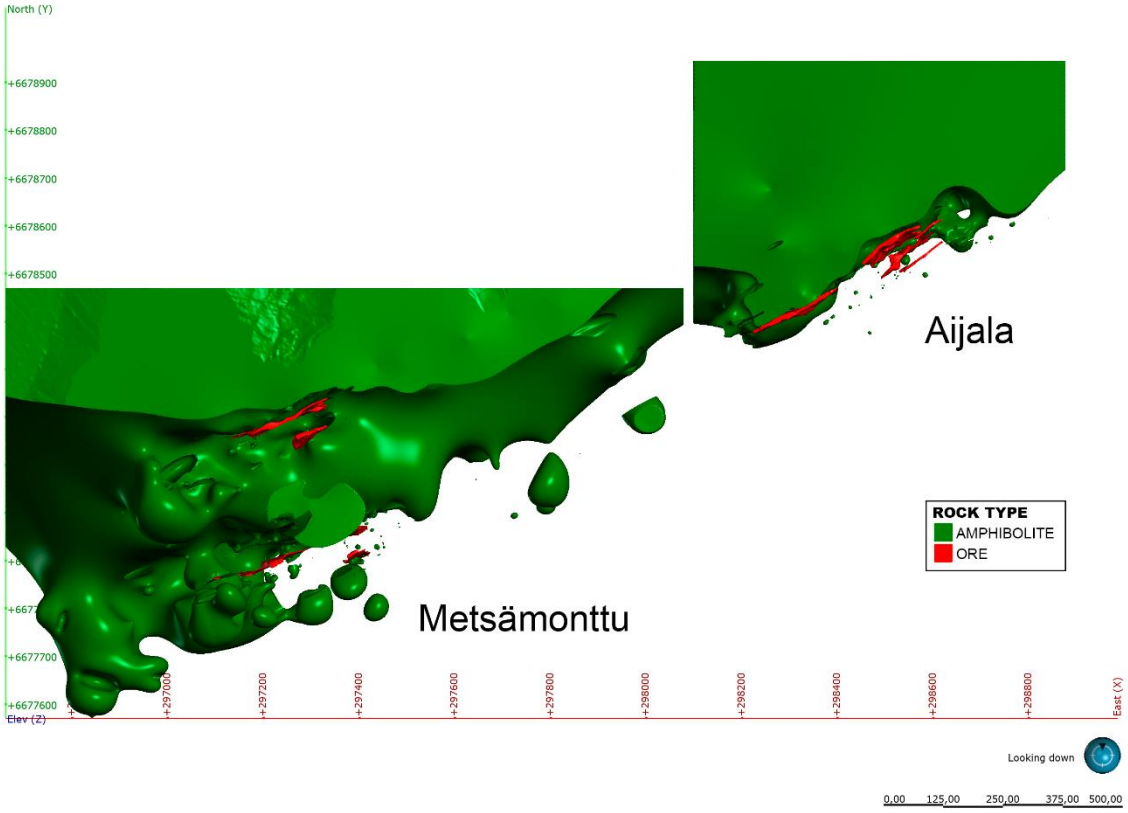

Figure 8. Distribution of the hanging wall amphibolite and sulphide ores. A fault has displaced sulphide lenses 270 m to the north in Metsämonttu. Looking down, and the north is up.

Table 8 shows the average concentrations of the metals mined from Aijala and Metsämonttu deposits (Cu, Pb, Zn, Ag, and Au). Averages were calculated using only those assays obtained from ore lithologies of geological models. The Aijala deposit is rich in Cu (2.23 wt.% Cu), Zn (1.13 wt.% Zn), but has only traces of Pb (0.14 wt.% Pb). Precious metals concentrations are 12.7 g/t Ag and 0.8 g/t Au in Aijala. The Metsämonttu deposit is rich in both Zn (5.37 wt.% Zn) and Pb (1.46 wt.% Pb), and in addition contains 42.1 g/t Ag, 2.7 g/t Au, and has minor (0.22 wt.%) amounts of Cu.

Table 8. Average concentrations of utilised metals mined from Aijala and Metsämonttu deposits. These concentrations differ from those reported by Mäkelä (1989) because assays used to obtain averages below represent sulphide-bearing samples.

Unit	Element	Aijala	Metsämonttu
wt.%	Cu	2.23	0.22
	Pb	0.14	1.46
	Zn	1.13	5.37
g/t	Ag	12.7	42.1
	Au	0.8	2.7

6.2. Geological 3D model of Aijala

The Aijala model reaches an elevation of -550 metres and contains three SSE and two NNW dipping faults. The major Metsämonttu-Aijala shear zone runs on the north side and interacts with neither the orebodies nor altered rocks. The fault dipping 50° NNW cuts the orebodies at an elevation of -253 metres and displaces the hanging wall 80 m towards the south. Ore extensions are at an elevation of -125 metres (Fig. 9).

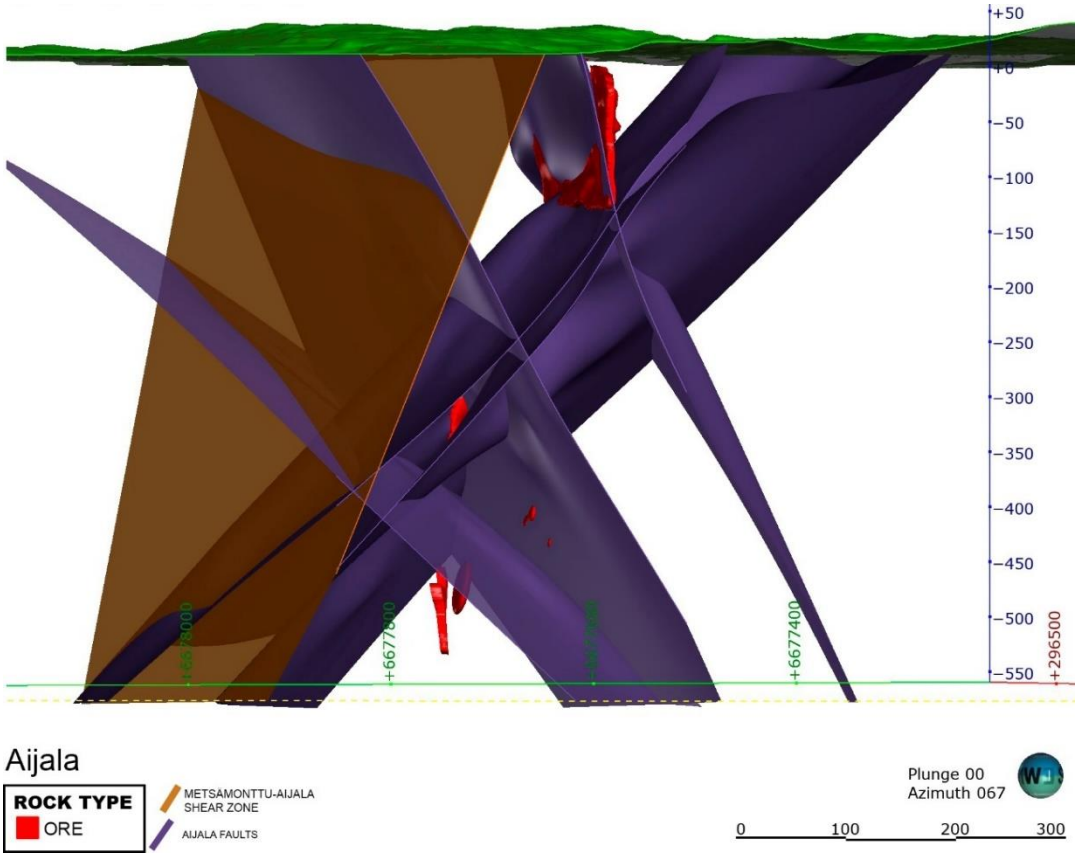

Figure 9. Sulphide ore lenses (red) in Aijala on the south side of the major Metsämonttu-Aijala shear zone (brown). Three faults (purple) dipping 45–75° towards SSE and two faults (purple) dipping 50° towards NNW cut the orebodies and displaces the overlying block 80 m towards the south. Looking towards ENE.

Figures 10a and b show the Aijala model divided into the footwall quartz-porphyry and the hanging wall amphibolite with all rocks between them. Cordierite-schist occurs to a greater extent at deeper and some in the upper part in modelled bedrock, while sericite-schist occurs in the middle of the modelled bedrock. The largest pegmatite unit is in the middle of the modelled bedrock.

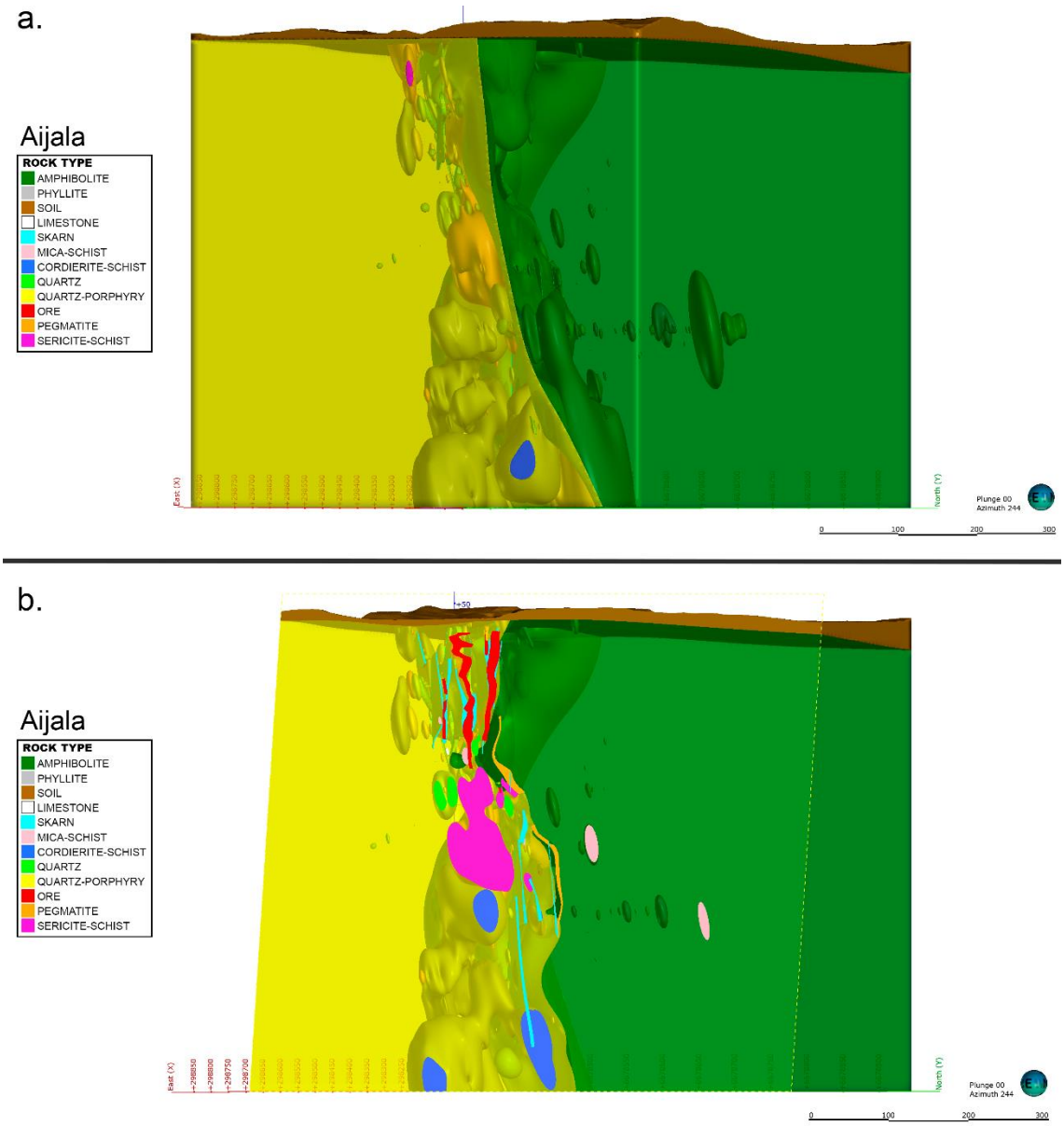

Figure 10. Aijala's geological 3D model in its entity. Amphibolite and quartz-porphyry are transparent. **a.**) All lithologies and overburden are shown. Some mica-schists are within the hanging wall amphibolite. Looking towards WSW. **b.**) Cross-section with all lithologies and overburden. All the lithologies at or near the interface between the hanging wall and the footwall are enclosed by the quartz-porphyry. Looking towards WSW.

The orebodies are close to the interface between the footwall quartz-porphyry and the hanging wall amphibolite, mainly within the footwall quartz-porphyry (Appendix 1). The Aijala deposit is divided into the west and east parts. The western part of the Aijala deposit has a single major sulphide lens, while the eastern part has two major and two-medium sized sulphide lenses a few tens of metres apart (Fig. 12a and b). In addition, three small sulphide accumulations occur deeper in the eastern Aijala deposit. The distribution of sulphide ores is more concentrated in the north side, the hanging wall side, than skarn veins (Fig. 11a and b).

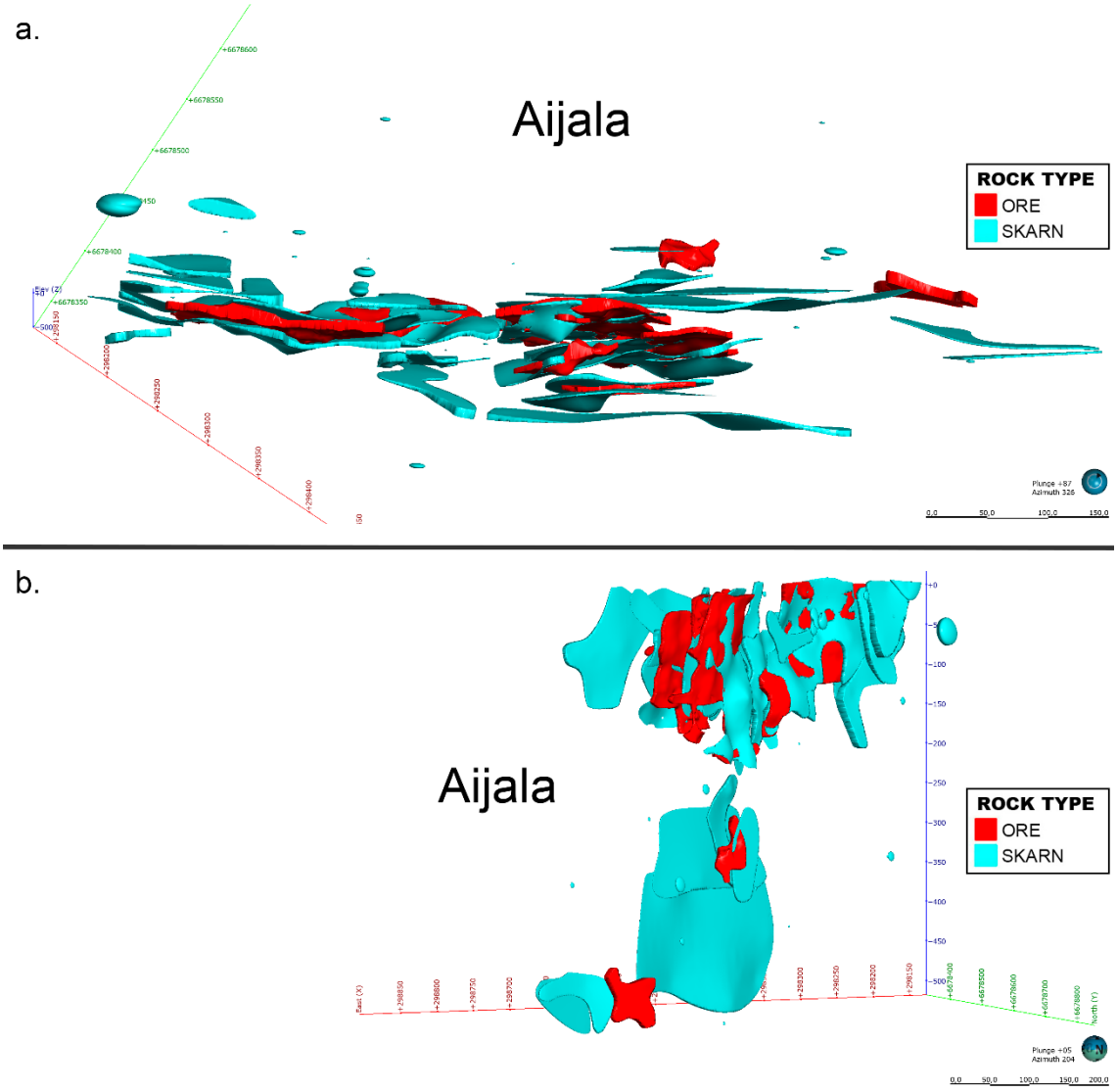

Figure 11. Sulphide orebodies and skarn in Aijala, **a.**) Looking down and the north is up. **b.**) Looking towards SSW.

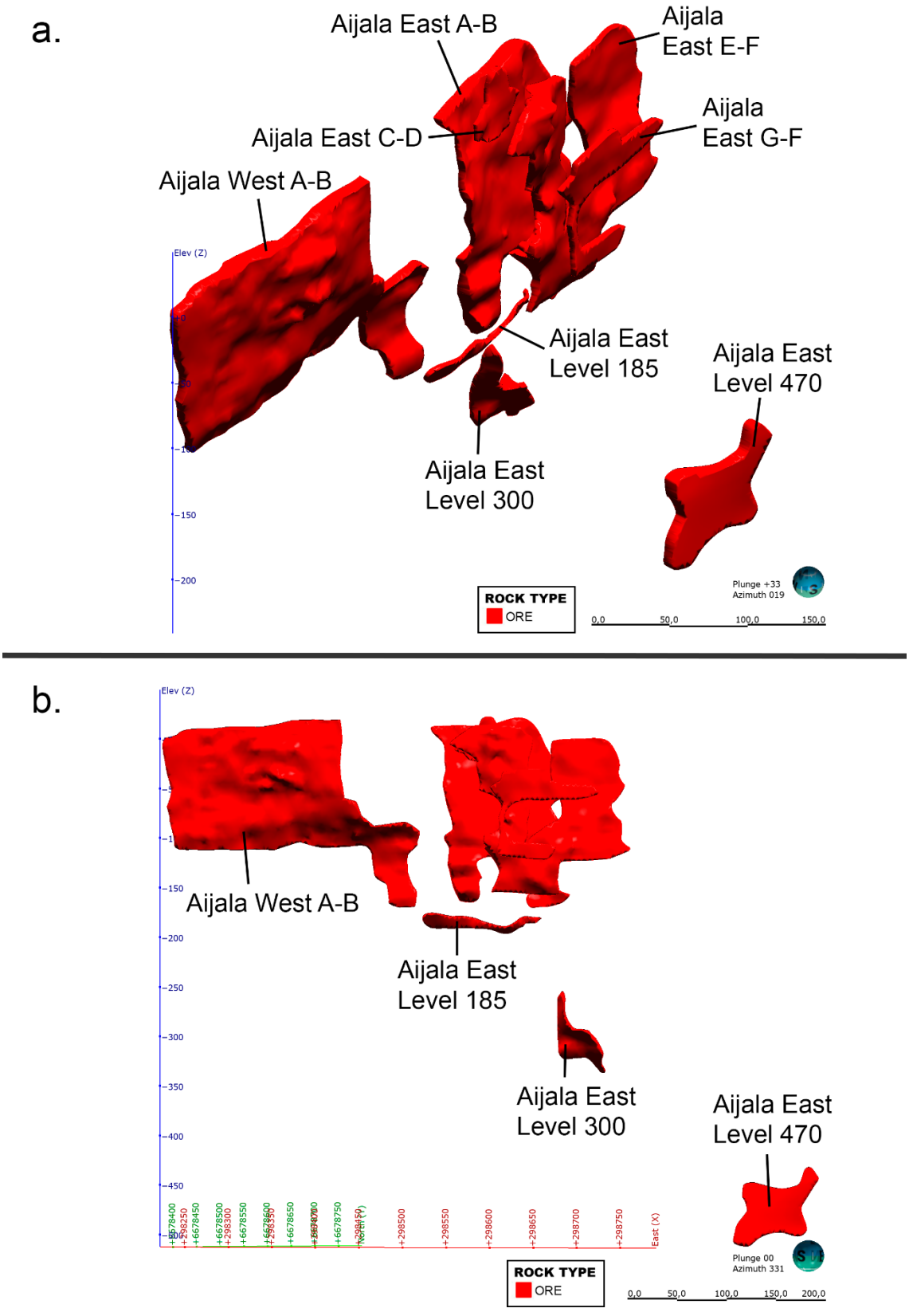

Figure 12. **a.** and **b.**) Sulphide orebodies in Aijala. The names of the orebodies West and East A-B, and C-D, E-F, and G-F in Aijala are the names given by Outokumpu Oy. Aijala East Level 470 ore has not been mined and the modelled orebody is based on four ore lithology intervals, which are 5–8 m long.

6.3. Numerical grade models of the Aijala deposit

Numerical models show the distribution and concentrations of base and precious metals for Aijala and Metsämonttu. The distribution of Cu is concentrated in West Aijala, and Cu is also present in the upper parts of East Aijala but less abundant. In the lower part of East Aijala Cu is absent. Minor Pb occurs in the deeper parts of East Aijala (-300 and -470 metres) and delimited areas in the upper parts of West and East Aijala. In the western and eastern Aijala Zn is distributed evenly all around. However, the highest concentrations of Zn are in the upper East Aijala. The highest Ag concentrations occur on the north side of sulphide orebodies in West Aijala and the western end of East Aijala. In addition, some distinct Ag-rich bodies occur in the deeper parts of East Aijala. Gold occurs as distinct domains mainly in deeper parts of East Aijala (Fig. 13, and 14a-b).

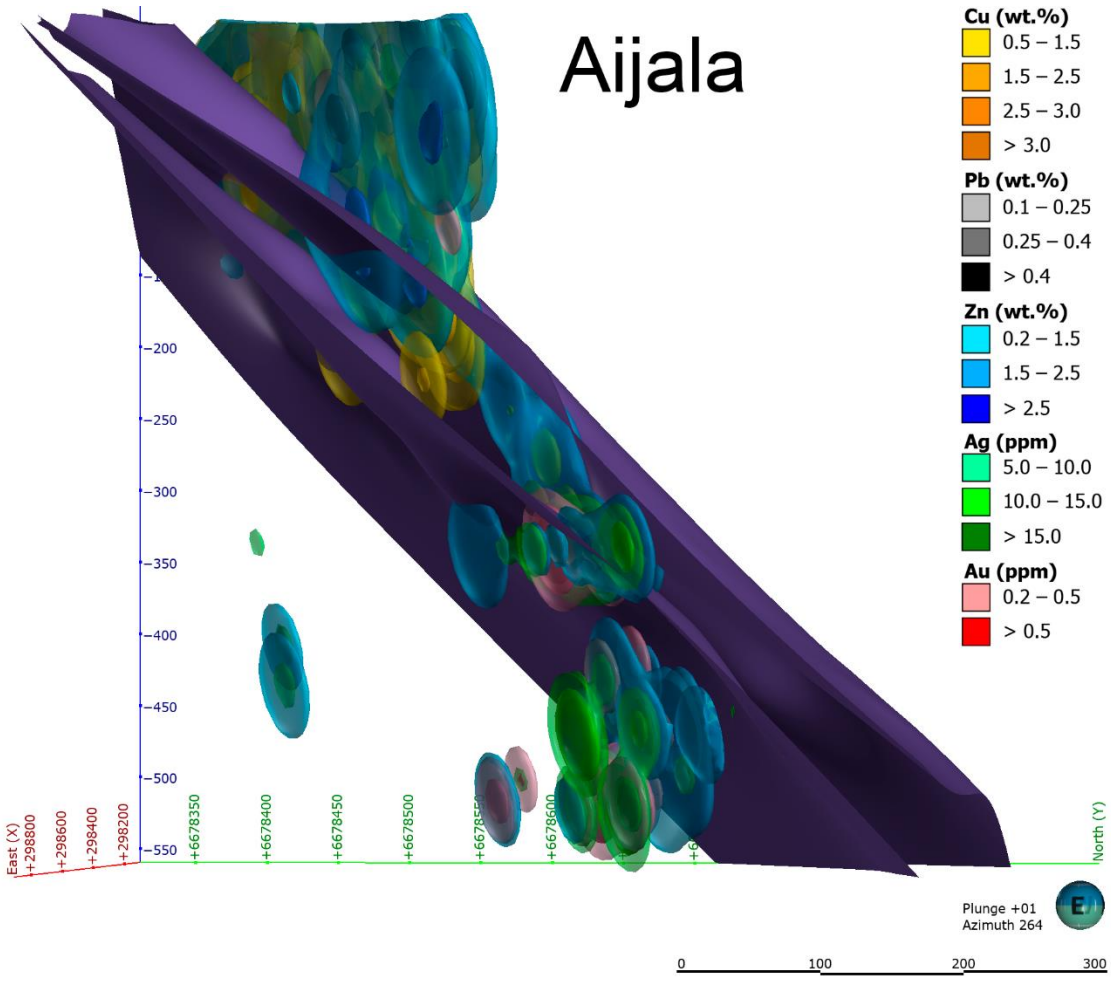

Figure 13. Numerical grade models for the economic metals in the Aijala deposit. North dipping faults has displaced the overlying block 80 m towards the south. Looking towards the west.

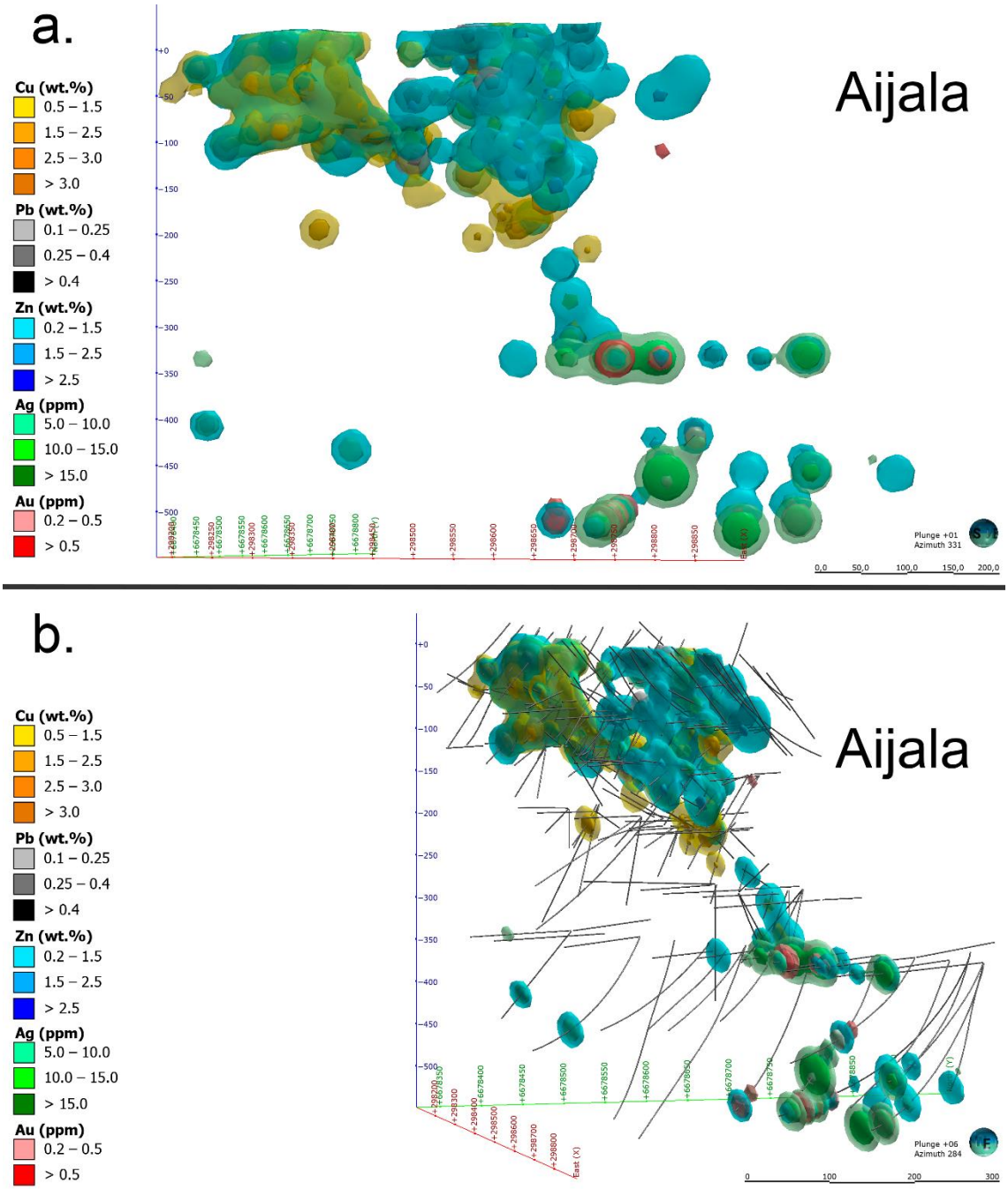

Figure 14. Numerical grade models for the economic metals in the Aijala deposit. **a.**) Looking towards NNW. **b.**) Drill hole traces are in grey. Looking towards WNW.

Figure 15 is a cross-section from the Aijala West A-B sulphide lens. The dominant base metal is Cu and it occur on the footwall side. Lead occurrence is concentrated on the topmost of the Aijala West A-B sulphide lens. Zinc is abundant on the hanging wall side of the sulphide lens and occurs around Cu. Silver and gold occur on the topmost in the Aijala West A-B sulphide lens, where minor Pb is also present.

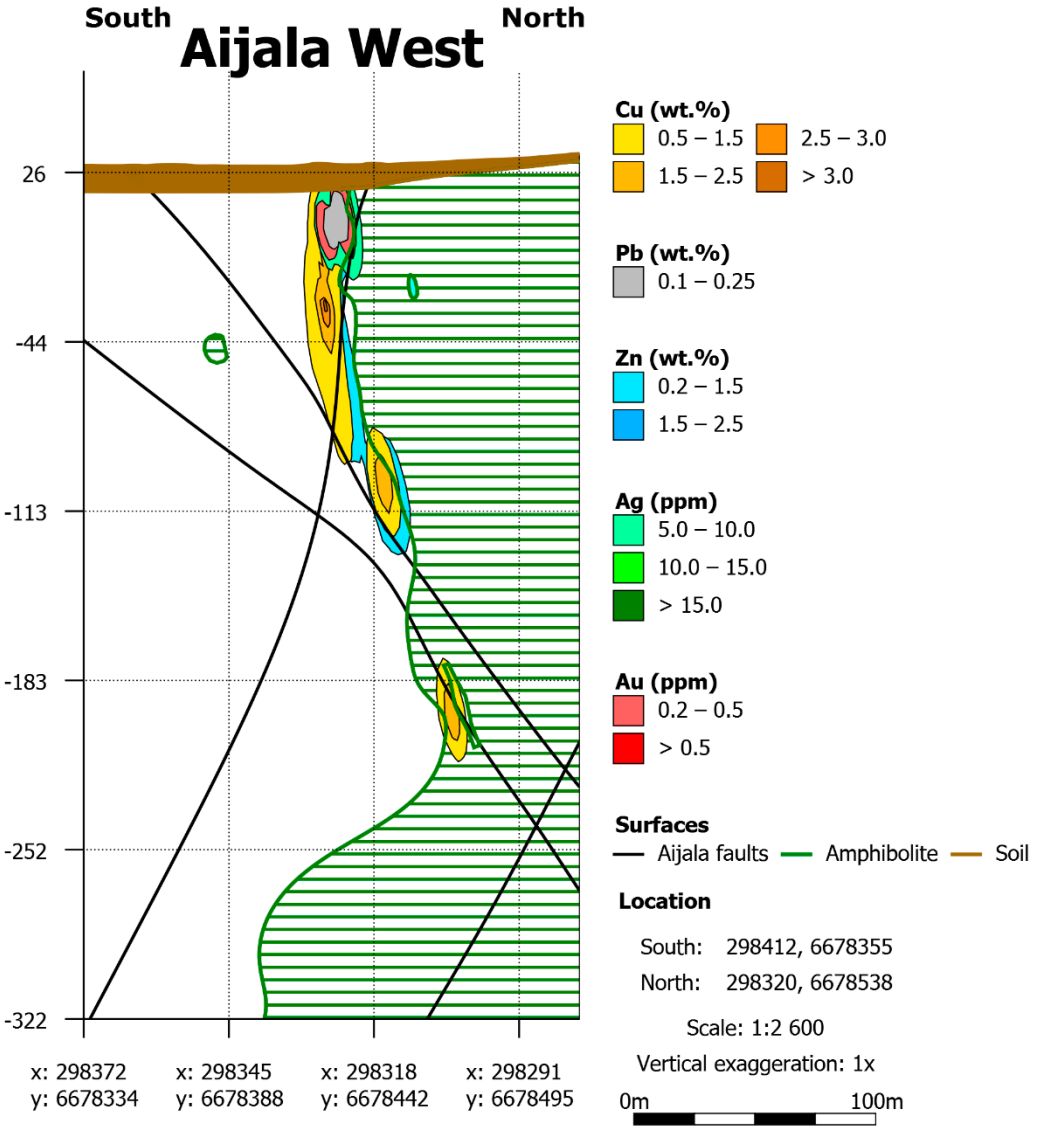

Figure 15. Cross-section from Aijala West A-B sulphide ores. The hanging wall amphibolite is shown as green hatch, and the two black lines represent the north-dipping faults. The numerical grade models do not take into account fault lines. Looking towards the west.

Figure 16 is a cross-section from the Aijala East. The cross-section shows the Aijala East A-B, C-D, E-F, and G-H ore lenses and Level 185, 300, 470 units. Zinc is the dominant base metal and occurs around Cu and Pb. Copper ores are most abundant in A-B, C-D, and E-F lenses. Lead occurs on the topmost in the Aijala East A-B and E-F sulphide lenses, and Pb is less abundant in the C-D lens between them. Silver and gold are absent in the upper parts of the eastern end of the Aijala East sulphide lenses. At Level 300, Ag and Au occur separately. At Level 470 is an occurrence of Ag, Au and Zn (Fig. 13 and 14a-b). Figure 17 shows the average concentrations of utilised base and precious metals per ore lithology unit.

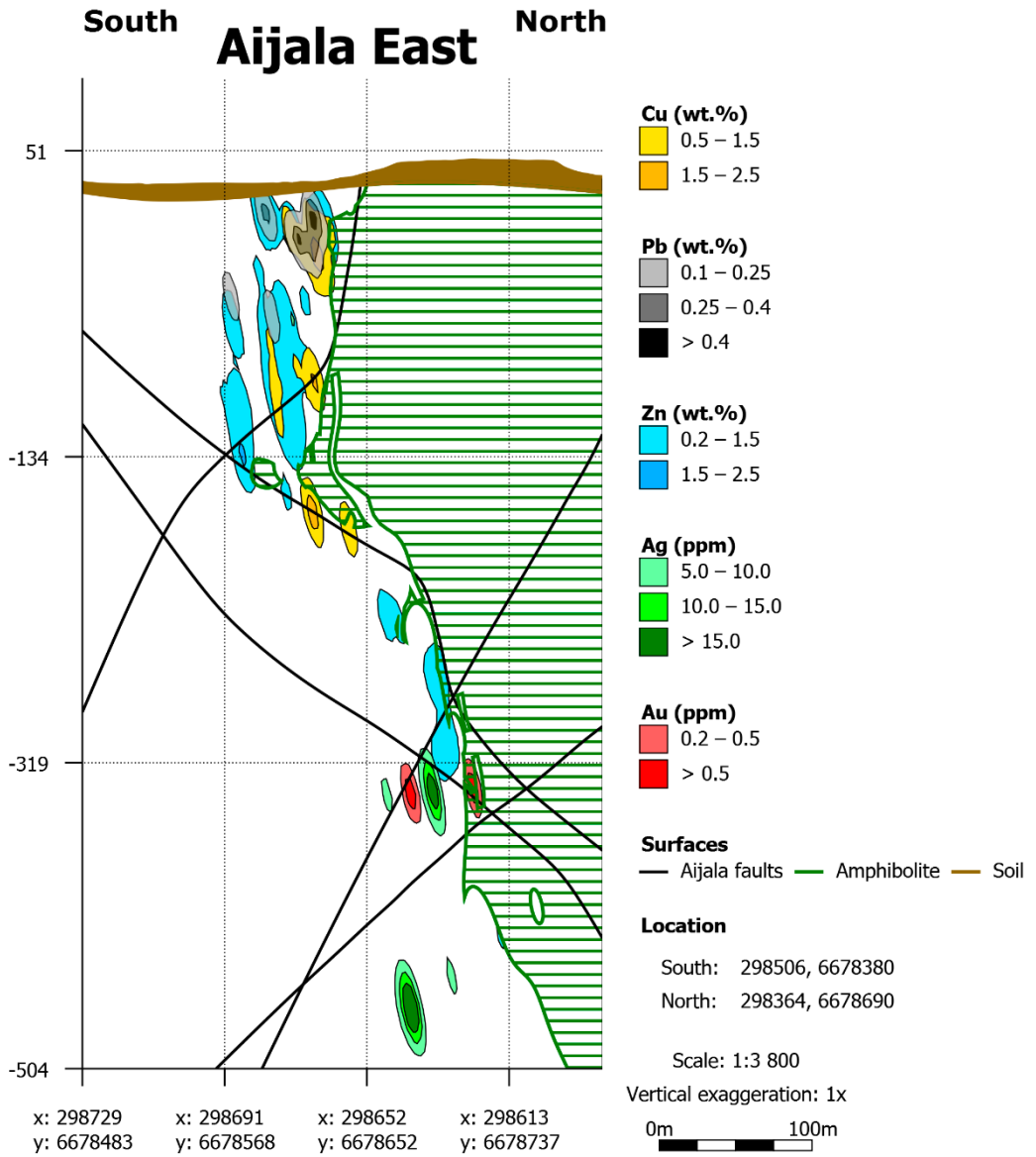

Figure 16. Cross-section from Aijala East. Includes Aijala East A-B, C-D, E-F, and G-H ore lenses and Level 185, 300, 470 ore units. The hanging wall amphibolite is the green hatch, and the two black lines represent the north-dipping faults. The numerical grade models do not take into account fault lines. Looking towards the west.

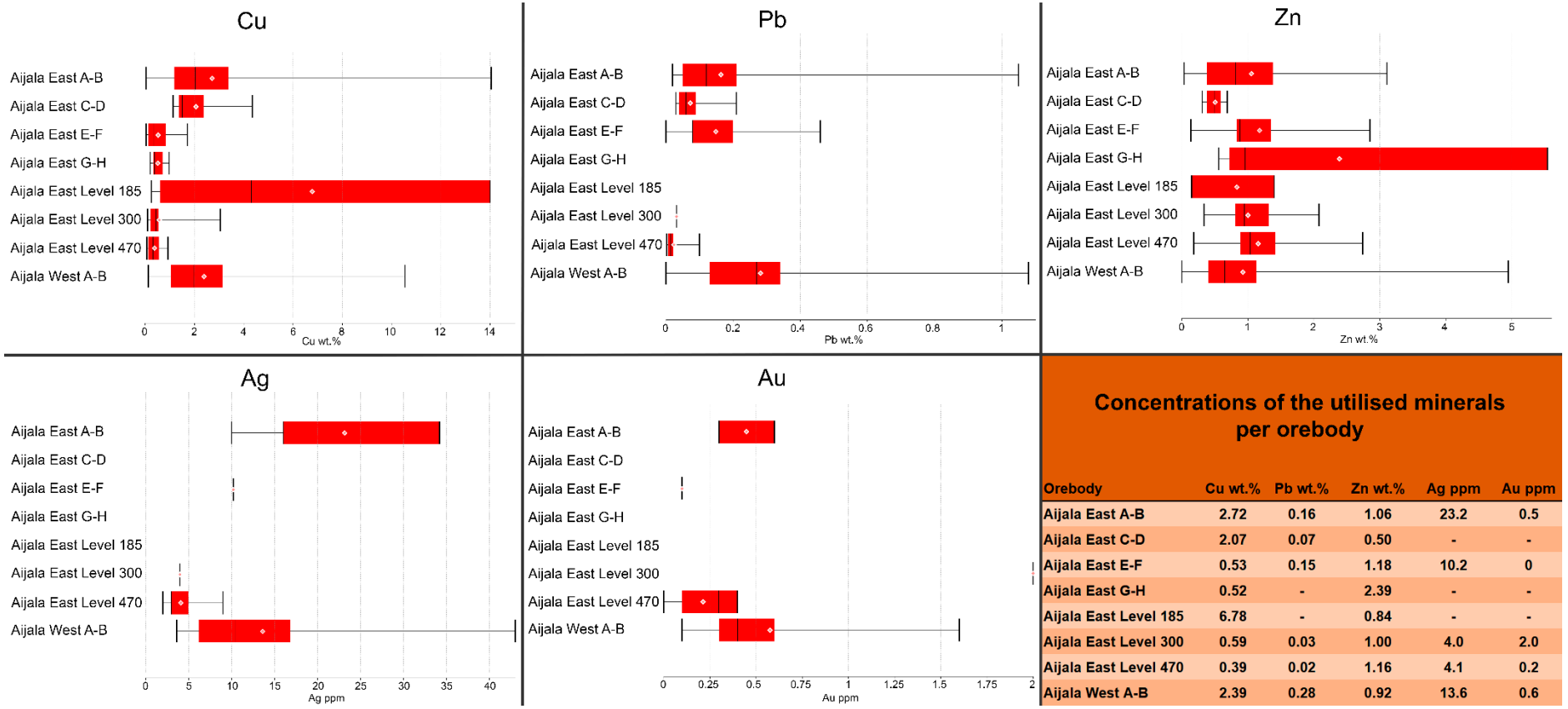

Concentrations of the utilised minerals per orebody

Orebody	Cu wt.%	Pb wt.%	Zn wt.%	Ag ppm	Au ppm
Aijala East A-B	2.72	0.16	1.06	23.2	0.5
Aijala East C-D	2.07	0.07	0.50	-	-
Aijala East E-F	0.53	0.15	1.18	10.2	0
Aijala East G-H	0.52	-	2.39	-	-
Aijala East Level 185	6.78	-	0.84	-	-
Aijala East Level 300	0.59	0.03	1.00	4.0	2.0
Aijala East Level 470	0.39	0.02	1.16	4.1	0.2
Aijala West A-B	2.39	0.28	0.92	13.6	0.6

Figure 17. Average concentration box plots of the selected utilised minerals from ores in Aijala. Aijala East Level 470 was never mined. Aijala East E-F contains two assays of Ag and Au. Aijala East Level 300 contains one assay of Pb, Ag, and Au.

Figures 18 and 19 present the average concentrations of the utilised minerals from the orebodies. The dominant base metal in the main sulphide lenses is Cu except for Aijala East E-F and G-H, where Zn is dominant. Silver and gold have not been analysed from the Aijala East C-D and G-H lenses and Level 185 unit. Silver is most abundant in the largest sulphide lenses West A-B, East A-B, and East E-F. Concentrations of Au are low in Aijala. Only one assay result (Ag and Au) is from Aijala East Level 300.

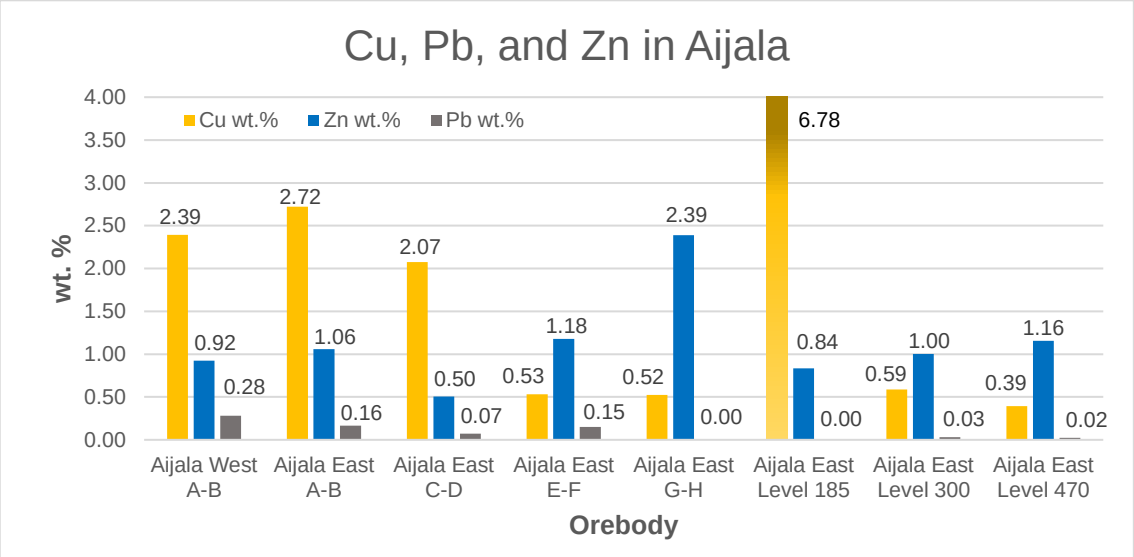

Figure 18. The average base metals concentrations of the Aijala deposit. Aijala East Level 470 is included, although it was not mined. Lead was not analysed from Aijala East G-H and Aijala East Level 185 orebodies.

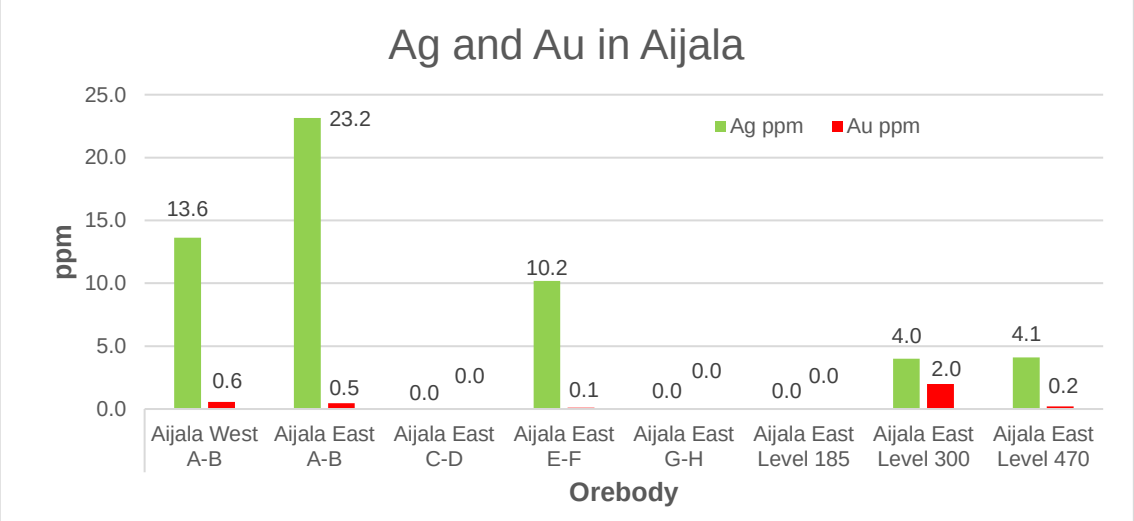

Figure 19. The average precious metals concentrations of the Aijala deposit. Aijala East Level 470 is included, though it was not mined. Silver and gold were not analysed from Aijala East C-D, G-H, and Level 185 orebodies.

6.4. Geological 3D model of Metsämonttu

The Metsämonttu model reaches a depth of -710 metres, includes four faults dipping towards the south, and features the major Metsämonttu-Aijala shear, which continues towards Aijala. The uppermost fault dips 20° towards the south and cuts the orebodies and has displaced the overlying block 270 metres towards the north. The lowermost fault cuts off the bottom edge of the ore lenses. However, the geological model does not continue below the lowermost fault because of the scarcity of drilling data (Fig. 20).

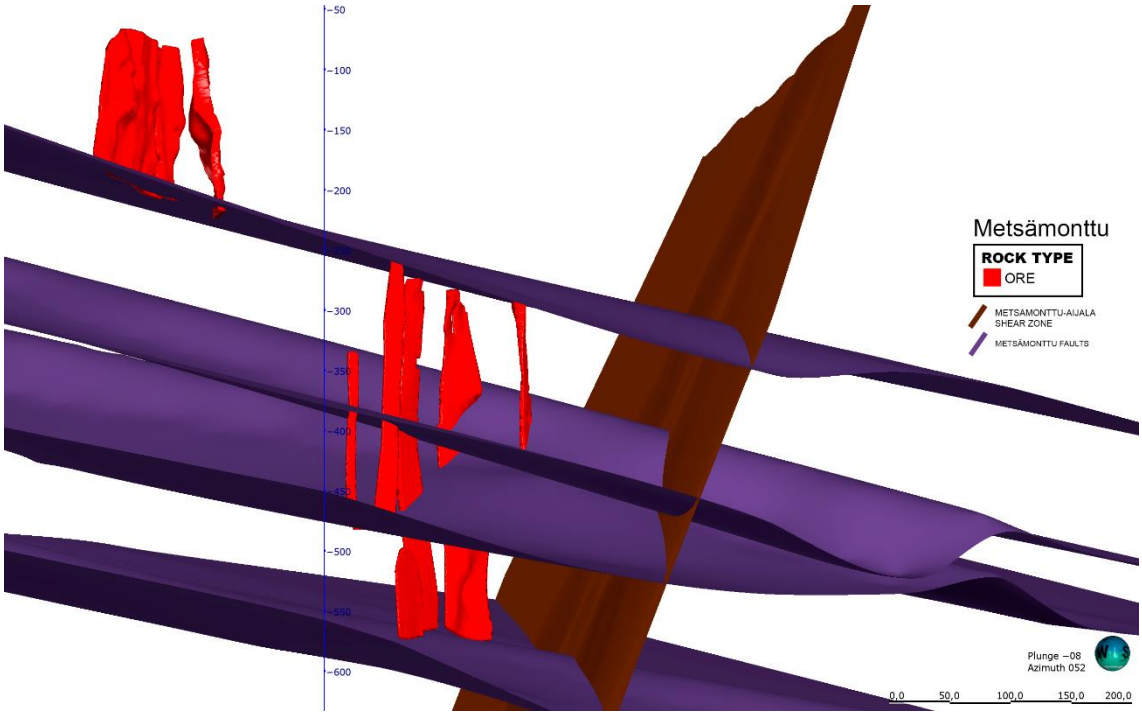

Figure 20. Metsämonttu sulphide orebodies (red) on the north side of the major Metsämonttu-Aijala shear zone (brown). Four Metsämonttu faults (purple), dipping 20° towards the south. Fault at elevation -84 m displace overlying block 300 m towards the north. Mining ended in 1974 at elevation 453 m when traces of ore ran out. Looking towards NE.

Figures 21a and b show the Metsämonttu geological model divided into the footwall quartz-porphyry and the hanging wall amphibolite and has all rocks between them. Skarns and sulphide ores are on the north side of the cordierite schists, inside the footwall, close to the hanging wall amphibolite. The large pegmatite unit is in the lower part of Metsämonttu, and some tiny units are on its west side.

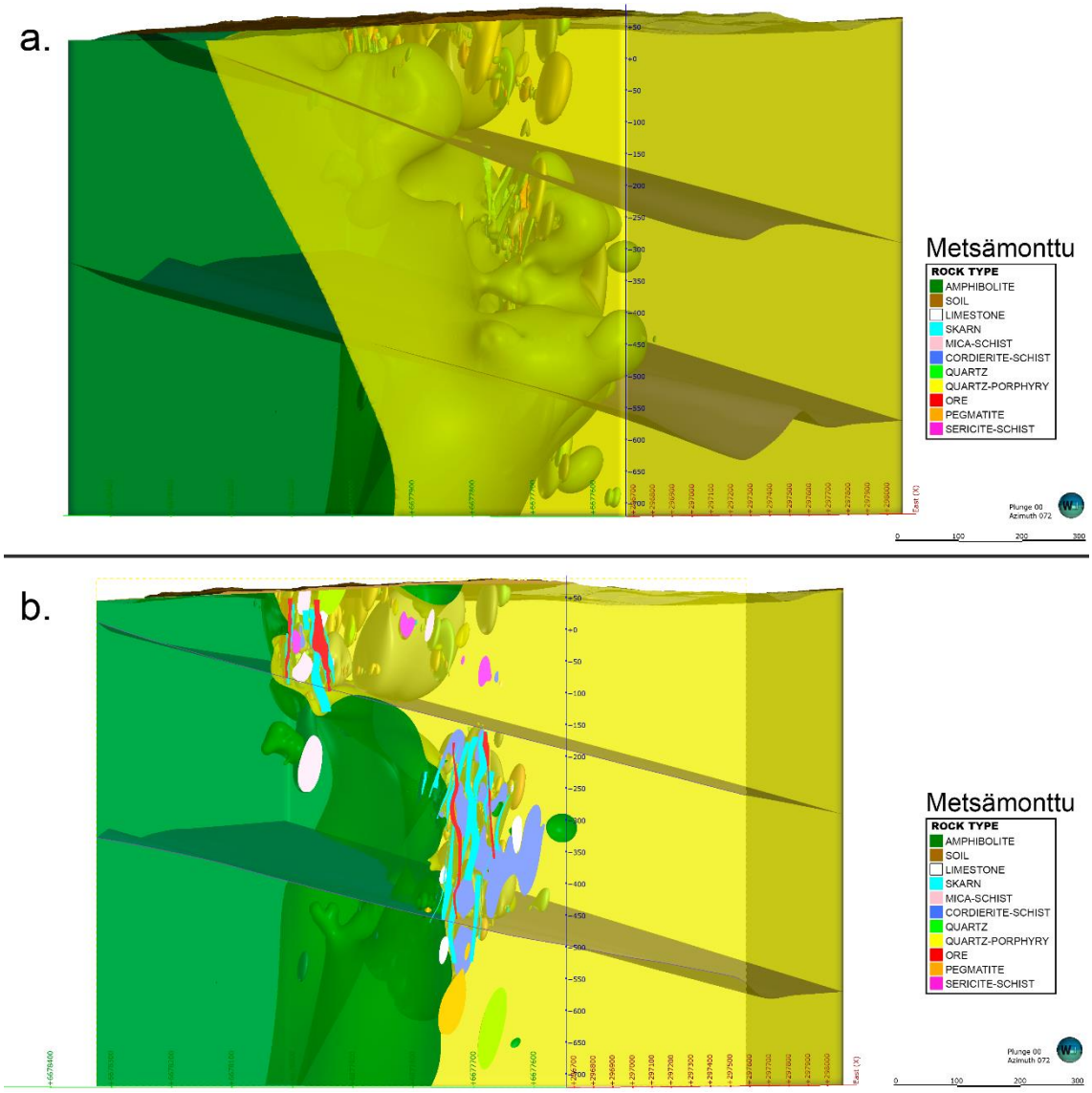

Figure 21. The Metsämonttu model in its entity with the uppermost and lowermost faults. **a.**) All lithologies and overburden are shown. Looking towards ENE. **b.**) Cross-section with all lithologies included. Almost all the lithologies at or near the interface between amphibolite and quartz-porphyry are enclosed by the quartz-porphyry. Looking towards ENE.

Figures 22a and b present sulphide orebodies in Metsämonttu. Sulphide lenses of G-H, I-J, K-L, M-N, and O-P in Uusi Metsämonttu, have been modelled with a few mine tunnel maps and structural cross-sections, and their boundaries based on drafting on the report. The Metsämonttu deposit is divided into the upper and the lower parts. The upper Metsämonttu deposit comprises three large sulphide lenses, and the lower Metsämonttu (Uusi Metsämonttu) unit comprise four large and one smaller sulphide lenses. The distribution of sulphide ores is more concentrated on the north, hanging wall side than skarn veins (Fig. 23a and b).

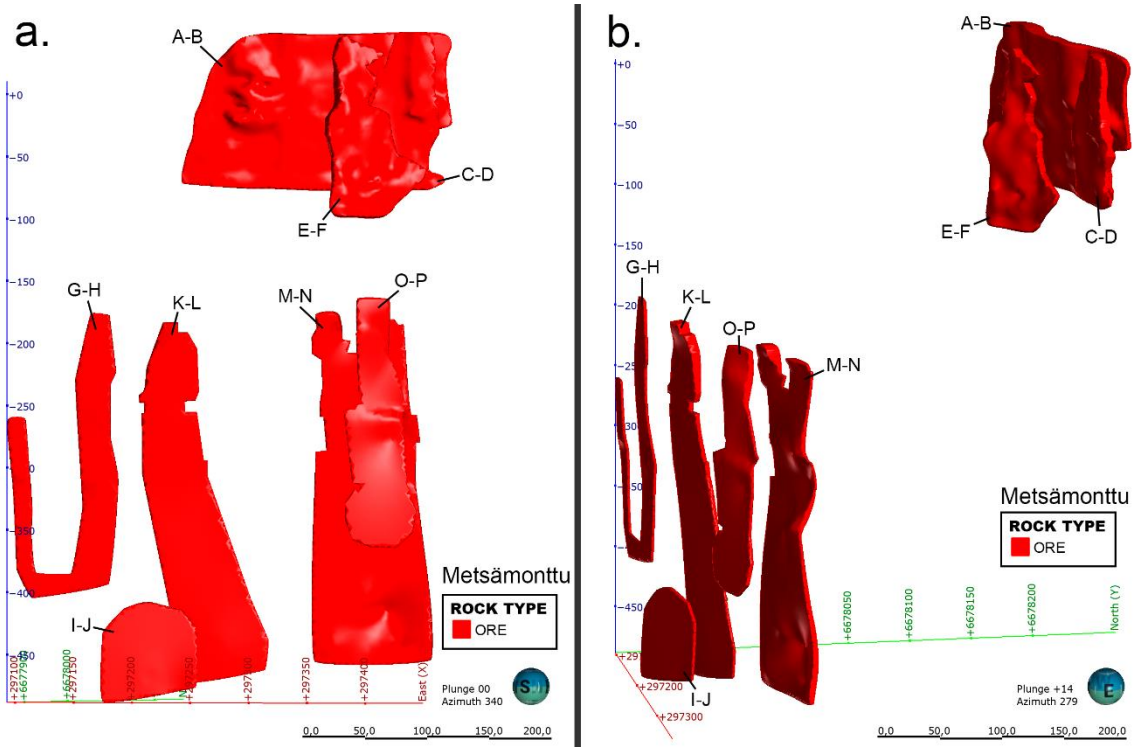

Figure 22. Orebodies A-B, C-D, and E-F are in the upper part of Metsämonttu and were first discovered. Orebodies G-H, I-J, K-L, M-N, and O-P are in the lower part of Metsämonttu, which is also called Uusi Metsämonttu. The names of the orebodies A-B, C-D, and E-F are the names given by Outokumpu Oy. **a.**) Looking towards NNW. **b.**) Looking towards W.

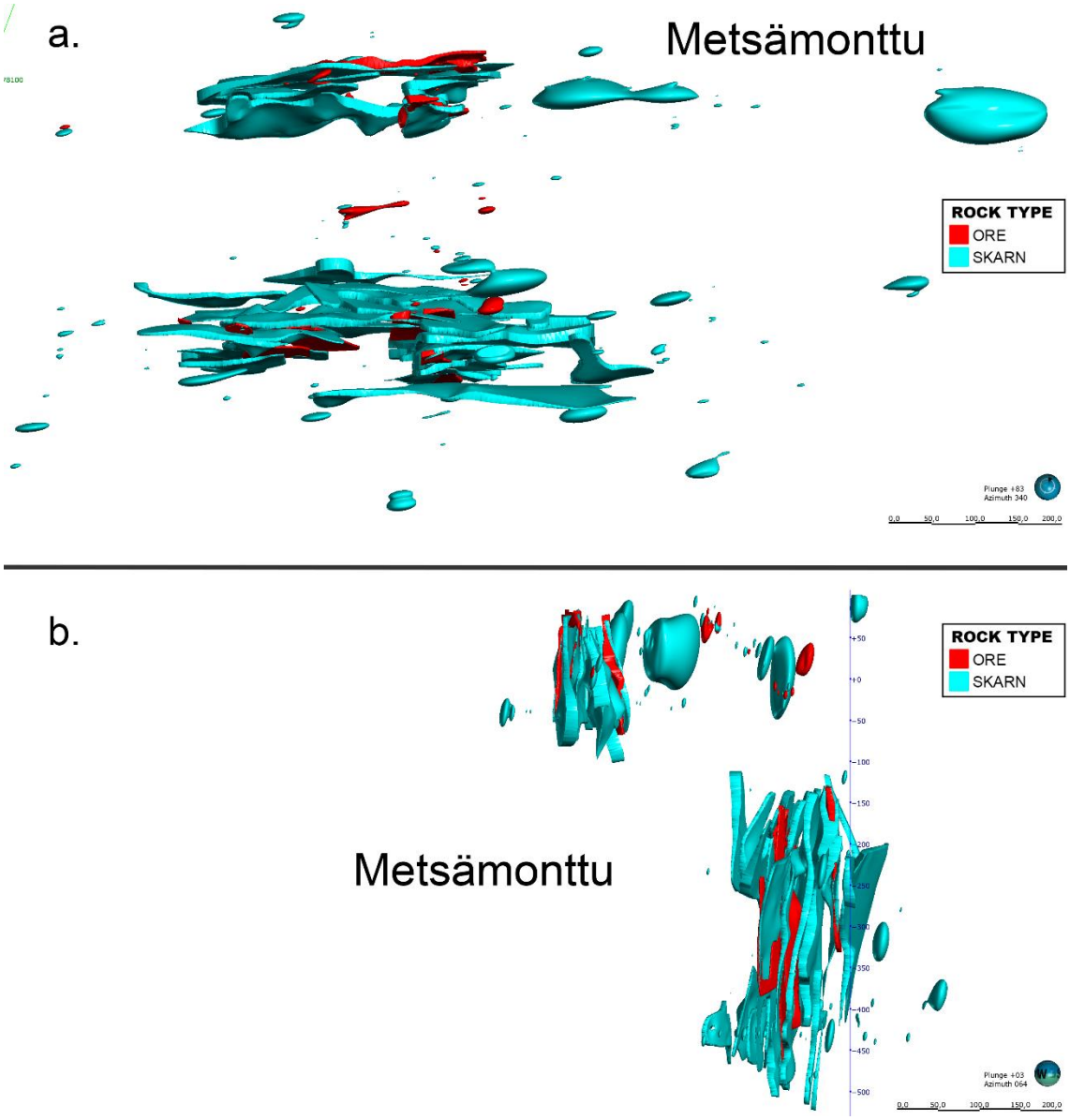

Figure 23. Sulphide ores and skarn in Metsämonttu. **a.**) Looking down and the north is up **b.**) Looking towards ENE.

6.5. Numerical grade models of the Metsämonttu deposit

Numerical models show the distribution and concentrations of base and precious metals. In contrast to Aijala deposit, Cu is minor in Metsämonttu and occurs mainly in the lower part of the deposit (Uusi Metsämonttu M-N sulphide lens). Lead is abundant and occurs in high concentrations. Like in Aijala, Zn has distributed widely and is present throughout every sulphide lens. Silver has distributed well to the eastern end and, to a lesser extent,

to the western end in the upper part of the Metsämonttu deposit (Fig. 24a-b and 25). Gold occurs as distinct domains focused on a particular locale. The highest concentrations of Au are in the lower part of the deposit, with sulphide lenses of Uusi Metsämonttu (Appendix 2).

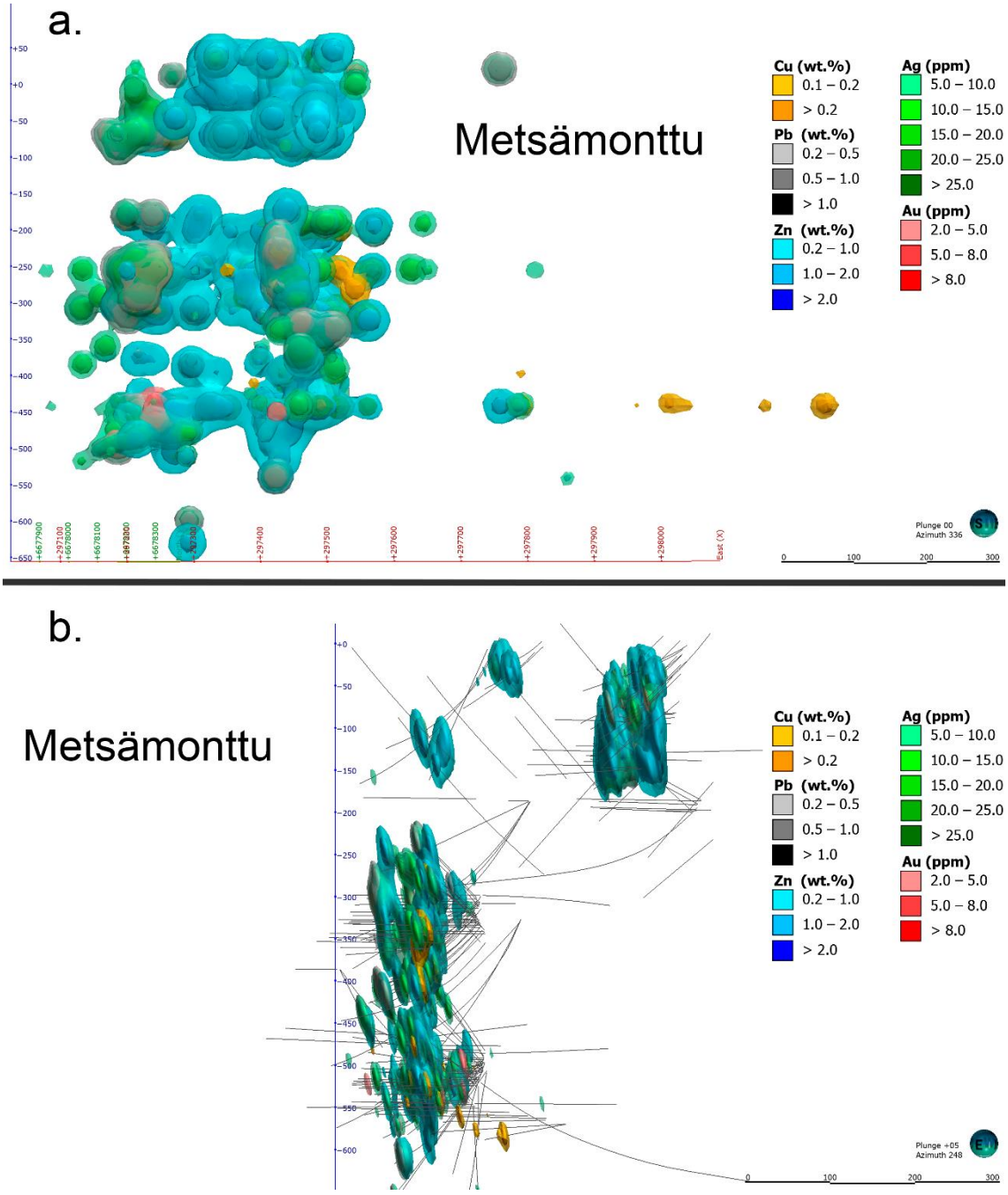

Figure 24. Numerical grade models for the economic metals in the Metsämonttu deposit. **a.**) Looking towards NNW. **b.**) Drill hole traces are in grey. Looking towards WSW.

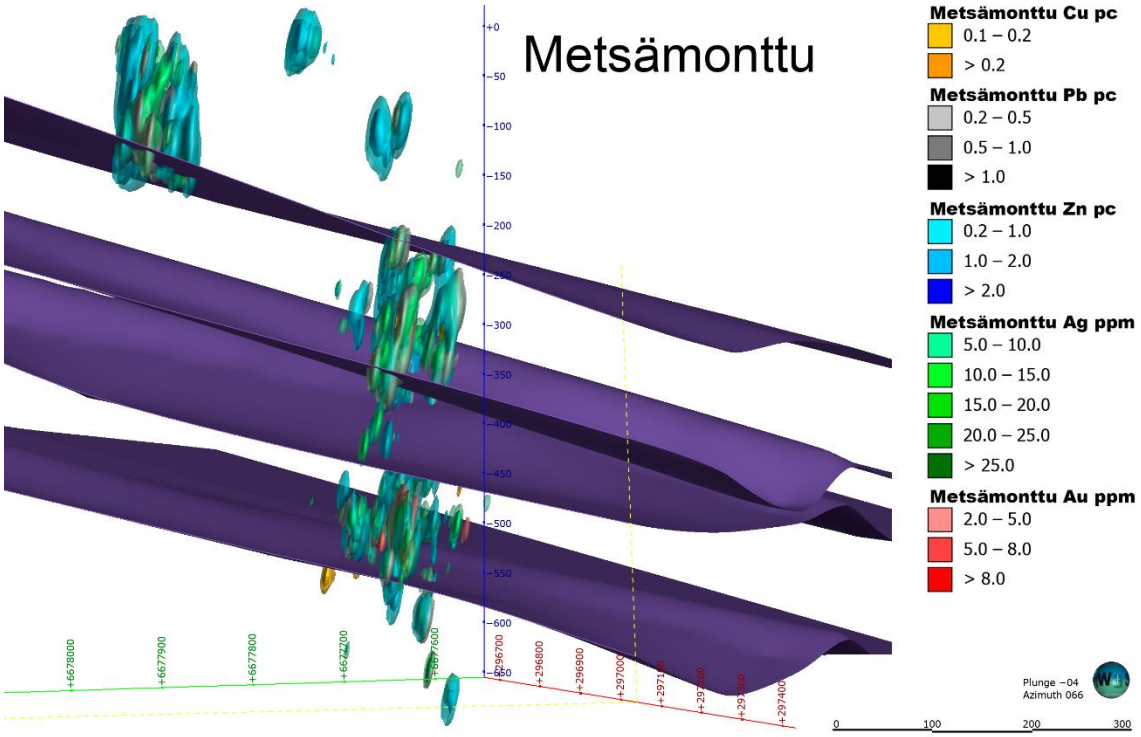

Figure 25. Numerical grade models for the economic metals in the Metsämonttu deposit. The uppermost south-dipping fault has displaced the overlying block 270 m towards the north. Looking towards ENE.

Figure 26 is a cross-section from the west end of the Metsämonttu deposit. Zinc is an evenly distributed predominant base metal and has accumulated distinct high-concentrated pockets. Copper is minor, and it is bounded within Pb presence. Lead occurs as compact ore pockets and has high-concentrated cores. Silver is present in Uusi Metsämonttu's K-L sulphide lens, and the highest content of Ag is in the topmost part, where Pb is present. Gold is abundant in Uusi Metsämonttu's I-J and K-L sulphide lenses and correlates with the emplacement of the Pb ore.

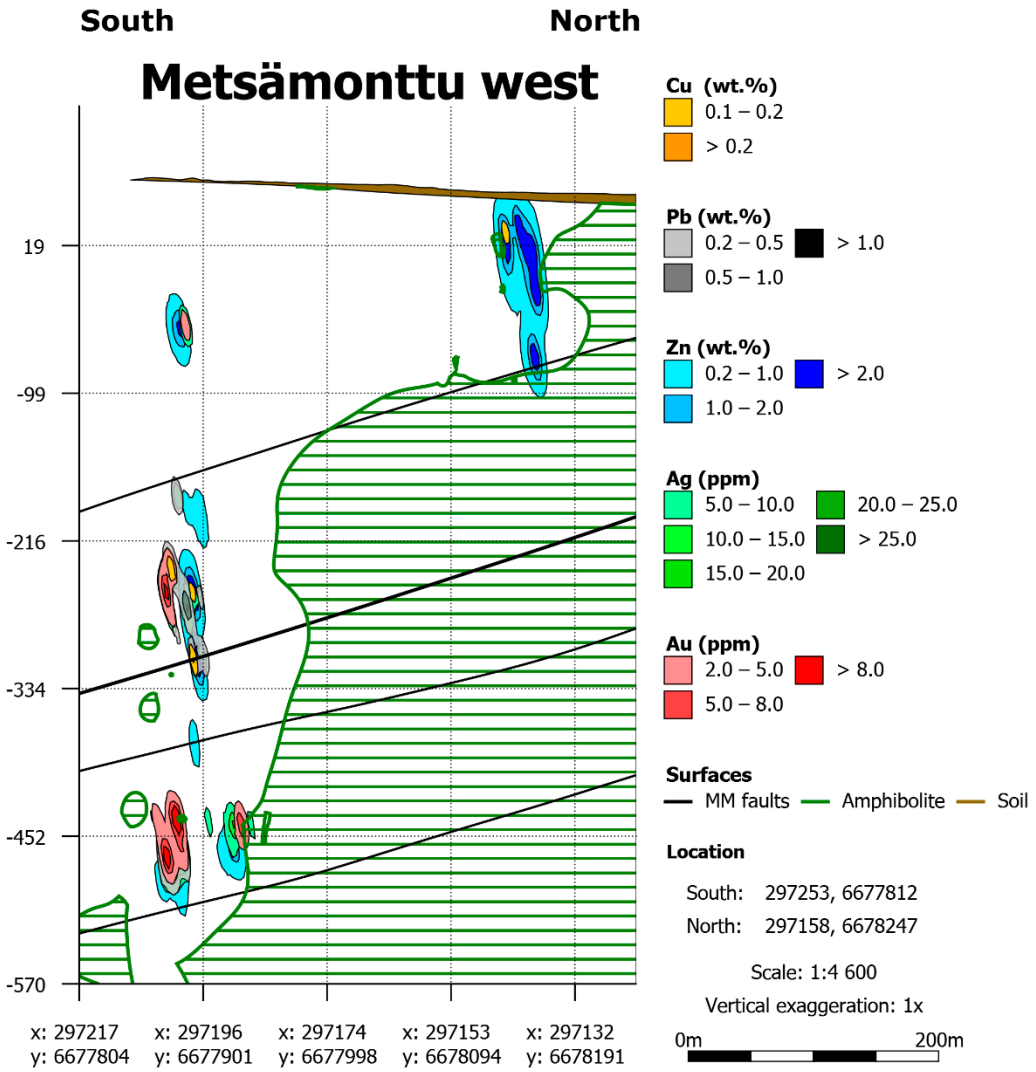

Figure 26. Cross-section from the western end of Metsämonttu. The hanging wall amphibolite is the green hatch, and the four black lines represent south-dipping faults. The numerical grade models do not take into account fault lines. Looking towards the west.

Figure 27 shows the base and precious metals distribution in the east end of the Metsämonttu deposit. Sulphide lens A-B, closer to the hanging wall, consist of primarily Zn ore. The lower part of the M-N sulphide lens has pockets with high-concentrated Ag and Au that correlate with Pb ore emplacement. Sulphide lenses O-P and E-F are most rich in metal minerals. Zinc is most widely distributed and also occurs in compact ore pockets. Minor Cu is bounded to Pb occurrence. Lead occurs as distinct compact high-concentrated ore pockets. Gold and silver follow Pb ore and occur as most rich within Pb ore pockets. Figure 28 present the average concentrations of utilised base and precious metals per ore lithology unit.

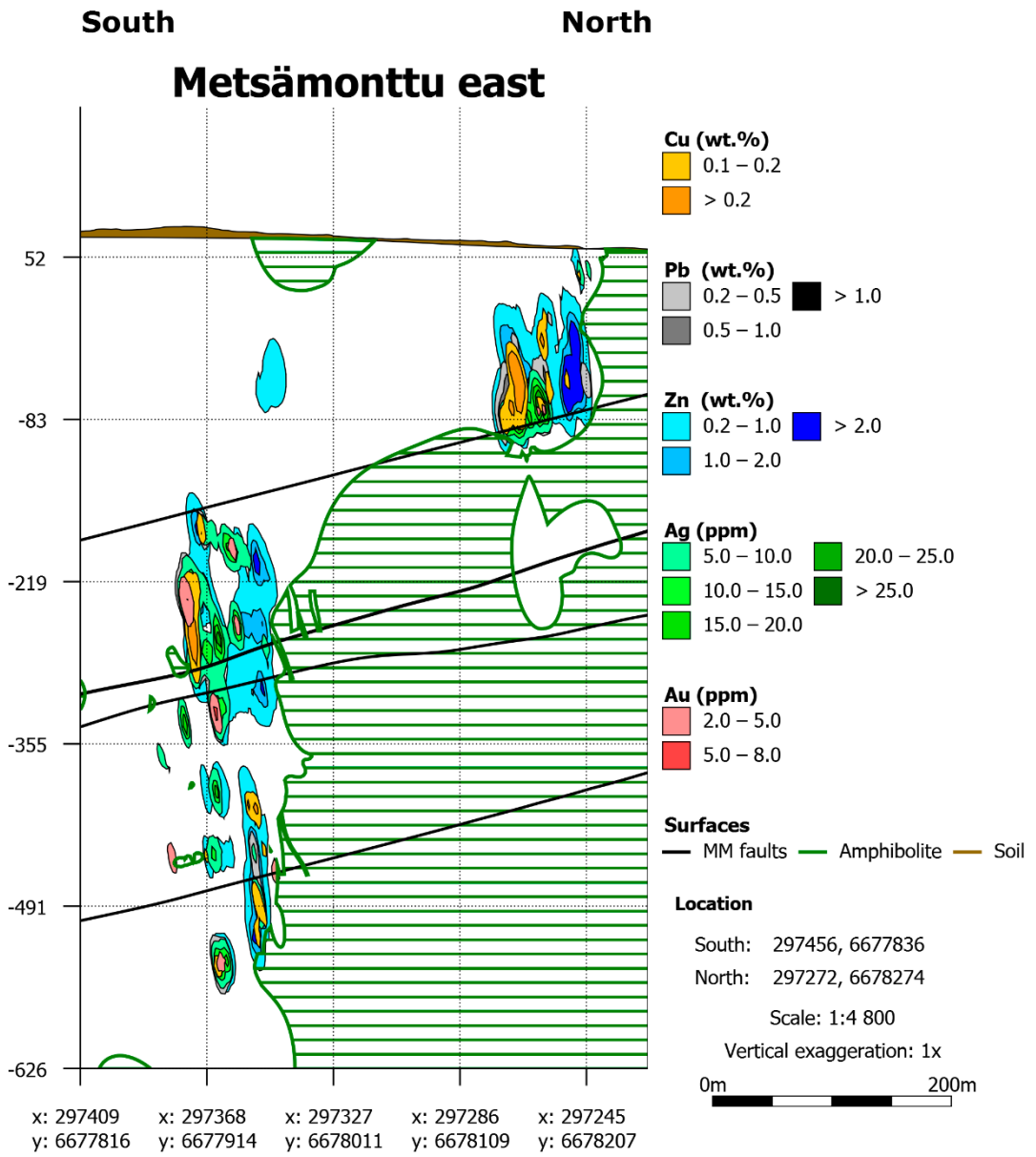

Figure 27. Cross-section from the eastern end of Metsämonttu. The hanging wall amphibolite is shaded by the green lines, and the four black lines represent south-dipping faults. The numerical grade models do not take into account fault lines. Looking towards the west.

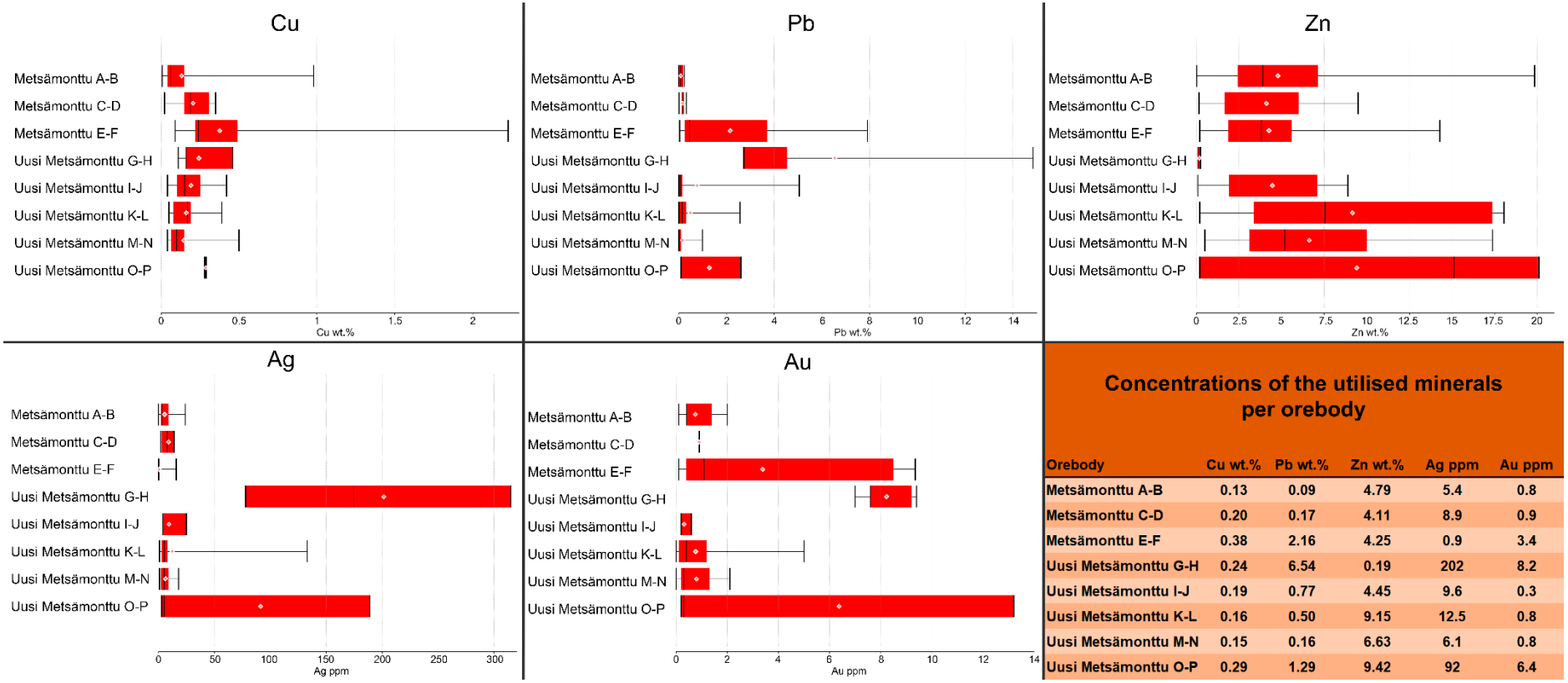

Concentrations of the utilised minerals per orebody

Orebody	Cu wt.%	Pb wt.%	Zn wt.%	Ag ppm	Au ppm
Metsämonttu A-B	0.13	0.09	4.79	5.4	0.8
Metsämonttu C-D	0.20	0.17	4.11	8.9	0.9
Metsämonttu E-F	0.38	2.16	4.25	0.9	3.4
Uusi Metsämonttu G-H	0.24	6.54	0.19	202	8.2
Uusi Metsämonttu I-J	0.19	0.77	4.45	9.6	0.3
Uusi Metsämonttu K-L	0.16	0.50	9.15	12.5	0.8
Uusi Metsämonttu M-N	0.15	0.16	6.63	6.1	0.8
Uusi Metsämonttu O-P	0.29	1.29	9.42	92	6.4

Figure 28. Average concentration box plots of the selected utilised minerals from mined ores in Metsämonttu. Orebody C-D contains one assay of Au.

Figures 29 and 30 show the average concentrations of the utilised minerals from the orebodies. Zinc is the dominant base metal in the Metsämonttu deposit. As an exception, Pb is the dominant metal mineral in the Uusi Metsämonttu G-H sulphide lens. Gold and silver are abundant within the G-H and O-P sulphide lenses.

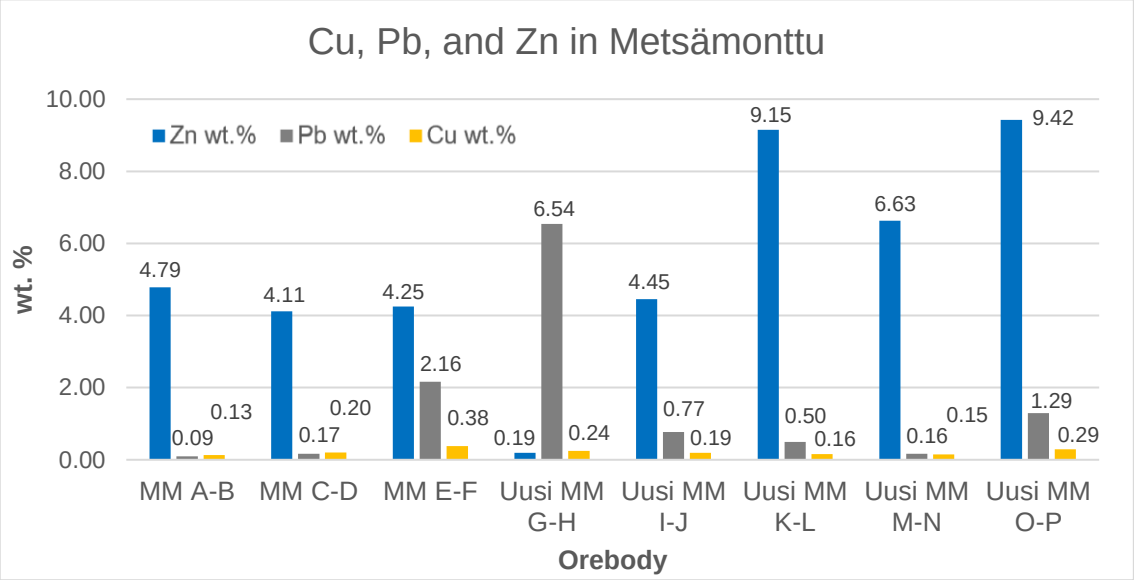

Figure 29. The average base metals concentrations of the Metsämonttu (MM) deposit.

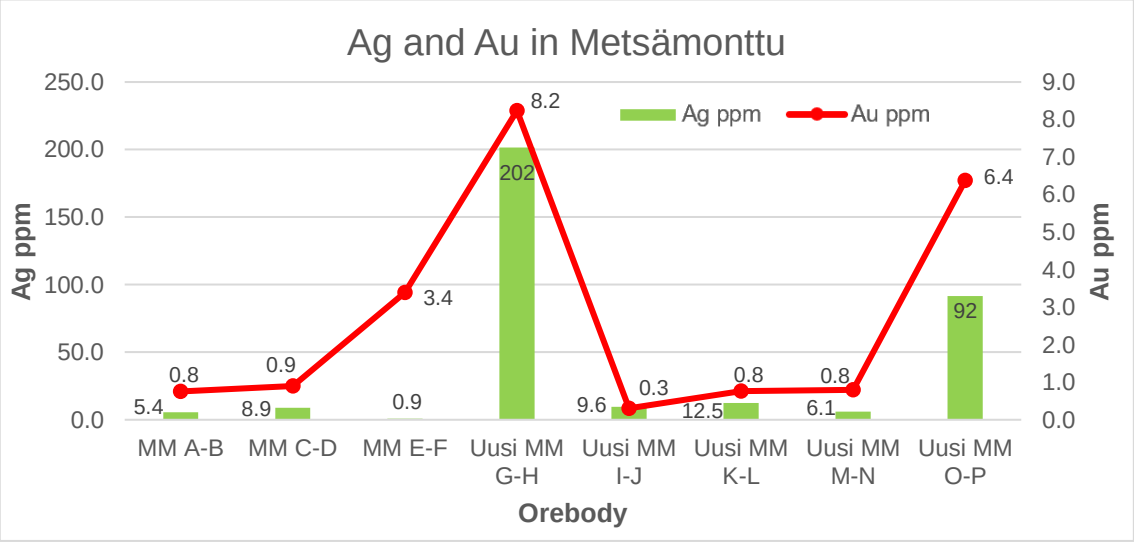

Figure 30. The average precious metals concentrations of the Metsämonttu (MM) deposit.

7. DISCUSSION

In this thesis, the first geological and numerical 3D models of the Aijala and Metsämonttu deposits were compiled. In Aijala and Metsämonttu, sulphide lenses consist of varying amounts of Zn-Pb-Cu and Ag-Au based on numerical grade models. Local faults affect both deposits, and those faults continuity is terminated by the major Metsämonttu-Aijala shear zone.

In the Aijala and Metsämonttu VMS deposits, sulphides occur mainly as disseminations within parallel and lenticular orebodies oriented vertically that are being cut by faults. The host rocks are skarn-carbonate and cordierite-gneiss or other associated schists (Parkkinen 1975a and b). The geological models were compiled using the original 11 lithologies (Table 6) as based on the historical data. Five major parallel sulphide lenses occur within the footwall in the upper parts of the Aijala deposit, and three more minor sulphide accumulation occur in the lower part. The presence of cordierite-schist and sericite-schist are concentrated in the footwall and lower parts in the Aijala deposit.

In the upper Metsämonttu deposit, three major parallel sulphide lenses occur within the footwall and four in the lower part of the deposit. The presence of sericite-schist is concentrated in the footwall and lower part of the deposit, and unlike the Aijala deposit, cordierite-schist occurs throughout the deposit within the footwall.

Sulphide ore lenses and altered rocks all locate between the footwall quartz-porphyry and hanging wall amphibolite. Mica-schist is more common in Aijala than Metsämonttu and occurs on the hanging wall and footwall contacts in both deposits. Sulphide lenses are frequently associated with skarn veins.

7.1. Validation of the Aijala and Metsämonttu models

The geological models were created using materials from 540 drill cores (52,074.00 m), including spatial information, lithologies, and assays. The Aijala geological model of lithologies consists of 266 drill cores (Fig. 31a-b). The Metsämonttu geological model of lithologies consists of 274 drill cores (Fig. 32a-b).

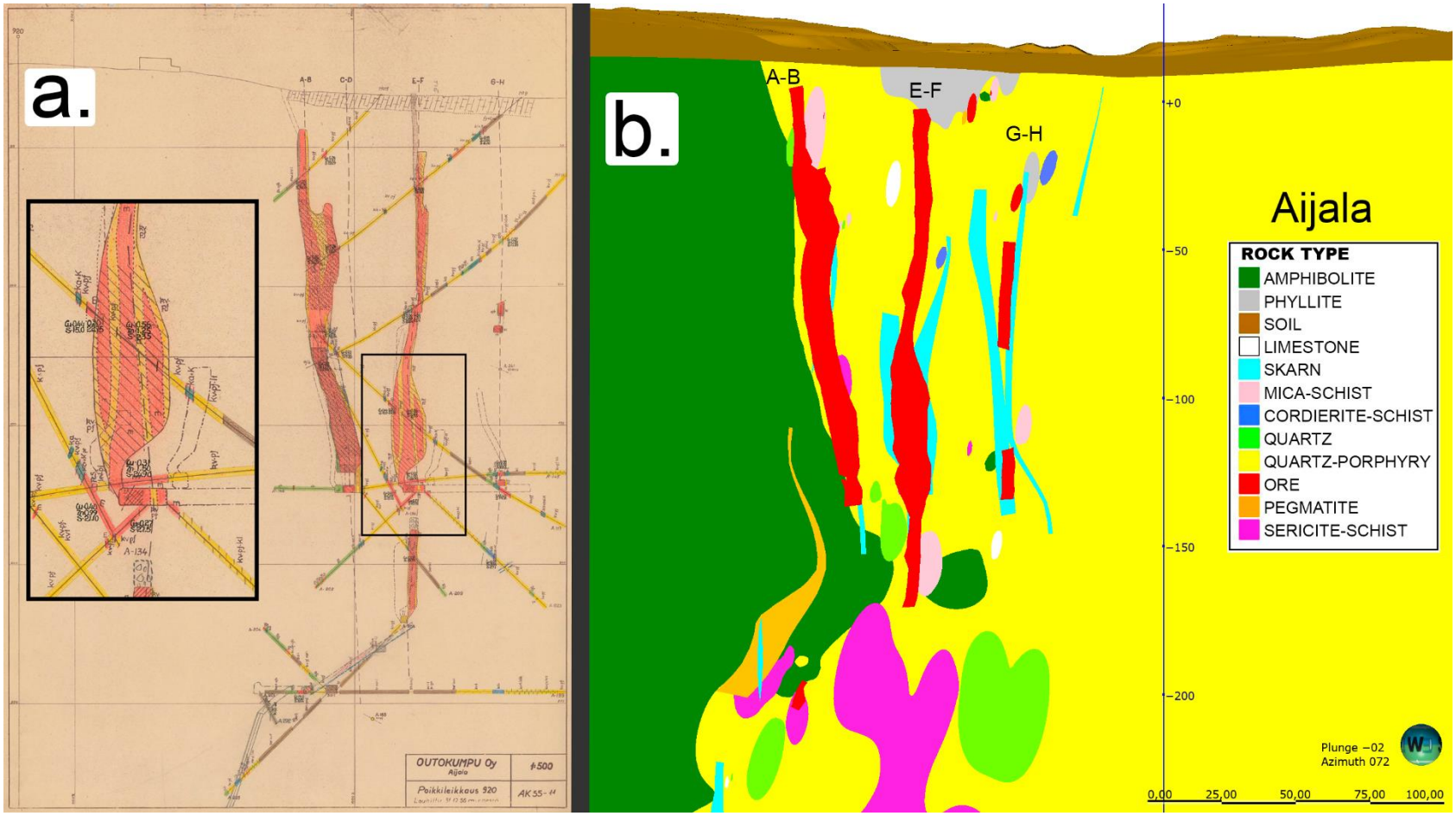

Figure 31. Details of the lithological unit boundaries are not as accurate as in the original historical material when using fRBF with drawn lines for modelling. **a.**) Original 1:500 cross-section of the east part of the Aijala deposit. Y = 10920 (in the local coordinate system). Modified after Outokumpu Oy (1950). **b.**) Cross-section of the Aijala lithological model from the same location as Figure 31a.

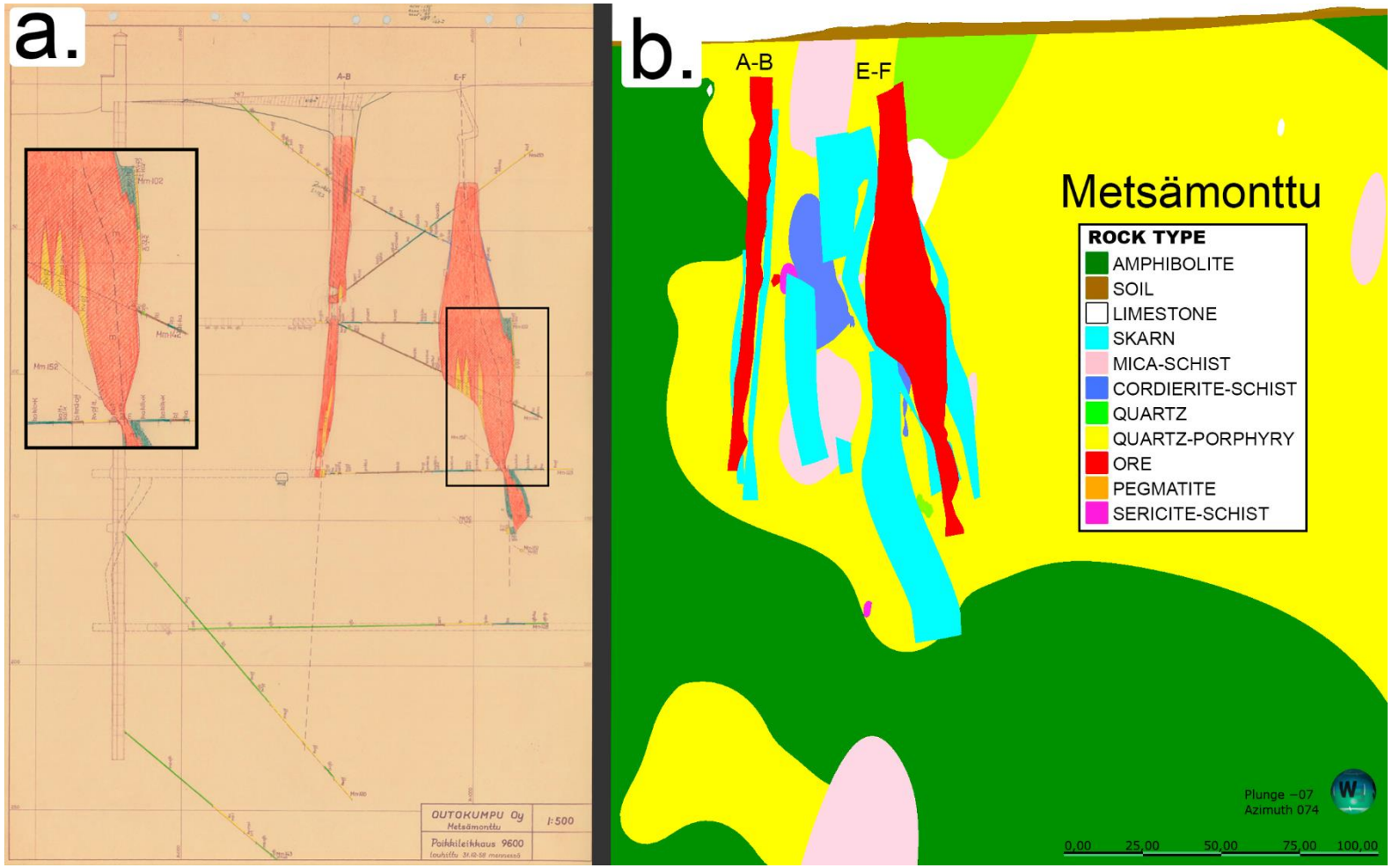

Figure 32. **a.**) Original 1:500 cross-section of the Metsämonttu deposit. Y = 9600 (in the local coordinate system). Modified after Outokumpu Oy (1951). **b.**) Cross-section of the Metsämonttu lithological model from the same location as Figure 32a.

Use of historical materials always causes some uncertainties. The 477 drill holes of 540 drill holes available haves all necessary spatial information (northing, easting, and elevation) (inaccuracy category 1). The 20 drill holes lack one piece of spatial information (inaccuracy category 2), and the 43 drill holes lack two or more spatial information (inaccuracy category 3). In this study, missing spatial information has been recovered from underground working maps, cross-sections or historical reports. The downhole surveys were available for 157 drill holes. For those 383 drill holes that lack survey data, azimuth and dip values, as recorded at the start of the drilling, were used throughout the drill holes.

The surface drill holes were drilled on both sides and perpendicular to sulphide lenses in Aijala and Metsämonttu. In contrast, at Uusi Metsämonttu, sulphide lenses were not drilled from the surface. The underground drill holes are perpendicular to sulphide lenses on the hanging wall side, and the starting angle is 45°, 0° or -45°. The distance between drill holes is 20–40 m. The 3D geological and numerical models are most accurate diagonally, from corner to corner in the middle of the boundary boxes where the drill holes are concentrated.

The hand-drawn mine tunnel maps (61 in total) and cross-sections (47 in total) containing the boundaries of lithologies were used to create geological models (Fig.33). The mine tunnel maps and cross-sections cover the entire Aijala deposit. As a result, the geological model of Aijala deposit is uniformly accurate throughout. In Metsämonttu, the mine tunnel maps and cross-sections cover the upper part of the deposit. A few mine tunnel maps and cross-sections cover the lower part of Metsämonttu. Aijala and the upper part of the geological model of the Metsämonttu and are most accurate. The lower part of the geological model of Metsämonttu (Uusi Metsämonttu) is based on the drill core data mainly and is not as accurate as of the models of Aijala or upper Metsämonttu. In addition, cross-sections containing structural information (11 in total) were used to modelling major shear and faults. Ellipsoid ratios of all the lithological units created using intrusion tool, were set to 3,3,1 for correspond to the historical material.

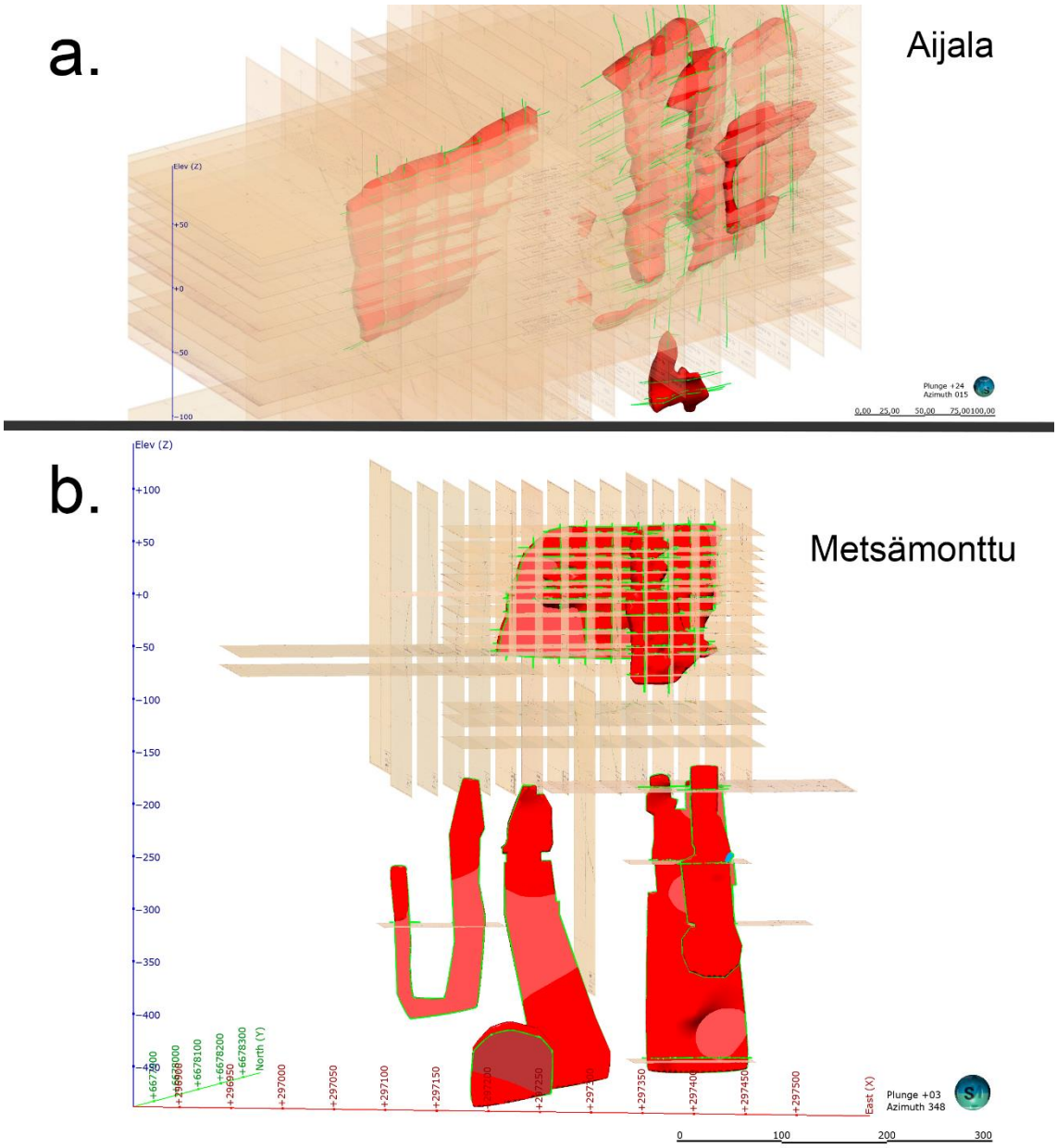

Figure 33. Cross-sections, mine level maps, orebodies (red), and drawn lines (green) of orebodies in the Aijala (**a.**) and Metsämonttu (**b.**) models. Aijala and upper part of Metsämonttu models are well covered with mine level maps and cross-section. The lower part of Metsämonttu (Uusi Metsämonttu) is covered with a few mine level maps that makes it less accurate than Aijala or upper Metsämonttu models. The outer boundaries of ore lenses in lower part of the Metsämonttu mine were drawn based on the sketch images found in the report of Heiskanen and Stenberg (1971) and Warma (1975).

7.2. Distribution of the sulphides

Numerical models were created using a fRBF interpolant. An fRBF interpolation presents continuous numeric models with varying grade distributions. The numerical data of the selected metals had to be processed before interpolation in order to obtain regularly-

spaced data from the unevenly-spaced raw data (Seequent Limited 2021), and this was done by creating numeric composites. The mean length of samples is 2.435 in Aijala and 2.708 m in Metsämonttu, and they were set as default. In addition, it was set, if the residual end length is less than 1.218 in Aijala and 1.354 m in Metsämonttu, they are evenly distributed. The numerical grade models of base and precious metals present the distribution without lithological and structural constraints based on RFB interpolation.

Grades and distribution of the possible ore extensions of both deposits are unclear in the deeper parts based on the historical drillings. Mining was ended because ore depletion and few drillings did not clarify the matter. Precious metals and Pb-Zn ore in Aijala and Cu ore in Metsämonttu in high concentrations are absent.

7.2.1. Aijala Cu-Zn sulphides

The Aijala deposit is rich in Cu and Zn sulphides and has traces of Pb sulphides (Fig. 17, 18, and 19). The presence of Cu ore pockets follows the hanging wall and footwall contacts. Cu-Zn rich sulphide lens is situated within the footwall quartz-feldspar-porphyry, close to the hanging wall amphibolite in the West Aijala. In the East Aijala, Cu rich sulphide lenses with Cu ore pockets are close to the hanging wall, and sulphide lenses mainly composed of Zn ore are situated more to the south. Minor Pb accumulations occur mainly in the upper parts of the deposit with the Zn ore (Appendix 1). According to Parkkinen (1975b), chalcopyrite remobilised and concentrated in pockets during the early stages of shear movements.

The north-dipping fault at an elevation of -253 m displaced the overlying block 80 m towards the south. The four drill cores from the deepest mine tunnel in the East Aijala at an elevation -335 m reach an elevation -516 m and indicate the continuation of the deposit below the lowermost fault at an elevation -423 m (Fig. 9). However, concentrations of Cu (0.39 wt.%), Zn (1.16 wt.%), Ag (4.1 ppm), and Au (0.2 ppm) remain rather low (Fig. 17).

7.2.2. Metsämonttu Zn-Pb-Cu sulphides

The Metsämonttu deposit has higher grades of Zn and Pb (as compared to Aijala) but is lower in Cu (Fig. 28, 29, and 30). The sulphide lenses are located within the footwall, near the contact of the hanging wall amphibole and the footwall quartz-porphyry. The orebodies in the western end of the Metsämonttu deposit are small in size and are located further to the south from the contact of amphibolite and quartz-porphyry than the orebodies in the eastern end of the deposit (Appendix 2). The composition and the location of the sulphide lenses indicate that O-P orebody in the lower Metsämonttu is a continuation to E-F orebody in the upper Metsämonttu, and M-N orebody is a continuation to A-B and C-D orebodies (Fig. 22 and 28). According to Parkkinen (1975a), Cu-Zn-bearing iron sulphides represent the first generation of sulphides deposited, while the younger complex Pb ore, locally associated with iron sulphides, deposited later.

Four parallel south-dipping faults were identified in the Metsämonttu. Two of them are important; the uppermost and the lowermost. The uppermost fault displaced the overlying block 270 m towards the north (Fig. 20 and 21a-b). The displacement of the overlying block of the lowermost fault is 80 metres (Latvalahti 1979). The two faults in between have not displaced blocks to a significant extent.

7.3. Distribution of precious metals in Aijala and Metsämonttu deposits

The distribution of precious metals within the Aijala and Metsämonttu deposits has not been studied in detail before (Huhma and Latvalahti 1975; Parkkinen 1975a, b; Latvalahti 1979; Mäkelä 1989). Precious metals are present in both deposits, although they have higher grades in the Metsämonttu deposit (Table 8; Fig. 17 and 28).

In the upper parts of the Aijala deposit, trace amounts of precious metals occur mainly within Zn and Cu ores. In the lower parts of the deposit, where drill core data is limited, precious metals are associated with sulphides (Fig. 13 and 14a-b; Appendix 1). Continuity of precious metals deeper in Aijala is one possibility that needs to be considered based on the models. Some gold has been analysed at a depth of -500 m in Aijala East: 13.4 ppm/1.05 m Au, 8.1 ppm/1.1 m Au, 7 ppm/0.75 m Au, 5 ppm/1.12 m Au, 2 ppm/3.15 m Au, 2 ppm/2.1 m Au, and 2 ppm/1.2 m Au.

Within the Metsämonttu deposit, precious metals are abundant in the western end and concentrations increase deeper, where Pb ore dominates. Ag-mineralised zones tend to be wider than the Au-mineralised zones, and the occurrences of both are highlighted on the south side of the mineralised zones (Fig. 24a-b). However, the distribution of precious metals is associated with the distribution of base metals (Appendix 2). According to Parkkinen (1975a), concentrations of S-Cu-Zn-Pb-Ag depend on the host rock; skarn rock and cordierite-gneiss have the highest Ag and Pb concentrations. According to Latvalahti (1979) cordierite-gneiss and sericite-schist are more abundant in the lower parts of the Metsämonttu deposit than in the upper parts.

7.4. Further research

Dynamic updates can be performed for geological 3D models using an additional data set (Seequent Limited 2021). Data can be historical or new. Uusi Metsämonttu is poorly covered with mine level maps and has only structural cross-sections, unlike upper Metsämonttu and Aijala that are well covered. Therefore, it would be useful to find out if more material of Uusi Metsämonttu has been stored in Outokumpu Oy archives. Using additional material would make the 3D geological model of Metsämonttu more detailed.

8. CONCLUSIONS

1. By creating a 3D model using implicit modelling on historical material, the results can be interpreted in a 3D environment. However, model accuracy depends on how detailed the data is recorded and does it cover the area under study evenly. Also, the human factor is present in the hand-drawn maps and digitising process. Aijala and the upper part of Metsämonttu can be considered good reproductions of the deposit models in a 3D environment. Uusi Metsämonttu is poorly covered by mine level maps and cross-sections compared to the upper Metsämonttu or Aijala, which makes it unreliable.

2. Element concentrations can be obtained per lithological unit due to numerical grade models and solids combined. The location and composition of sulphide lenses indicate that orebody M-N in the lower Metsämonttu is a continuation to

A-B and C-D orebodies in the upper Metsämonttu and orebody O-P in the lower Metsämonttu is a continuation to E-F orebody in the upper Metsämonttu.

3. The deposits differ in their metal assemblages. The Aijala deposit is Cu-rich. In contrast, the Metsämonttu deposit is Zn-Pb-rich, such Zn-Pb ores have not been encountered in the Aijala area.

4. Precious metals occur in both deposits associated with base metals and mostly on the sulphide lenses within the footwall. The Metsämonttu deposit has higher concentrations of precious metals than the Aijala deposit, and concentrations increase from east to west and deeper in Metsämonttu.

9. ACKNOWLEDGMENTS

I would like to thank the Geological Survey of Finland for providing the historical material and my supervisors Petri Peltonen and Janne Hokka for their guidance in this thesis. I would also thank Jonathan Pownall for his review and suggestions for improvement. I want to thank Konsta Kuorikoski, Jukka Kaunismäki and Juha Vuohelainen who helped digitise the historical material.

10. REFERENCES

Barrie, C.T. and Hannington, M.D. 1999. Introduction: Classification of VMS deposits based on host rock composition. In: Barrie, C.T. and Hannington, M.D. (Eds) Volcanic-Associated Massive Sulfide Deposits: Processes and Examples in Modern and Ancient Settings: Reviews. (8), 13–51.

Blengini, G.A., Latunussa, C.E., Eynard, U., de Matos, C.T., Wittmer, D., Georgitzikis, K., Pavel, C., Carrara, S., Mancini, L., Unguru, M., Mathieux, F., Pennington, D., Huisman, J., Bobba, S., Blagoeva, D., Dondi, M., Barakos, G., Krueger, M.-., Le Gleuher, M., Komnitsas, K., Rietveld, E., Lundhaug, M., Muller, D., Fernanda, M., Dewulf, J., Ciacci, L., Auberger, A., Dittrich, M., Planchon, M. and Devauze, C. 2020. European Commission, Study on the EU's list of Critical Raw Materials – Final Report (2020). European Commission, Luxembourg, 155 pp.

Bucher, K. and Grapes, R. 2011. Petrogenesis of Metamorphic Rocks. 8. edition. Springer-Verlag, Berlin Heidelberg, 257–292.

Colley, H. and Westra, L. 1987. The Volcano-Tectonic Setting and Mineralization of the Early Proterozoic Kemiö-Orijärvi-Lohja Belt, SW Finland. Geological Society, London, Special Publications 33, 95–107.

Ehlers, C., Lindroos, A. and Selonen, O. 1993. The late Svecofennian granite-migmatite zone of southern Finland—a belt of transpressive deformation and granite emplacement. Precambrian Research, 64 (1), 295–309.

Eilu, P., Ahtola, T., Äikäs, O., Halkoaho, T., Heikura, P., Hulkki, H., Iljina, M., Juopperi, H., Karinen, T., Kärkkäinen, N., Konnunaho, A., Kontinen, A., Kontoniemi, O., Korkiakoski, E., Korsakova, M., Kuivasaari, T., Kyläkoski, M., Makkonen, H., Niiranen, T. and Västi, K. 2012. Metallogenic areas in Finland. Geological Survey of Finland, Special Paper, 53, 207–342.

Eskola, P. 1914. On the petrology of the Orijärvi region in southwestern Finland. PhD thesis, Bulletin de la Commission Geológique de Finlande 40, 277 pp.

Eynard, A., Georgitzikis, K., Wittmer, D., EL Latunussa, C., Torres de Matos, C., Mancini, L., Unguru, M., Blagoeva, D., Bobba, S., Pavel, C., Carrara, S., Mathieux, F., Pennington, D. and Blengini, G.A. 2020. European Commission, Study on the EU's list of Critical Raw Materials (2020), Factsheets on Non-critical Raw Materials. European Commission, 595 pp.

Franklin, J.M. 1996. Volcanic-associated massive sulphide base metals. In: Eckstrand, O.R., Sinclair, W.D. and Thorpe, R.I. (Eds) Geology of Canadian Mineral Deposit Types. Geological Survey of Canada. Geology of Canada, no. 8, 158–183.

Franklin, J.M., Gibson, H.L., Jonasson, I.R. and Galley, A.G. 2005. Volcanogenic Massive Sulfide Deposits. In: Hedenquist, J.W., Thompson, J.F.H., Goldfarb, R.J. and Richards, J.P. (Eds) One Hundredth Anniversary Volume. Society of Economic Geologists, Littleton, 523–560.

Galley, A.G., Hannington, M.D. and Jonasson, I.R. 2007. Volcanogenic massive sulphide deposits, in mineral deposits of Canada: A synthesis of major deposit types. Earth Sciences Sector, 141–162.

Geological Survey of Finland. 2019a. Aijala Mineral Deposit Report. Geological Survey of Finland, 21 pp.

Geological Survey of Finland. 2019b. Metsämonttu Mineral Deposit Report. Geological Survey of Finland, 20 pp.

Geological Survey of Finland. 2021. Spatial data products. Webpage visited 16.4.2021. https://hakku.gtk.fi/en/locations/search

Hannington, M.D. 2014. 13.18 - Volcanogenic Massive Sulfide Deposits. In: Holland, H.D. and Turekian, K.K. (Eds) Treatise on Geochemistry (Second Edition). Elsevier, Oxford, 463–488.

Heiskanen, R. and Stenberg, A. 1971. Outokumpu Oy Aijalan kaivos. Outokumpu Oy, 27 pp.

Huhma, M. and Latvalahti, U. 1975. Uuden Metsämontun jatkotutkimukset 1974. Geological Survey of Finland, 23 pp.

Korja, A., Lahtinen, R. and Nironen, M. 2006. The Svecofennian orogen: A collage of microcontinents and island arcs. Geological Society, London, Memoirs, 32, 561–578.

Kuorikoski, K. 2019. Aijala-Metsämontun kaivoskoordinaatiston muunnos EUREF-FIN-koordinaatistoon. Geological Survey of Finland. Internal report, 9 pp.

Lahtinen, R., Korja, A. and Nironen, M. 2005. Chapter 11 Paleoproterozoic tectonic evolution. In: Lehtinen, M., Nurmi, P.A. and Rämö, O.T. (Eds) Precambrian Geology of Finland – Key to the Evolution of the Fennoscandian Shield. Elsevier B.V., Amsterdam, 481–531.

Lahtinen, R., Korja, A., Nironen, M. and Heikkinen, P. 2009. Palaeoproterozoic accretionary processes in Fennoscandia. Geological Society, London, Special Publications, 318, 237–256.

Large, R.R. 1992. Australian volcanic-hosted massive sulfide deposits; features, styles, and genetic models. Economic Geology, 87 (3), 471–510.

Latvalahti, U. 1979. Cu-Zn-Pb Ores in the Aijala-Orijarvi Area, Southwest Finland. Economic Geology, 74, 1035–1059.

Leväniemi, H., Hokka, J., Hulkki, H., Huovinen, I., Karjalainen, J., Kaunismäki, J., Kuikka, J., Sandström, J., Stenberg, R. and Vuohelainen, J. 2020. Tiedonkeruukäytännöt Aijala-Metsämonttu - projektin kairasydänmittauksissa 2019-2020. Geological Survey of Finland, Espoo, 60 pp.

Mäkelä, U. 1989. Geological and Geochemical Environments of Precambrian Sulphide Deposits in Southwestern Finland. PhD thesis, Geological Survey of Finland, Espoo, 102 pp.

National Land Survey of Finland. 2021. File Service of Open Data. Webpage visited 9.4.2021. https://tiedostopalvelu.maanmittauslaitos.fi/tp/kartta?lang=en

Outokumpu Oy. 1950. Aijala Poikkileikkaus 920 1:500. Geological Survey of Finland. Not published.

Outokumpu Oy. 1951. Metsämonttu Poikkileikkaus 9600 1:500. Geological Survey of Finland. Not published.

Outokumpu Oy. 1957. Aijala itä taso +175 m, 1:500. Geological Survey of Finland. Not published.

Outokumpu Oy. 1975. Malminetsintä. Kaivosoikeudesta luopuminen. In the archives of the Geological Survey of Finland, 10 pp.

Parkkinen, J. 1974a. Metsämontun puhkeaman pintakartoitus 16.4.74. In the archives of the Geological Survey of Finland, 16 pp.

Parkkinen, J. 1974b. Muodostumaryhmien analyysi ja lyijy-sinkkimalmit. Outokumpu Oy, 17 pp.

Parkkinen, J. 1974c. Raportti vierailusta Aijalassa 12.2.74. In the archives of the Geological Survey of Finland, 31 pp.

Parkkinen, J. 1975a. Aijala Rakennegeologinen ja malmipetrografinen tutkimus. Outokumpu Oy, 28 pp.

Parkkinen, J. 1975b. Uusi Metsämonttu Rakennegeologinen ja malmipetrografinen tutkimus. Outokumpu Oy, 61 pp.

Ploegsma, M. and Westra, L. 1990. The Early Proterozoic Orijärvi triangle (southwest Finland): a key area on the tectonic evolution of the Svecofennides. Precambrian Research, 47 (1), 51–69.

Puustinen, K. 2003. Suomen kaivosteollisuus ja mineraalisten raaka-aineiden tuotanto vuosina 1530–2001, historiallinen katsaus erityisesti tuotantolukujen valossa. Geologian tutkimuskeskus, arkistoraportti M10.1/2003/3, 578 pp.

Rasilainen, K., Eilu, P., Halkoaho, T., Karvinen, A., Kontinen, A., Kousa, J., Lauri, L., Luukas, J., Niiranen, T., Nikander, J., Sipilä, P., Sorjonen-Ward, P., Tiainen, M., Törmänen, T. and Västi, K. 2014. Quantitative assessment of undiscovered resources in volcanogenic massive sulphide deposits, porphyry copper deposits and Outokumpu-type deposits in Finland. Geological Survey of Finland, Report of Investigation 208, Espoo, 60 pp.

Seequent Limited. 2021. User Manual for Leapfrog Geo Version 6.0. Webpage visited 12.3.2021. https://help.seequent.com/Geo/6.0/en-GB/LeapfrogGeoUserManual.pdf

Simonen, A. 1980. The Precambrian in Finland. Geological Survey of Finland, Bulletin 269, 58 pp.

Singer, D.A. 1995. World class base and precious metal deposits; a quantitative analysis. Economic Geology, 90, 88–104.

Skyttä, P. 2007. Svecofennian crustal evolution in the Uusimaa Belt area, SW Finland. PhD thesis, Geological Survey of Finland, Espoo, 17 pp.

Skyttä, P. and Mänttäri, I. 2008. Structural setting of late Svecofennian granites and pegmatites in Uusimaa Belt, SW Finland: Age constraints and implications for crustal evolution. Precambrian Research, 164 (1), 86–109.

Tuominen, H.V. 1957. The structure of an Archean area: Orijärvi, Finland. Bulletin de la Commission Geológique de Finlande 177, 32 pp.

Väisänen, M. 1988. Geology of the Orijärvi-Aijala Area. In: Gaal, G. and Gorbatschev, R. (Eds) Tectonic Setting of Proterozoic Volcanism and Associated Ore Deposits. Geological Survey of Finland, Guide 22, Espoo, 81–86.

Väisänen, M., Mänttäri, I. and Hölttä, P. 2002. Svecofennian magmatic and metamorphic evolution in southwestern Finland as revealed by U-Pb zircon SIMS geochronology. Precambrian Research, 116 (1), 111–127.

Varma, A. 1954. The copper-zinc ore deposits of Aijala and Metsämonttu. In: Aurola, E. (Ed) The mines and quarries of Finland. Geological Survey of Finland, Helsinki, 20–24.

Warma, A. 1975. Outokumpu Oy:n Aijalan ja Metsämontun kaivosten vaiheita. (Eds) Vuoriteollisuus N:o 2. Vuorimiesyhdistys R.Y., 94–98.

Wei, C., Powell, R. and Clarke, G.L. 2004. Calculated phase equilibria for low- and medium-pressure metapelites in the KFMASH and KMnFMASH systems. Journal of Metamorphic Geology, 22, 495–508.

Wennervirta, H. and Papunen, H. 1974. Heavy metals as lithogeochemical indicators for ore deposits in the Iilinjärvi and Aijala fields, SW-Finland. Geological Survey of Finland, Bulletin 269, 21 pp.

APPENDICES

1. Cross-sections of the Aijala deposit
2. Cross-sections of the Metsämonttu deposit
3. Excel formulas for coordinate transformation
4. Lithologies created for the Aijala and Metsämonttu models
5. List of 540 drill holes used to create the models
6. Mine level maps and cross-sections of the Aijala and Metsämonttu deposits

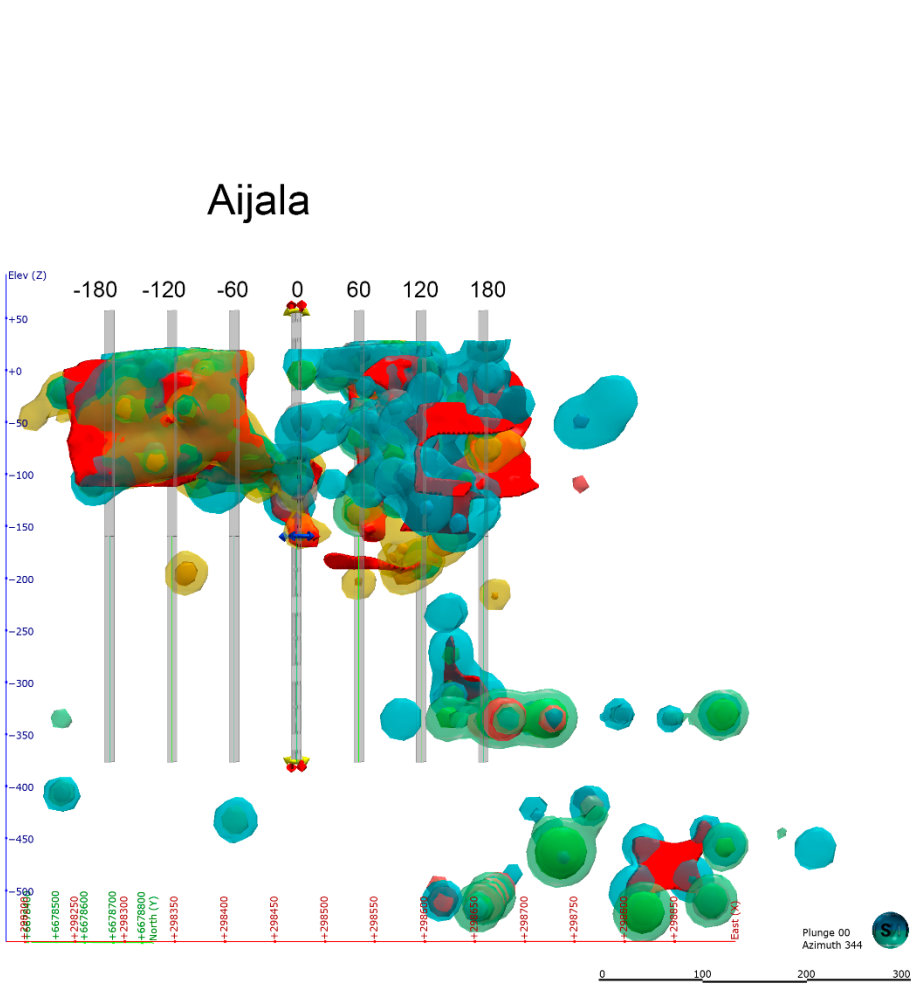

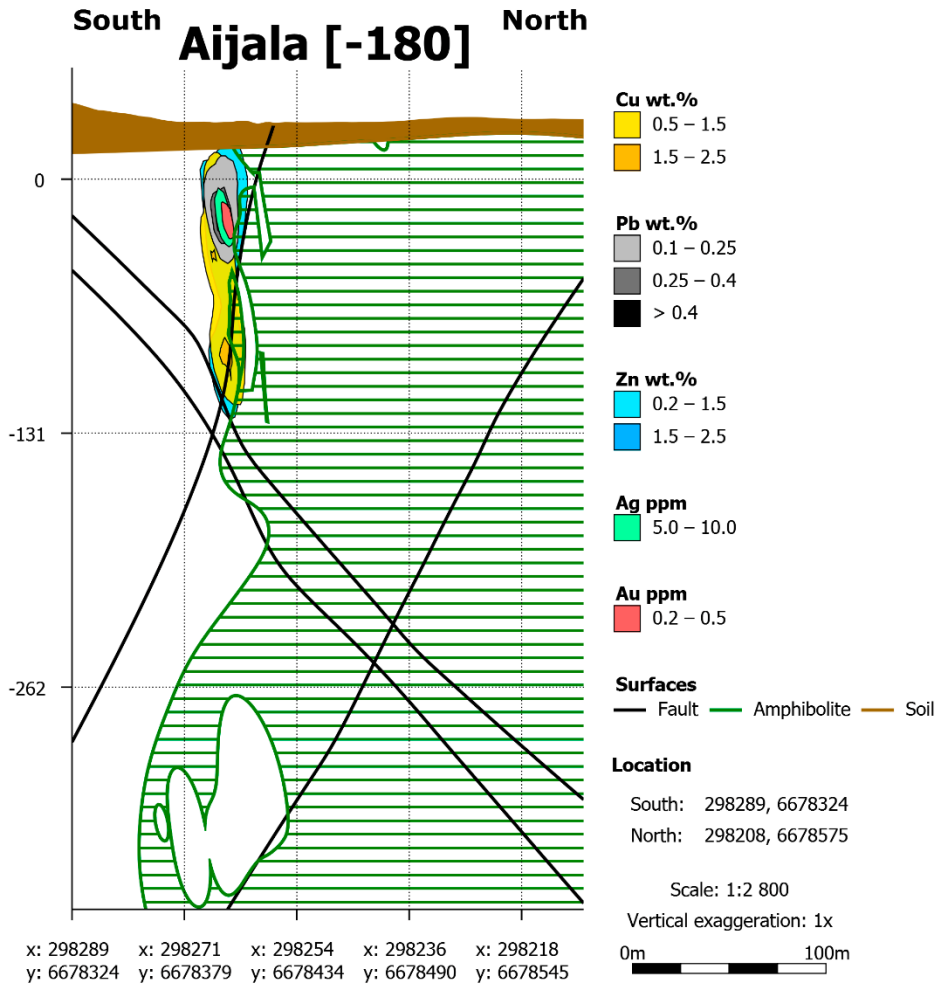

Appendix 1. Cross-sections of the Aijala deposit.

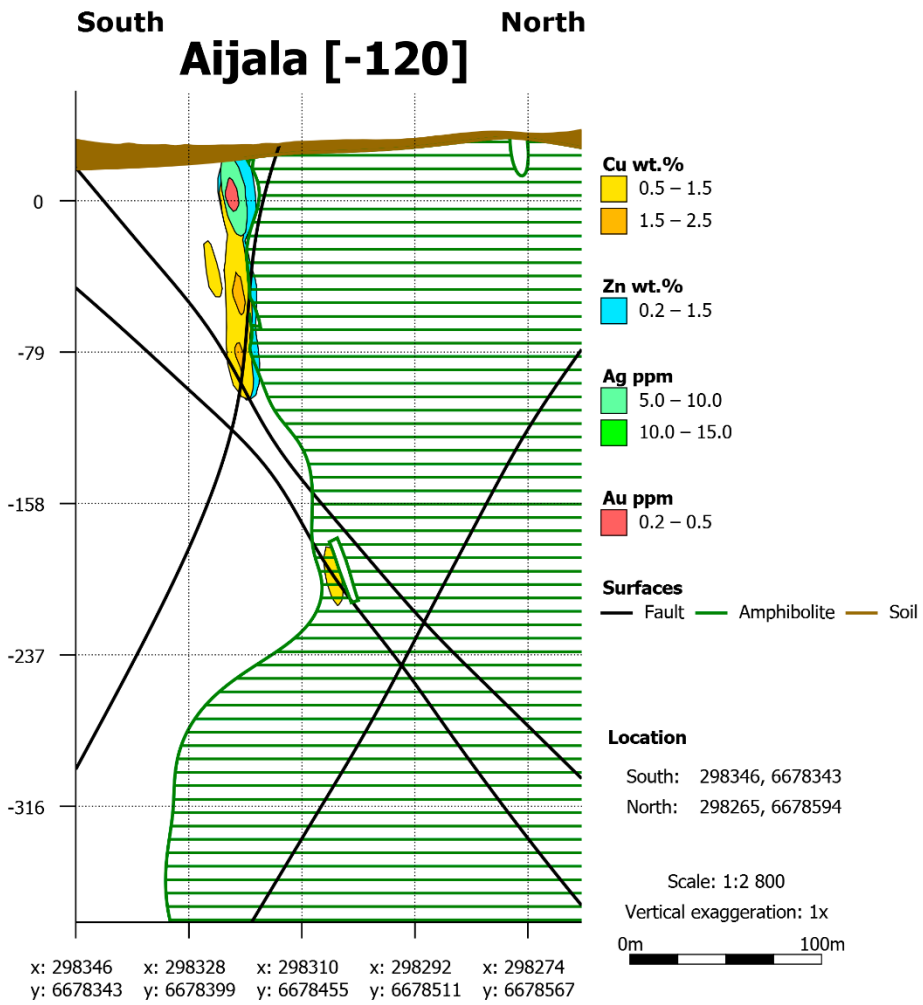

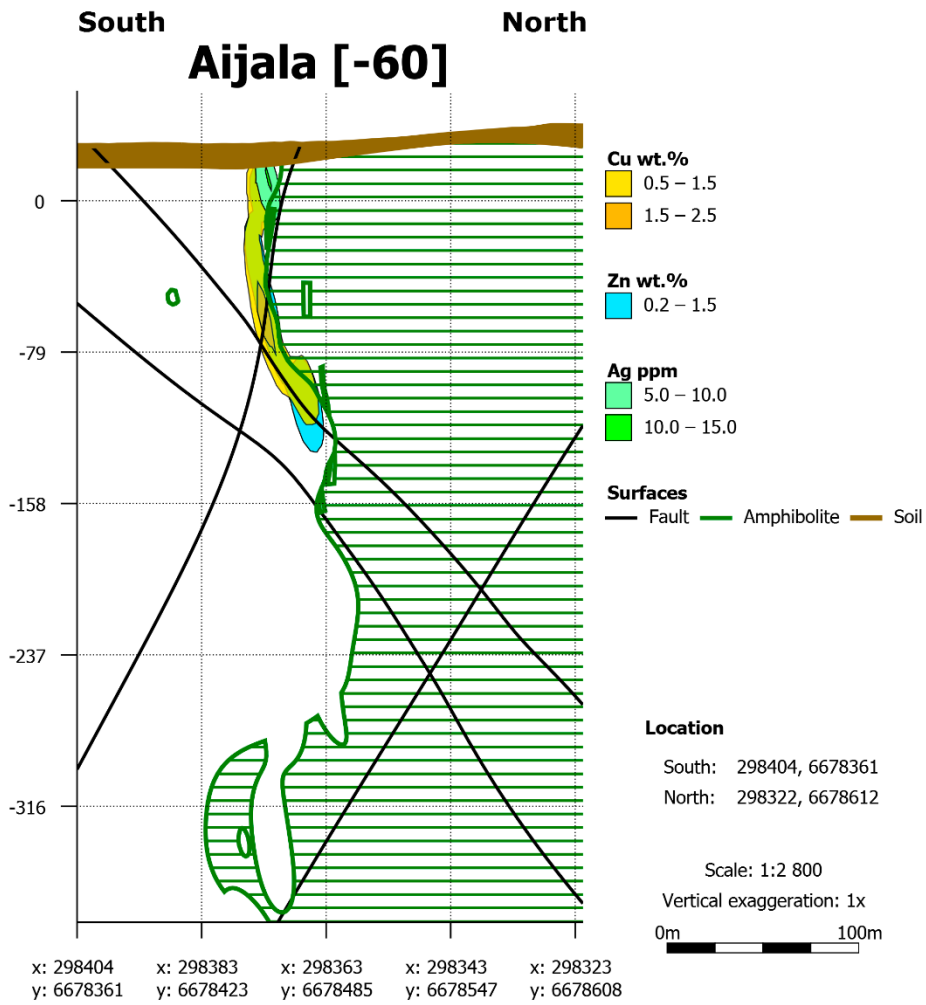

Appendix 1. Continues. Cross-sections of the Aijala deposit.

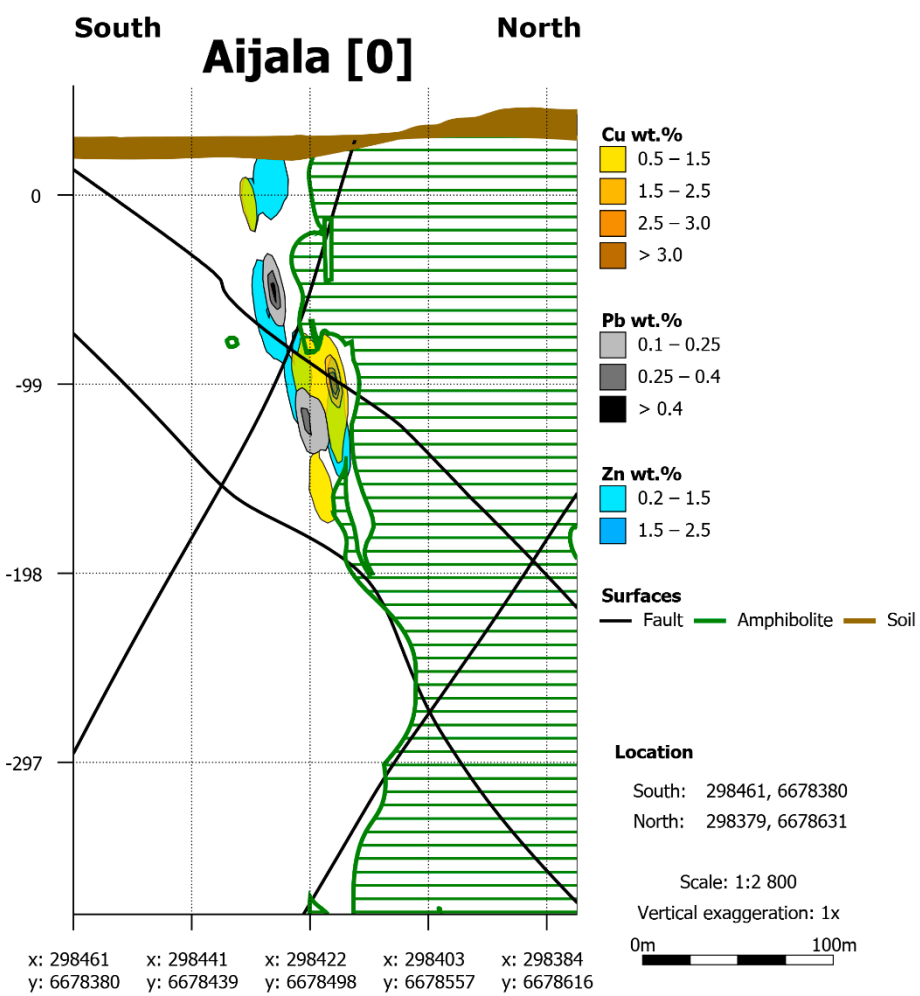

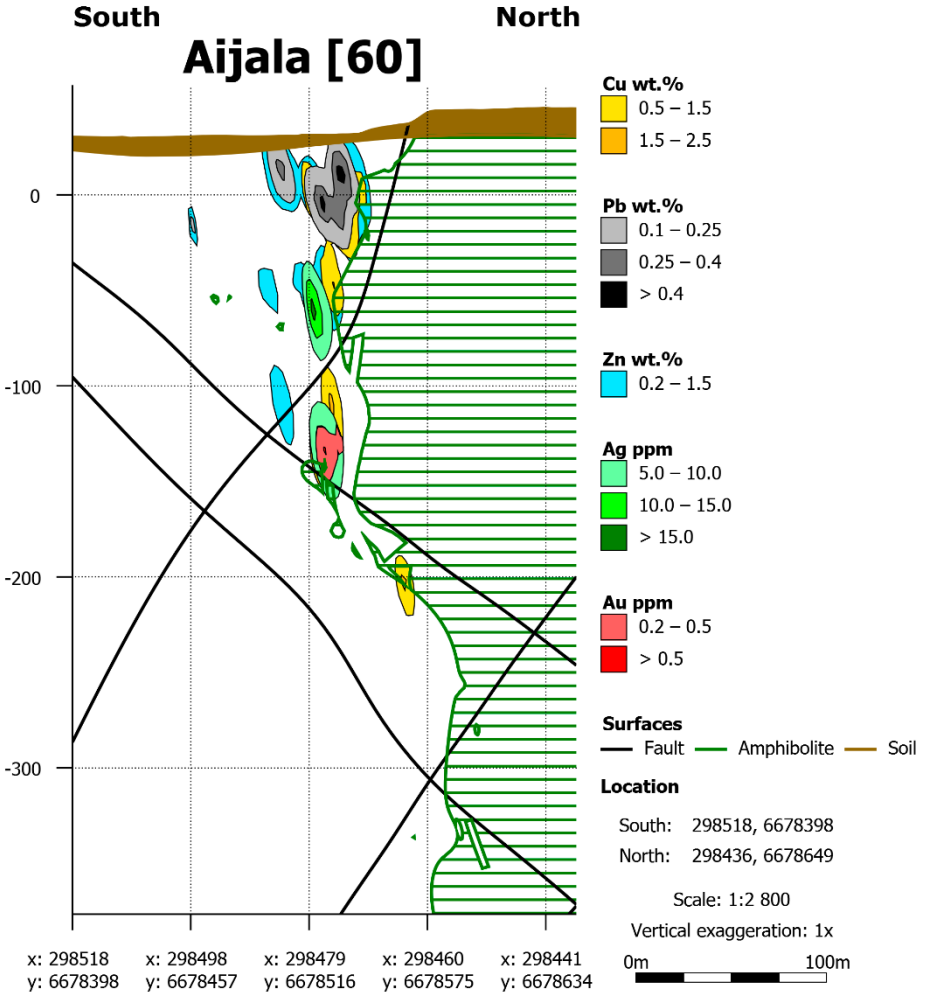

Appendix 1. Continues. Cross-sections of the Aijala deposit.

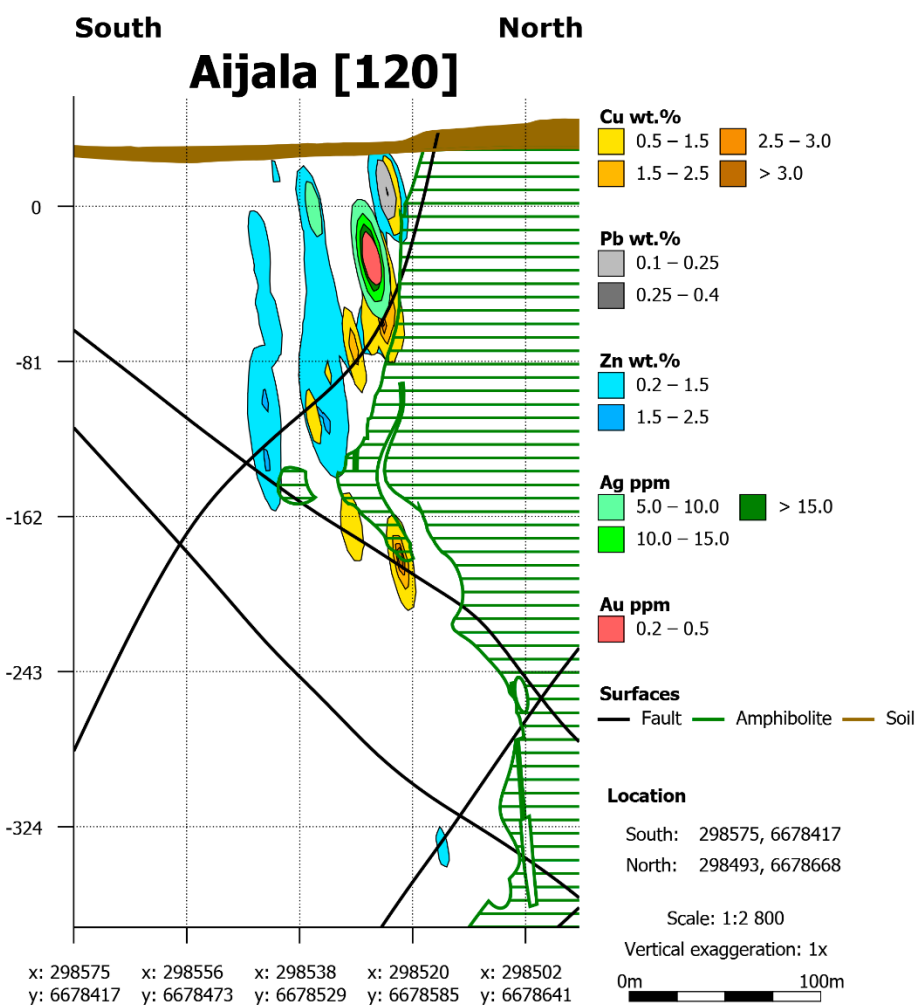

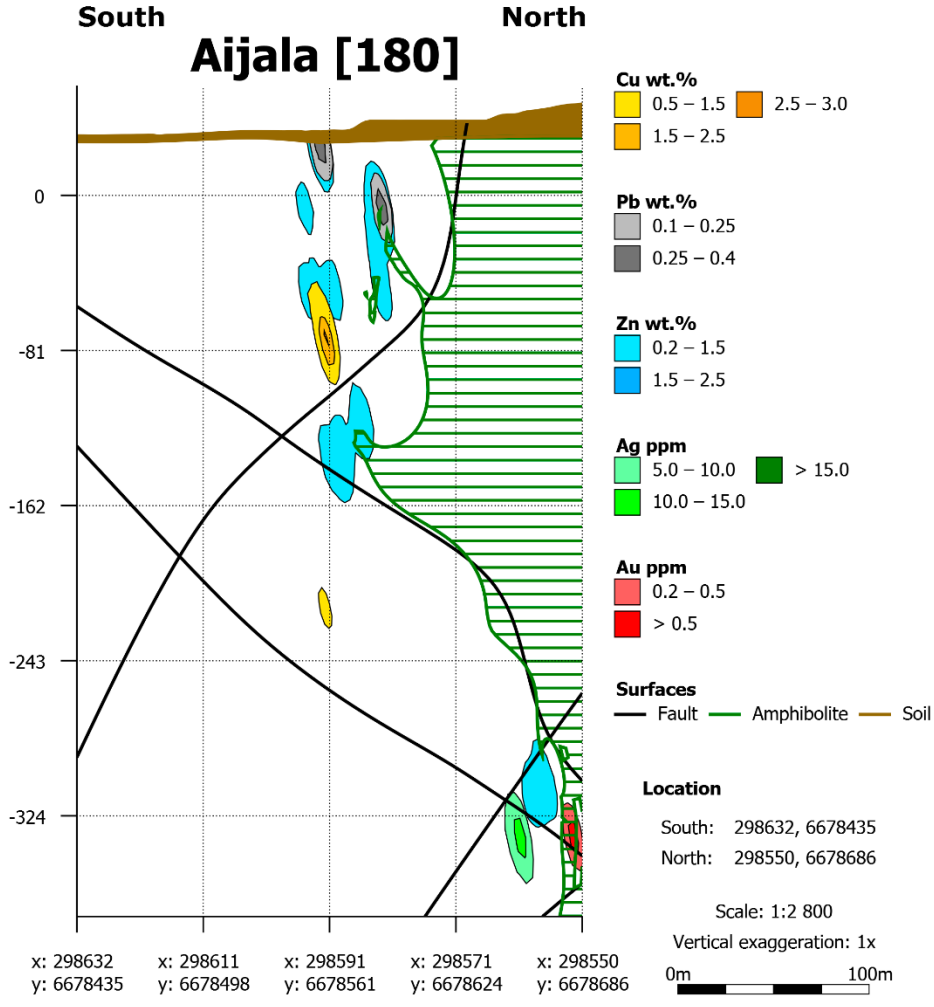

Appendix 1. Continues. Cross-sections of the Aijala deposit.

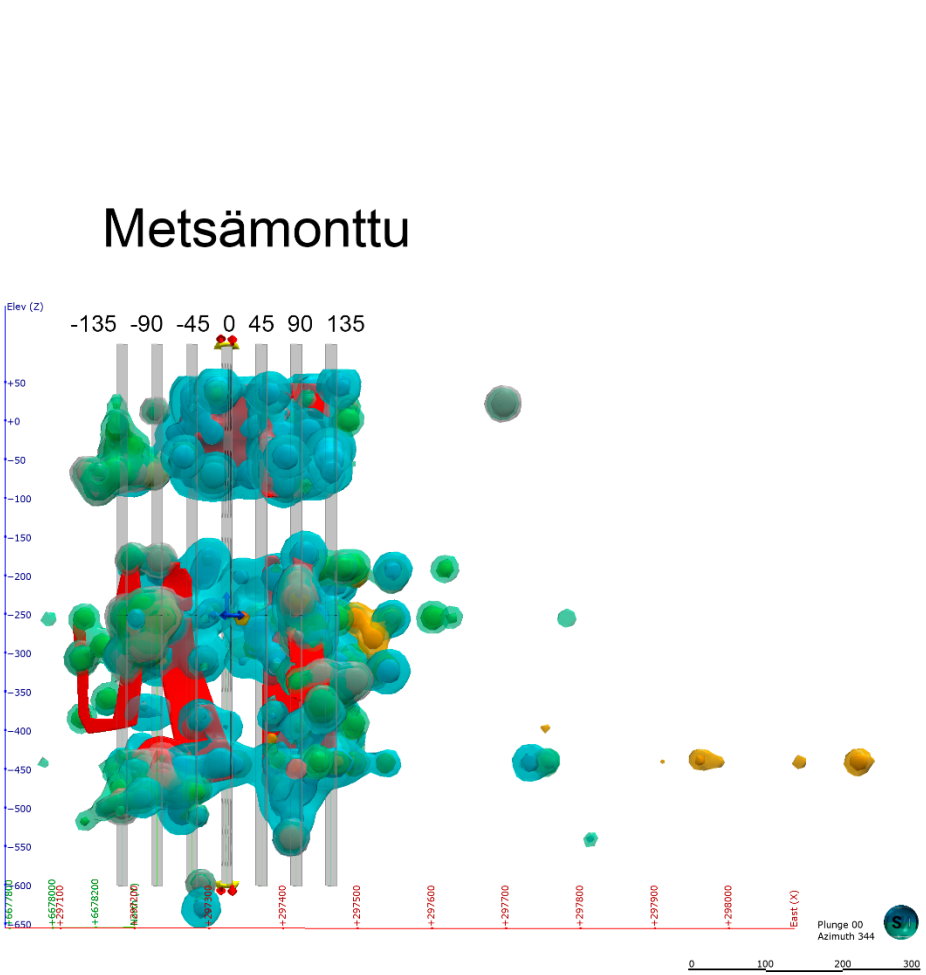

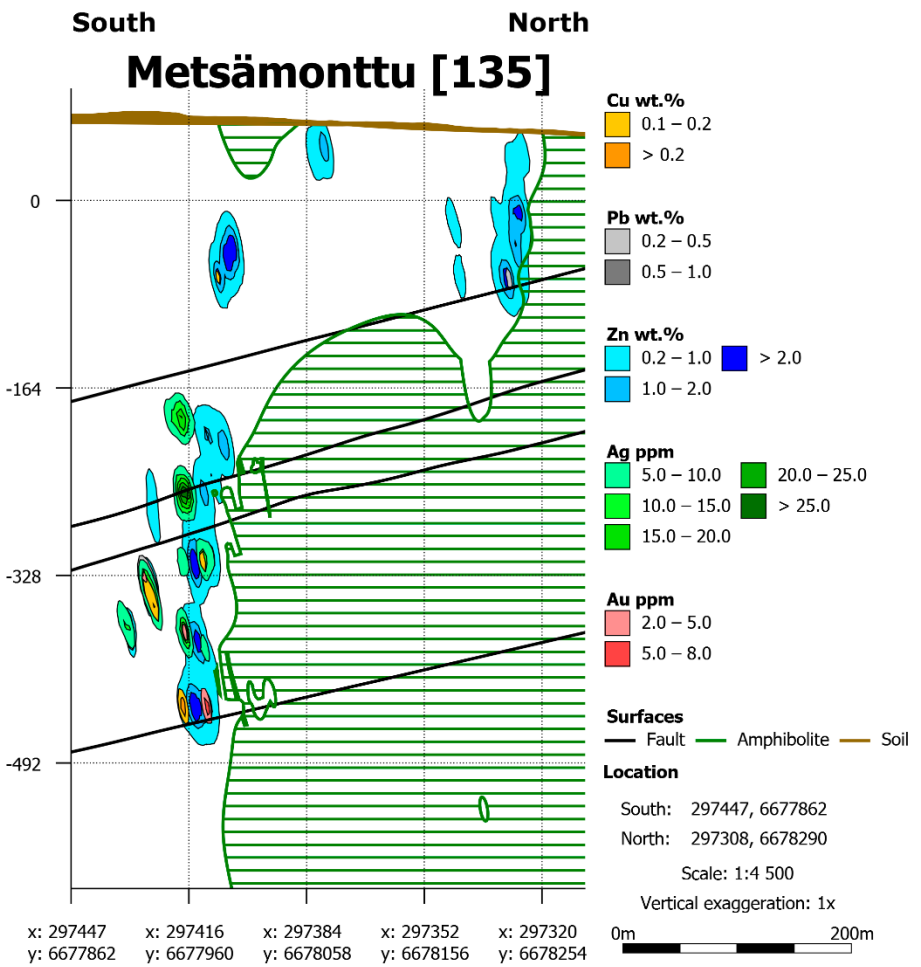

Appendix 2. Cross-sections of the Metsämonttu deposit.

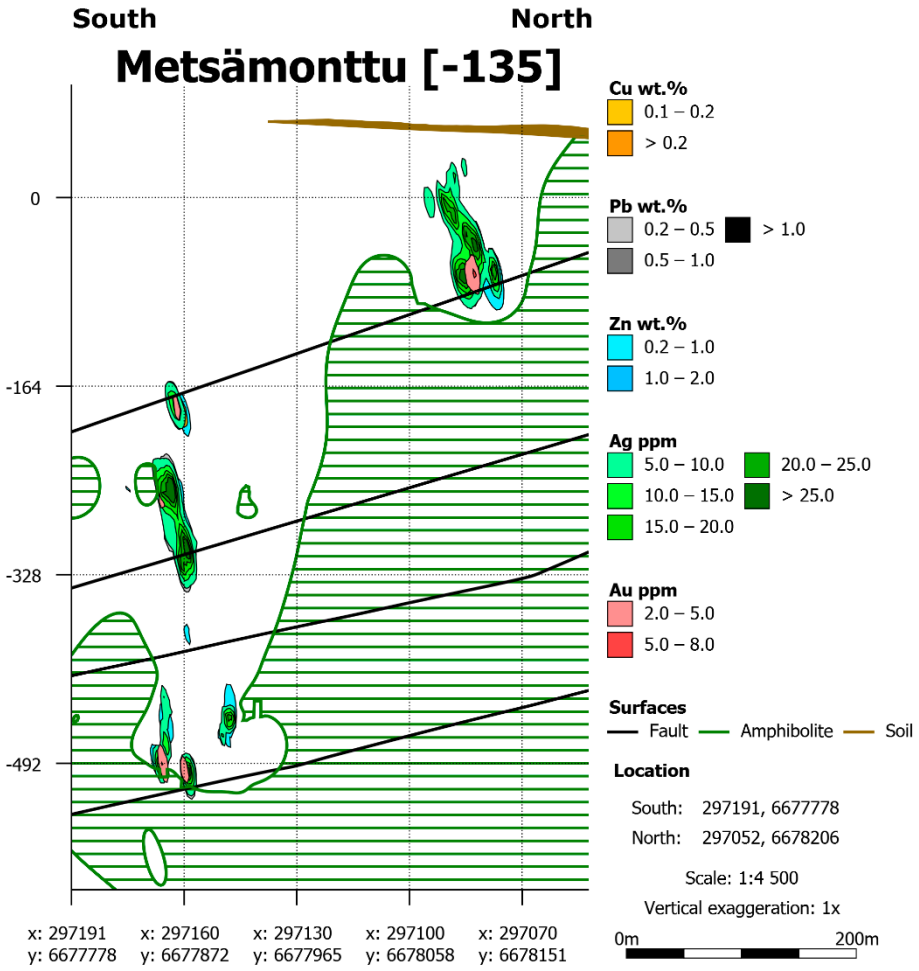

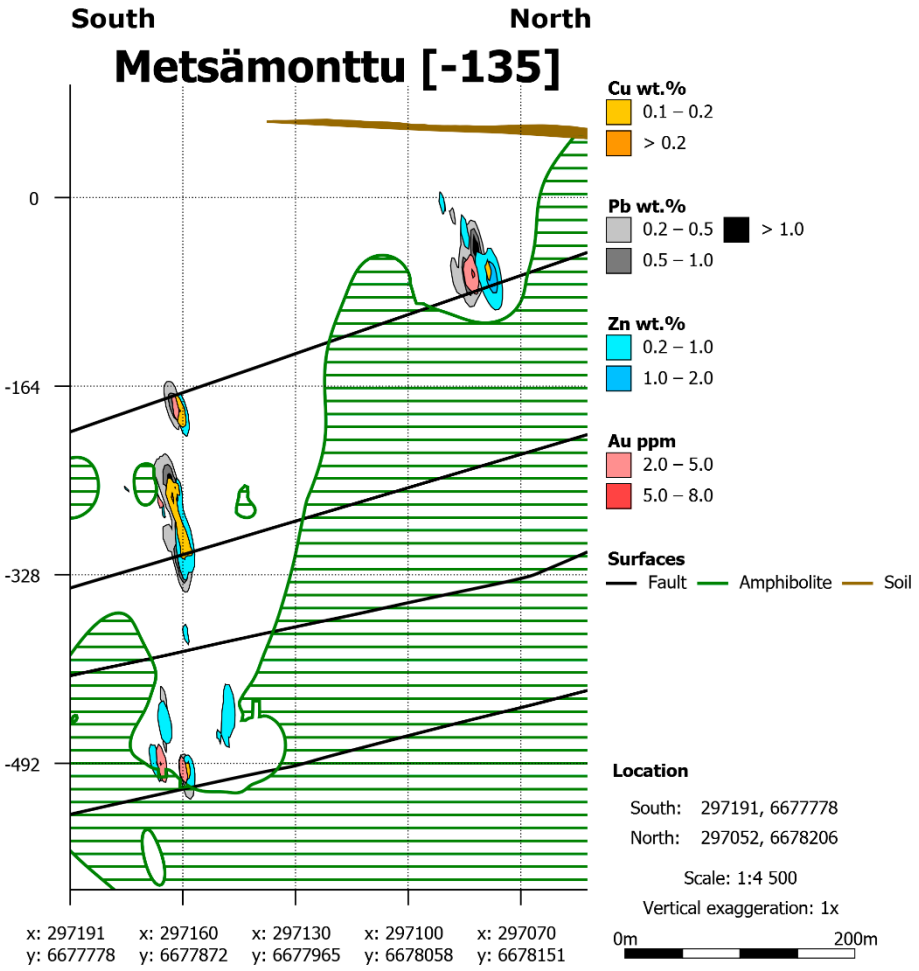

Appendix 2. Continues. Cross-sections of the Metsämonttu deposit. The second one is without Ag.

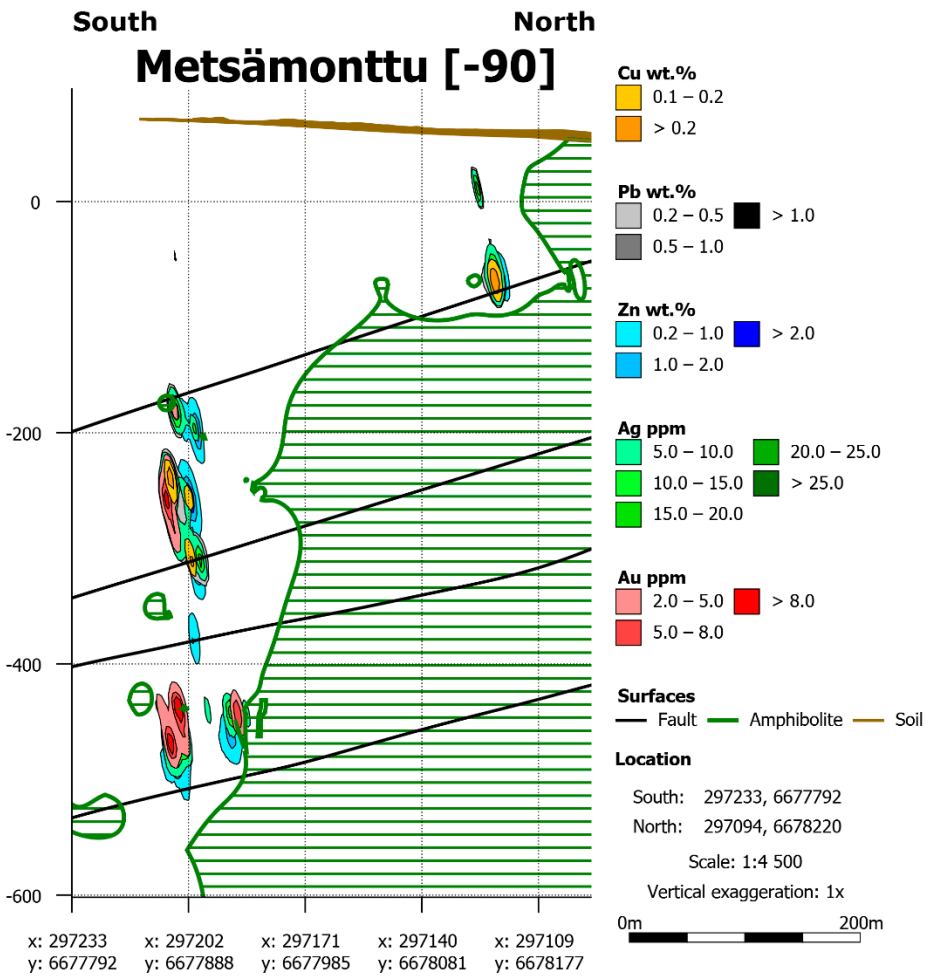

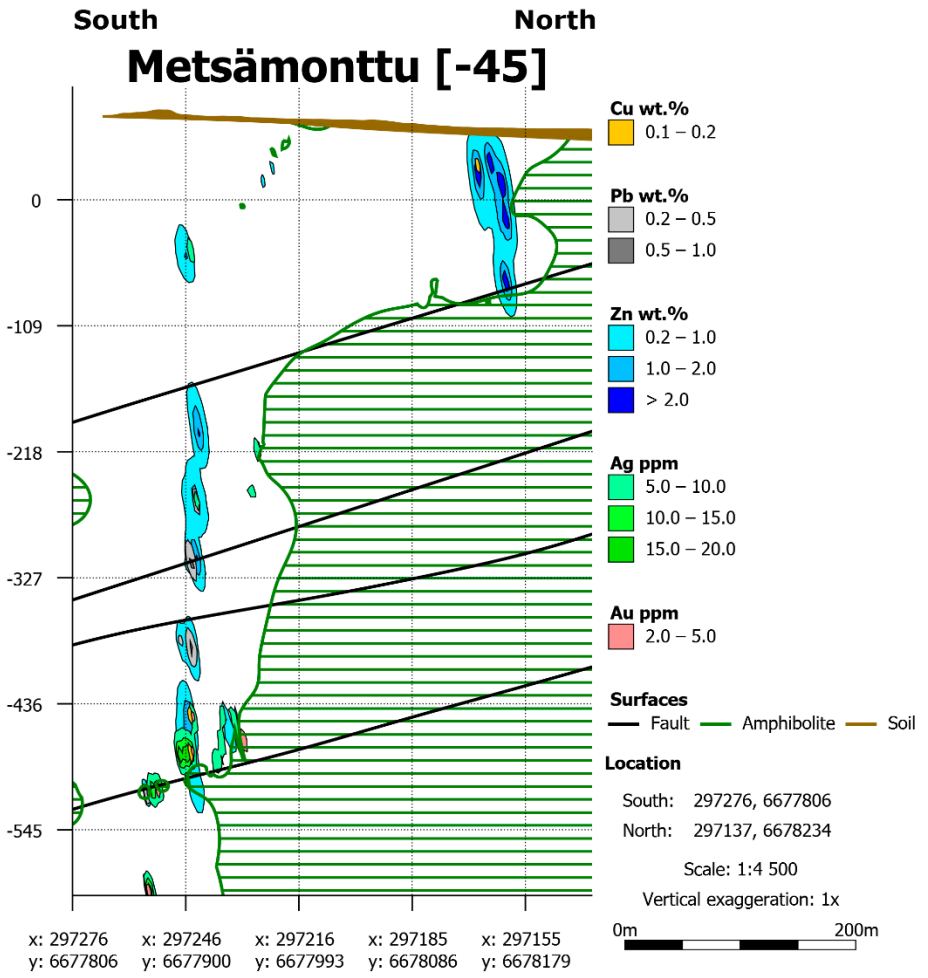

Appendix 2. Continues. Cross-sections of the Metsämonttu deposit.

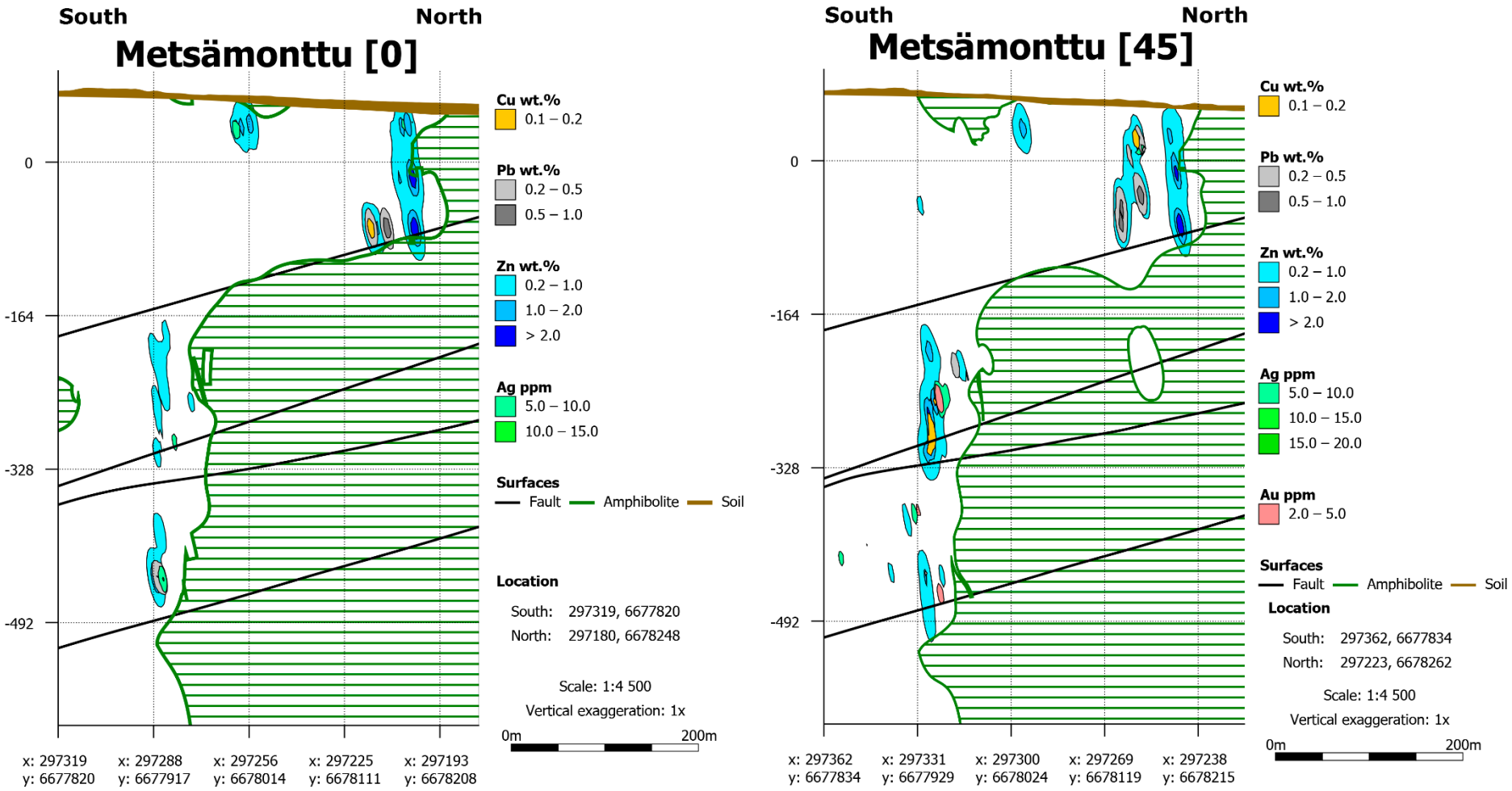

Appendix 2. Continues. Cross-sections of the Metsämonttu deposit.

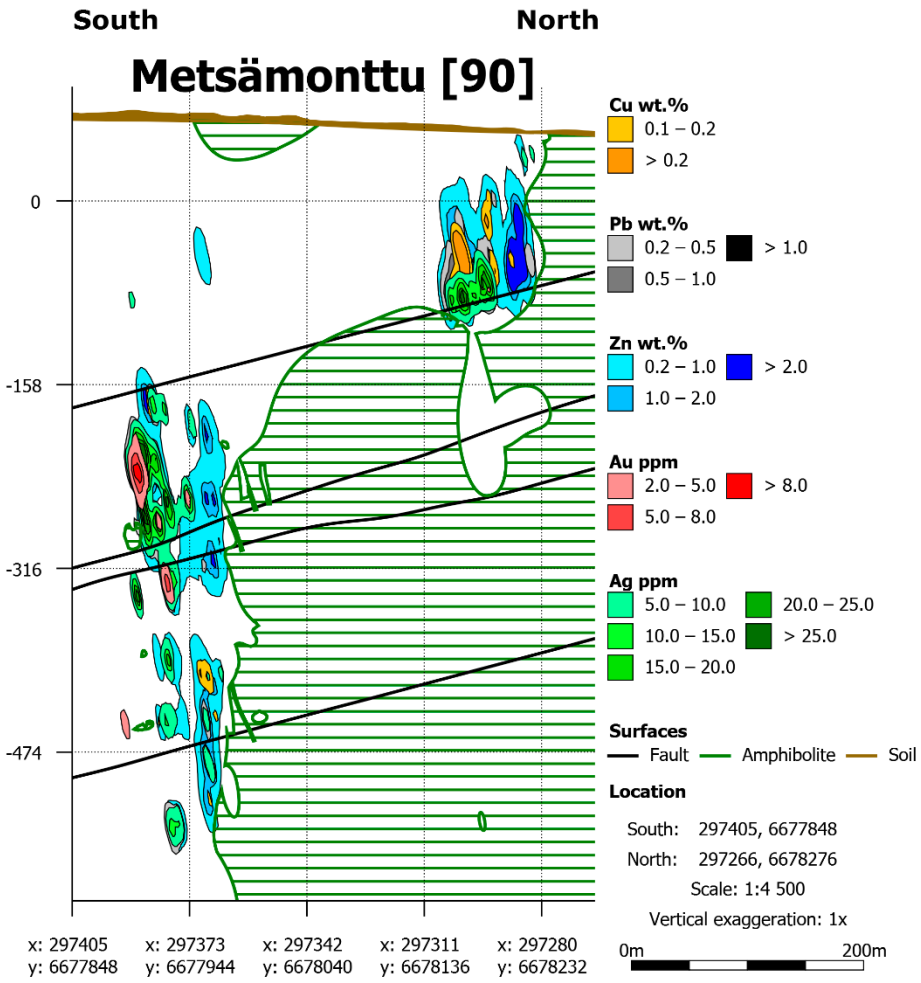

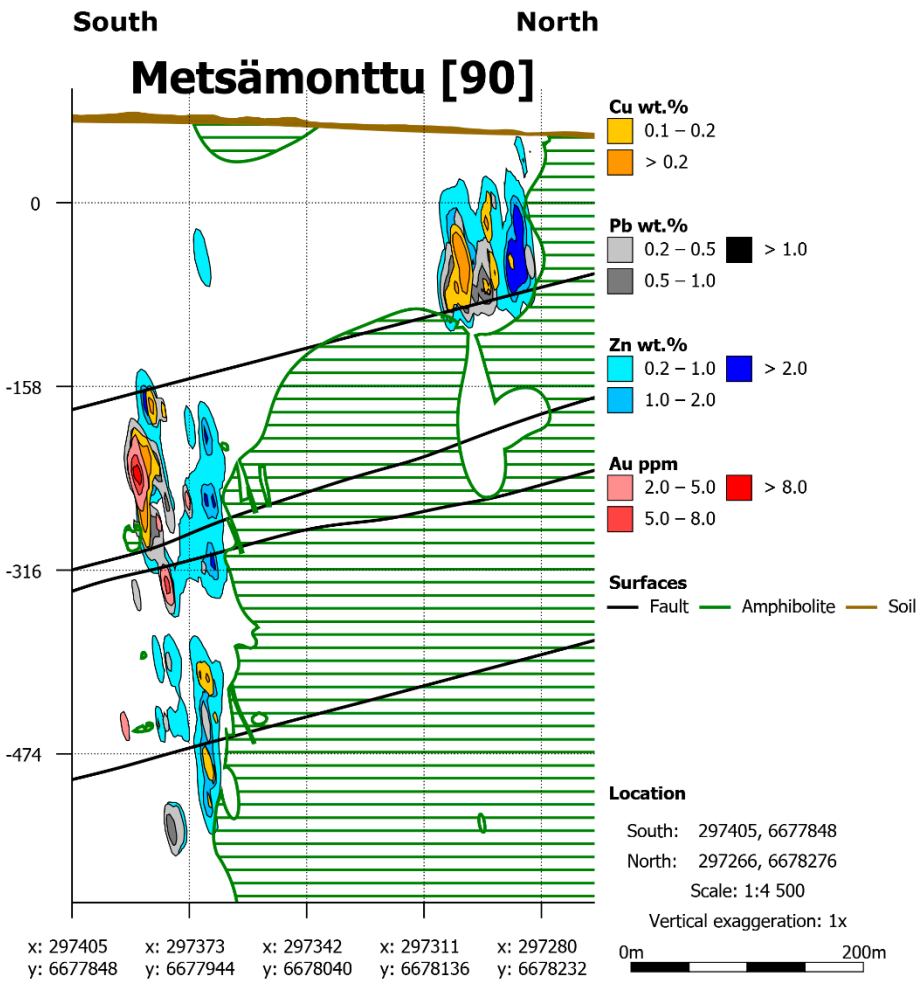

Appendix 2. Continues. Cross-sections of the Metsämonttu deposit. The second one is without Ag.

Appendix 3. Excel formulas for coordinate transformation.

Degree to radian =((α /360)*(2*PI()))

Radian to degree =(α /(2*PI()))*360)

The scale coefficient λ.

=SQRT(*N-orignal*^2 + *E-original*^2) / SQRT(*N-new*^2 + *E-new*^2)

The rotation angle α. Excel uses radians.

= – (ATAN(*E-new* / *N-new*) - ATAN(*E-original* / *N-original*))

The rotation matrix *R*.

=COS(α)	= – SIN(α)
=SIN(α)	=COS(α)

The inverse rotation matrix R^{-1}. Array formulas are accepted with Ctrl+Shift+Enter.

=MINVERSE(<rotation_matrix>)	=MINVERSE(<rotation_matrix>)
=MINVERSE(<rotation_matrix>)	=MINVERSE(<rotation_matrix>)

The translation vector *M* (yx).

= *N-orignal* : *E-original* – λ * MMULT([rotation_matrix] ; *N-new* : *E-new*)
= *N-orignal* : *E-original* – λ * MMULT([rotation_matrix] ; *N-new* : *E-new*)

Final form of Helmert transformation formula *U* (yx).

=(1/λ)*MMULT(inverse_rotation_matrix ; (*N-orignal* : *E-original* – translation_vector_Y))
=(1/λ)*MMULT(inverse_rotation_matrix ; (*N-orignal* : *E-original* – translation_vector_X))

Elevation correction formula.

Z_N2000 = (Z_loc-64)*(-1)

Appendix 4. Lithologies created for the Aijala and Metsämonttu models. Both models also have irtomaa (soil) unit.

Count	Aijala lithologies
1	AMFIBOLIITTI
2	FYLLIITTI
3	KALKKIKIVI
4	KARSI
5	KARSI_AIJALA_ITA_001
6	KARSI_AIJALA_ITA_002
7	KARSI_AIJALA_ITA_003
8	KARSI_AIJALA_ITA_004
9	KARSI_AIJALA_ITA_005
10	KARSI_AIJALA_ITA_006
11	KARSI_AIJALA_ITA_007
12	KARSI_AIJALA_ITA_A-B_KAAKKO
13	KARSI_AIJALA_ITA_A-B_LUODE
14	KARSI_AIJALA_ITA_E-F_KAAKKO
15	KARSI_AIJALA_ITA_E-F_LUODE
16	KARSI_AIJALA_ITA_G-H_KAAKKO
17	KARSI_AIJALA_ITA_G-H_LUODE
18	KARSI_AIJALA_LANSI_002
19	KARSI_AIJALA_LANSI_004
20	KARSI_AIJALA_LANSI_A-B_KAAKKO
21	KARSI_AIJALA_LANSI_A-B_LUODE
22	KIILLELIUSKE
23	KORDIERIITTILIUSKE
24	KVARTSI
25	KVARTSIPORFYYRI
26	MALMI
27	MALMI_AIJALA_ITA
28	MALMI_AIJALA_ITA_A-B
29	MALMI_AIJALA_ITA_C-D
30	MALMI_AIJALA_ITA_E-F
31	MALMI_AIJALA_ITA_G-H
32	MALMI_AIJALA_ITA_TASO_185
33	MALMI_AIJALA_ITA_TASO_300
34	MALMI_AIJALA_ITA_TASO_470
35	MALMI_AIJALA_LANSI
36	MALMI_AIJALA_LANSI_A-B
37	PEGMATIITTI
38	PEGMATIITTI_AIJALA_02
39	SERISIITTILIUSKE

Count	Metsämonttu lithologies
1	AMFIBOLIITTI
2	FYLLIITTI
3	KALKKIKIVI
4	KARSI
5	KARSI_MM_001
6	KARSI_MM_002
7	KARSI_MM_003
8	KARSI_MM_004
9	KARSI_MM_005
10	KARSI_MM_A-B_KAAKKO
11	KARSI_MM_A-B_LUODE
12	KARSI_MM_E-F_KAAKKO
13	KARSI_MM_E-F_LUODE
14	KARSI_U_MM_001
15	KARSI_U_MM_002
16	KARSI_U_MM_003
17	KARSI_U_MM_004
18	KARSI_U_MM_005
19	KARSI_U_MM_006
20	KARSI_U_MM_007
21	KARSI_U_MM_008
22	KARSI_U_MM_009
23	KARSI_U_MM_010
24	KARSI_U_MM_011
25	KARSI_U_MM_012
26	KARSI_U_MM_013
27	KARSI_U_MM_014
28	KARSI_U_MM_015
29	KARSI_U_MM_016
30	KARSI_U_MM_017
31	KARSI_U_MM_018
32	KARSI_U_MM_019
33	KIILLELIUSKE
34	KORDIERIITTILIUSKE
35	KVARTSI
36	KVARTSIPORFYYRI
37	MALMI
38	MALMI_MM_A-B
39	MALMI_MM_C-D
40	MALMI_MM_E-F
41	MALMI_UUSI_MM_Y9400_A-A
42	MALMI_UUSI_MM_Y9450_A-A
43	MALMI_UUSI_MM_Y9475_A-A
44	MALMI_UUSI_MM_Y9625_A-A
45	MALMI_UUSI_MM_Y9625_C-C
46	PEGMATIITTI
47	SERISIITTILIUSKE

Appendix 5. List of 540 drill holes used to create the models

Count	Hole ID	Easting	Northing	Z
1	A-001	298550.46	6678372.90	36.85
2	A-002	298460.42	6678559.94	31.50
3	A-003	298424.57	6678501.75	30.84
4	A-004	298299.44	6678440.25	30.95
5	A-005	298234.40	6678439.34	29.55
6	A-006	298351.08	6678467.40	30.54
7	A-008	298651.44	6678580.84	37.80
8	A-009	298549.16	6678504.94	32.15
9	A-010	298598.06	6678550.44	33.89
10	A-011	298492.41	6678487.06	31.50
11	A-012	298178.23	6678416.92	29.75
12	A-013	298327.76	6678539.31	34.65
13	A-014	298206.81	6678426.03	29.70
14	A-015	298534.11	6678553.30	33.05
15	A-016	298466.58	6678467.85	30.95
16	A-017	298577.38	6678515.19	33.45
17	A-018	298520.67	6678495.54	31.75
18	A-019	298403.17	6678436.46	30.05
19	A-020	298220.29	6678481.70	29.70
20	A-021	298275.38	6678506.35	32.80
21	A-022	298268.26	6678430.56	29.65
22	A-023	298330.78	6678529.99	34.10
23	A-024	298323.70	6678456.52	31.30
24	A-025	298410.01	6678545.02	34.70
25	A-026	298384.17	6678430.19	29.95
26	A-027	298511.60	6678426.26	31.60
27	A-028	298421.57	6678444.53	30.30
28	A-029	298534.60	6678452.59	31.35
29	A-030	298484.32	6678510.40	31.55
30	A-031	298560.05	6678471.36	31.50
31	A-032	298508.46	6678533.21	32.80
32	A-034	298775.91	6678567.54	37.00
33	A-036	298271.39	6678551.05	37.20
34	A-037	298401.60	6677922.62	35.00
35	A-042	298275.79	6678180.90	35.60
36	A-043	295668.56	6678145.50	29.55
37	A-044	298719.64	6678368.26	39.05
38	A-046	295997.29	6677990.87	28.15
39	A-047	299219.05	6678805.70	39.55
40	A-050	297294.03	6678015.17	55.60
41	A-051	297366.80	6678033.93	69.33
42	A-052	297224.14	6677990.82	68.76
43	A-055	297435.97	6678308.75	55.58
44	A-056	297484.99	6678318.08	56.73
45	A-057	297539.82	6678310.72	54.04
46	A-058	297593.40	6678307.77	56.01
47	A-059	297623.81	6678364.46	55.75
48	A-060	297712.10	6678419.85	50.65
49	A-061	297819.42	6678432.63	51.46
50	A-062	297962.91	6678313.44	50.37
51	A-063	297997.79	6678502.04	39.75
52	A-064	297590.57	6678154.33	56.40
53	A-065	296961.48	6678151.70	56.97
54	A-066	298634.17	6678534.72	34.61
55	A-067	299075.11	6678828.14	49.40
56	A-068	298660.02	6678551.89	34.94
57	A-069	299045.03	6678823.64	46.65
58	A-070	298729.80	6678531.44	36.17
59	A-071	299129.10	6678856.16	45.52
60	A-072	299239.18	6678743.63	43.50
61	A-073	298755.81	6678543.04	38.28
62	A-074	299296.09	6678762.66	42.42
63	A-075	298858.17	6678564.14	38.08
64	A-076	299482.18	6678837.15	39.00
65	A-077	298675.51	6678504.35	33.79
66	A-078	298259.63	6678684.58	31.66
67	A-079	298190.92	6678249.06	49.15
68	A-080	298097.41	6678212.27	42.38
69	A-081	297462.63	6677900.49	73.99
70	A-082	296925.32	6677936.50	68.05
71	A-083	298002.53	6678180.70	39.00
72	A-101	298463.38	6678554.35	-51.59
73	A-102	298456.43	6678571.48	-52.64
74	A-103	298452.87	6678512.89	-51.80
75	A-104	298452.69	6678513.62	-52.73
76	A-105	298509.13	6678548.71	-42.08
77	A-106	298427.86	6678489.85	-52.40
78	A-107	298503.52	6678554.60	-29.40
79	A-108	298428.38	6678488.60	-49.81
80	A-109	298519.08	6678565.09	-42.17
81	A-110	298502.67	6678555.14	-18.57
82	A-111	298538.33	6678580.44	-42.13
83	A-112	298538.77	6678579.37	-42.13
84	A-113	298523.89	6678575.04	-51.84
85	A-114	298376.21	6678454.86	-42.72
86	A-115	298377.46	6678450.87	-42.71
87	A-116	298386.71	6678462.22	-41.29
88	A-117	298386.32	6678462.59	-43.50
89	A-118	298414.02	6678475.50	-49.26
90	A-119	298328.18	6678440.59	-49.48
91	A-120	298411.53	6678478.89	-52.85
92	A-121	298327.75	6678442.52	-52.11
93	A-122	298347.07	6678438.24	-51.38
94	A-123	298299.80	6678431.30	-49.47
95	A-126	298271.58	6678421.71	-49.45
96	A-127	298271.08	6678423.12	-51.93
97	A-128	298320.87	6678418.34	-50.90
98	A-129	298319.60	6678422.07	-50.89
99	A-130	298245.73	6678403.52	-49.59
100	A-131	298220.56	6678384.45	-49.34
101	A-132	298219.67	6678386.79	-51.79
102	A-133	298189.50	6678381.89	-49.44
103	A-134	298523.47	6678575.92	-51.71
104	A-135	298553.46	6678591.66	-51.83
105	A-136	298373.75	6678460.19	-52.30
106	A-137	298355.77	6678453.86	-52.29
107	A-138	298189.35	6678382.01	-51.79
108	A-139	298157.74	6678383.19	-50.16
109	A-140	298487.06	6678535.19	-51.10
110	A-141	298501.19	6678555.20	-52.41
111	A-142	298377.37	6678451.15	-51.65
112	A-143	298477.08	6678539.40	-109.41
113	A-144	298508.37	6678541.36	-108.18
114	A-145	298531.13	6678559.65	-108.61
115	A-146	298528.99	6678569.12	-108.69
116	A-147	298454.23	6678505.86	-109.59
117	A-148	298477.09	6678533.02	-50.73
118	A-149	298482.99	6678511.97	-50.40
119	A-150	298551.57	6678574.87	-108.63
120	A-151	298392.70	6678467.90	-109.26
121	A-152	298355.90	6678452.79	-109.13
122	A-153	298376.21	6678455.70	-107.59

Appendix 5. Continues. List of 540 drill holes used to create the models

Count	Hole ID	Easting	Northing	Z
123	A-154	298357.01	6678449.74	-107.71
124	A-155	298357.39	6678448.73	-109.98
125	A-156	298377.34	6678453.76	-110.37
126	A-157	298335.70	6678444.13	-101.62
127	A-158	298336.54	6678440.04	-101.28
128	A-159	298336.35	6678441.06	-99.92
129	A-160	298392.79	6678467.43	-108.30
130	A-161	298393.28	6678464.22	-110.41
131	A-162	298393.80	6678465.03	-106.69
132	A-163	298442.75	6678612.62	-153.97
133	A-164	298268.22	6678437.80	-109.89
134	A-165	298269.74	6678438.27	-109.85
135	A-166	298273.65	6678424.08	-109.77
136	A-167	298427.54	6678488.30	-107.72
137	A-168	298428.36	6678488.44	-107.71
138	A-169	298453.63	6678509.62	-107.99
139	A-170	298453.23	6678509.18	-107.70
140	A-171	298439.92	6678600.04	-181.73
141	A-172	298427.71	6678488.23	-110.19
142	A-173	298491.62	6678494.13	-10.58
143	A-174	298393.27	6678466.15	-110.26
144	A-175	298427.46	6678488.49	-110.16
145	A-176	298493.20	6678491.28	-10.60
146	A-177	298453.81	6678509.34	-110.35
147	A-178	298377.13	6678453.13	-107.65
148	A-179	298429.05	6678485.07	-109.16
149	A-180	298409.05	6678547.20	-181.12
150	A-181	298375.32	6678527.38	-181.12
151	A-182	298311.67	6678487.58	-181.50
152	A-183	298269.61	6678465.00	-181.36
153	A-184	298508.65	6678562.92	-180.97
154	A-185	298408.82	6678547.26	-181.13
155	A-186	298343.83	6678458.09	-107.39
156	A-187	298223.88	6678373.38	-110.00
157	A-188	298223.26	6678375.31	-107.60
158	A-189	298428.42	6678488.07	-106.98
159	A-190	298428.35	6678487.49	-107.06
160	A-191	298326.04	6678447.37	-107.76
161	A-192	298393.59	6678465.99	-52.20
162	A-193	298395.18	6678464.31	-52.48
163	A-194	298328.25	6678441.27	-52.22
164	A-195	298500.48	6678557.47	-181.75
165	A-196	298428.37	6678490.96	-52.37
166	A-197	298410.86	6678480.28	-52.00
167	A-198	298512.81	6678531.47	-110.19
168	A-199	298528.74	6678568.17	-182.15
169	A-200	298469.82	6678551.20	-110.52
170	A-201	298527.57	6678572.07	-182.24
171	A-202	298538.32	6678541.39	-109.22
172	A-203	298551.84	6678593.33	-182.39
173	A-204	298527.55	6678572.15	-181.15
174	A-205	298527.73	6678571.83	-182.73
175	A-206	298528.63	6678568.28	-181.15
176	A-207	298515.52	6678561.60	-182.14
177	A-208	298485.94	6678555.51	-182.31
178	A-209	298531.17	6678559.79	-109.47
179	A-210	298551.77	6678575.07	-109.47
180	A-211	298508.05	6678543.37	-109.74
181	A-212	298552.75	6678590.46	-182.36
182	A-213	298553.60	6678590.91	-181.82
183	A-214	298554.85	6678587.73	-181.35
184	A-215	298431.11	6678562.97	-181.32
185	A-216	298431.10	6678563.03	-181.90
186	A-217	298453.65	6678558.43	-181.15
187	A-218	298510.02	6678559.84	-181.51
188	A-219	298539.97	6678583.01	-182.15
189	A-220	298390.59	6678540.57	-181.31
190	A-221	298550.66	6678584.06	-49.40
191	A-222	298159.41	6678385.62	-50.93
192	A-223	298538.47	6678539.29	-108.99
193	A-224	298512.89	6678615.80	-256.85
194	A-225	298511.71	6678621.28	-256.20
195	A-226	298552.06	6678593.18	-182.45
196	A-227	298407.06	6678553.82	-181.92
197	A-228	298564.01	6678649.41	-256.74
198	A-229	298532.65	6678649.51	-257.66
199	A-230	298532.62	6678649.73	-257.85
200	A-231	298532.95	6678648.61	-254.00
201	A-232	298431.07	6678562.96	-181.62
202	A-233	298563.34	6678557.72	-109.79
203	A-234	298555.39	6678563.49	-179.95
204	A-235	298526.82	6678669.32	-257.41
205	A-236	298526.25	6678670.86	-257.30
206	A-237	298581.75	6678598.64	-50.34
207	A-238	298611.12	6678607.03	-50.16
208	A-239	298588.57	6678568.39	-108.65
209	A-240	298585.09	6678588.60	-109.91
210	A-241	298523.25	6678526.12	-51.99
211	A-242	298612.39	6678601.15	-110.13
212	A-243	298581.69	6678598.53	-51.29
213	A-244	298581.71	6678598.55	-51.10
214	A-245	298612.41	6678601.06	-109.53
215	A-246	298629.79	6678609.60	-109.03
216	A-247	298652.55	6678618.64	-50.39
217	A-248	298564.02	6678559.71	-154.94
218	A-249	298515.58	6678515.39	-51.61
219	A-250	298514.00	6678529.31	-154.94
220	A-251	298485.70	6678509.12	-51.69
221	A-252	298514.06	6678528.62	-154.48
222	A-253	298474.33	6678516.62	-52.56
223	A-254	298555.04	6678563.21	-180.03
224	A-255	298429.13	6678486.13	-50.37
225	A-256	298638.98	6678616.26	-50.10
226	A-257	298611.33	6678606.65	-50.67
227	A-258	298650.70	6678678.27	-255.65
228	A-259	298629.98	6678610.06	-108.92
229	A-260	298611.02	6678604.58	-109.09
230	A-261	298650.21	6678681.82	-255.56
231	A-262	298520.68	6678688.93	-257.14
232	A-263	298652.46	6678618.77	-50.21
233	A-264	298481.56	6678528.74	-181.87
234	A-265	298521.46	6678689.38	-257.08
235	A-266	298441.84	6678576.42	-182.63
236	A-267	298311.54	6678488.75	-182.41
237	A-268	298519.90	6678689.02	-256.98
238	A-269	298549.91	6678604.68	-256.89
239	A-270	298310.47	6678490.26	-182.24
240	A-271	298269.51	6678465.75	-182.36
241	A-272	298374.89	6678528.98	-182.24
242	A-273	298310.93	6678489.58	-182.45
243	A-274	298549.59	6678604.23	-256.90
244	A-275	298452.08	6678595.10	-256.85

Appendix 5. Continues. List of 540 drill holes used to create the models

Count	Hole ID	Easting	Northing	Z
245	A-276	298554.41	6678588.23	-50.07
246	A-277	298587.74	6678591.91	-3.83
247	A-278	298629.94	6678609.58	-109.56
248	A-279	298549.39	6678604.73	-254.74
249	A-280	298550.20	6678604.91	-254.81
250	A-281	298269.81	6678466.40	-182.29
251	A-282	298374.60	6678528.78	-182.20
252	A-283	298431.13	6678563.48	-182.82
253	A-284	298437.90	6678604.52	-258.05
254	A-285	298242.20	6678506.52	-181.00
255	A-286	298440.05	6678602.23	-258.30
256	A-287	298243.38	6678509.02	-180.59
257	A-288	298242.70	6678509.54	-180.40
258	A-289	298468.60	6678552.79	-182.87
259	A-290	298414.98	6678509.42	-182.04
260	A-291	298518.44	6678593.48	-181.65
261	A-292	298518.45	6678594.04	-181.53
262	A-293	298482.13	6678530.11	-180.99
263	A-294	298552.51	6678592.42	-180.42
264	A-297	298437.62	6678602.54	-257.29
265	A-298	298443.98	6678598.22	-336.07
266	A-299	298416.25	6678622.91	-336.49
267	A-300	298389.01	6678651.58	-336.47
268	A-301	298431.33	6678679.38	-335.28
269	A-302	298468.95	6678712.25	-334.78
270	A-303	298508.44	6678745.05	-334.76
271	A-304	298430.47	6678679.77	-335.91
272	A-305	298278.72	6678549.63	-334.84
273	A-306	298355.30	6678614.84	-336.13
274	A-307	298278.56	6678549.87	-335.79
275	A-308	298546.72	6678775.98	-334.52
276	A-309	298582.68	6678809.26	-334.37
277	A-310	298582.33	6678809.66	-335.31
278	A-311	298579.75	6678812.80	-334.43
279	A-312	298240.52	6678516.22	-334.47
280	A-313	298202.69	6678484.57	-333.96
281	A-314	298201.01	6678488.30	-334.31
282	A-315	298202.55	6678485.04	-334.88
283	A-316	298388.93	6678651.71	-336.20
284	A-317	298545.17	6678777.42	-335.51
285	A-318	298621.45	6678842.63	-335.11
286	A-319	298622.28	6678841.61	-334.13
287	A-320	298658.73	6678873.61	-333.96
288	A-321	298658.00	6678874.52	-334.69
289	A-322	298658.30	6678875.05	-334.70
290	A-323	298657.60	6678874.96	-334.78
291	A-324	298591.45	6678875.04	-328.60
292	A-325	298591.25	6678874.84	-332.26
293	A-326	298467.72	6678713.77	-335.53
294	A-327	298317.09	6678582.44	-335.89
295	MM-007	297249.36	6678233.96	60.00
296	MM-033	297297.65	6678247.15	62.20
297	MM-035	297202.67	6678215.87	61.60
298	MM-038	297154.75	6678201.54	61.50
299	MM-039	297110.92	6678174.61	61.85
300	MM-040	297070.76	6678136.36	62.75
301	MM-041	297340.86	6678275.99	60.30
302	MM-045	297389.23	6678289.57	61.65
303	MM-048	297276.87	6678068.11	65.57
304	MM-049	297272.95	6678242.77	61.35
305	MM-053	297372.96	6678095.96	61.55

Count	Hole ID	Easting	Northing	Z
306	MM-054	297230.96	6678047.59	67.22
307	MM-084	296835.36	6678538.08	31.95
308	MM-085	297574.47	6678041.88	65.50
309	MM-101	297282.99	6678206.38	-18.11
310	MM-102	297258.18	6678210.13	-18.02
311	MM-103A	297304.07	6678224.80	-17.87
312	MM-103B	297307.35	6678214.16	-17.36
313	MM-104	297303.40	6678228.05	-17.89
314	MM-105	297274.37	6678215.07	-16.80
315	MM-106	297274.24	6678215.14	-19.10
316	MM-107	297213.11	6678182.09	-17.71
317	MM-108	297216.14	6678173.91	-10.60
318	MM-109	297327.57	6678235.97	-10.60
319	MM-110	297328.55	6678232.60	-10.75
320	MM-111	297191.83	6678169.69	-18.03
321	MM-112	297193.90	6678161.96	-18.04
322	MM-113	297169.60	6678155.48	-18.20
323	MM-114	297170.84	6678151.96	-18.12
324	MM-115	297168.28	6678166.92	3.84
325	MM-116	297181.40	6678157.20	0.75
326	MM-117	297181.79	6678154.87	-1.71
327	MM-118	297145.84	6678158.27	-18.01
328	MM-119	297238.64	6678189.35	-11.77
329	MM-120	297248.03	6678272.87	-90.25
330	MM-121	297187.07	6678183.15	-70.52
331	MM-122	297281.71	6678215.44	-70.92
332	MM-123	297259.33	6678203.40	-70.21
333	MM-124	297237.51	6678194.85	-70.18
334	MM-125	297304.72	6678224.95	-70.17
335	MM-126	297315.15	6678228.57	-69.70
336	MM-127	297285.39	6678202.39	-68.91
337	MM-128	297244.01	6678267.99	-124.09
338	MM-129	297213.13	6678182.07	-69.95
339	MM-130	297189.77	6678177.13	-69.29
340	MM-131	297166.31	6678168.47	-69.93
341	MM-132	297212.02	6678185.26	-69.70
342	MM-133	297258.32	6678198.40	-8.72
343	MM-134	297197.67	6678231.92	-123.01
344	MM-135	297197.63	6678232.16	-122.13
345	MM-136	297150.95	6678217.71	-123.00
346	MM-137	297150.94	6678217.62	-122.03
347	MM-138	297291.50	6678263.77	-122.75
348	MM-139	297291.46	6678264.09	-121.80
349	MM-140	297267.52	6678259.33	-123.15
350	MM-141	297304.58	6678225.17	-69.19
351	MM-142	297257.97	6678198.59	-18.70
352	MM-143	297238.26	6678268.48	-159.60
353	MM-144	297285.67	6678206.87	-50.28
354	MM-146	297299.22	6678160.98	-70.10
355	MM-147	297291.60	6678162.45	-17.90
356	MM-148	297326.35	6678219.15	-18.54
357	MM-149	297299.33	6678161.14	-70.68
358	MM-150	297221.13	6678241.72	-123.83
359	MM-151	297278.31	6678180.74	-70.95
360	MM-152	297276.89	6678149.70	-63.72
361	MM-153	297285.94	6678164.67	-71.00
362	MM-154	297286.05	6678164.53	-70.60
363	MM-155	297233.38	6678032.82	-123.44
364	MM-156	297234.93	6678033.47	-123.30
365	MM-157	297232.02	6678033.00	-123.31
366	MM-158	297284.99	6678200.58	-68.34

Appendix 5. Continues. List of 540 drill holes used to create the models

Count	Hole ID	Easting	Northing	Z
367	MM-159	297285.38	6678199.60	-69.61
368	MM-161	297307.12	6678175.29	-59.53
369	MM-162	297233.73	6678031.66	-122.36
370	MM-163	297233.65	6678031.93	-123.03
371	MM-164	297133.45	6678155.09	-69.38
372	MM-165	297133.56	6678158.79	-69.31
373	MM-166	297331.95	6678222.95	-68.78
374	MM-167	297234.16	6677964.62	-122.36
375	MM-168	297232.90	6677962.44	-256.88
376	MM-169	297232.72	6677963.19	-257.64
377	MM-170	297279.61	6677981.30	-256.73
378	MM-171	297323.70	6678001.68	-256.56
379	MM-172	297184.73	6677947.23	-256.86
380	MM-173	297138.02	6677928.93	-256.58
381	MM-174	297137.98	6677929.14	-257.58
382	MM-175	297232.84	6677962.51	-255.07
383	MM-176	297138.04	6677929.25	-254.85
384	MM-177	297136.90	6677932.11	-256.14
385	MM-178	297369.86	6678021.53	-255.67
386	MM-179	297459.89	6678067.31	-256.30
387	MM-180	297459.31	6678067.69	-257.30
388	MM-181	297371.04	6678022.65	-256.56
389	MM-182	297044.90	6677892.02	-255.79
390	MM-183	297092.11	6677907.17	-255.89
391	MM-184	297043.82	6677895.40	-255.78
392	MM-185	297091.83	6677907.94	-256.85
393	MM-186	297044.50	6677893.20	-256.64
394	MM-187	297091.98	6677907.59	-254.56
395	MM-188	297309.28	6678052.80	-255.61
396	MM-189	297183.34	6677950.11	-257.67
397	MM-190	297309.32	6678052.85	-255.62
398	MM-191	297183.80	6677947.67	-255.20
399	MM-192	297279.42	6677981.40	-257.62
400	MM-193	297308.76	6678052.62	-255.61
401	MM-194	297278.86	6677982.56	-255.02
402	MM-195	297505.24	6678087.49	-254.61
403	MM-196	297323.18	6678004.65	-257.33
404	MM-197	297505.14	6678088.00	-264.98
405	MM-198	297325.14	6678002.78	-254.56
406	MM-199	297520.11	6678087.49	-262.98
407	MM-200	297371.04	6678022.45	-254.05
408	MM-201	297415.94	6678043.19	-256.03
409	MM-202	297415.76	6678043.71	-256.88
410	MM-203	297415.04	6678045.03	-254.56
411	MM-204	297459.55	6678067.61	-254.56
412	MM-205	297392.51	6678035.32	-256.06
413	MM-206	297392.24	6678036.03	-256.87
414	MM-207	297392.52	6678035.60	-254.19
415	MM-208	297345.57	6678013.93	-256.58
416	MM-209	297346.79	6678014.81	-257.36
417	MM-210	297346.95	6678014.60	-254.67
418	MM-211	297095.89	6678138.45	-68.75
419	MM-212	297071.76	6678126.84	-67.87
420	MM-213	297071.75	6678127.01	-66.12
421	MM-214	297050.92	6678116.55	-67.78
422	MM-215	297051.24	6678116.97	-66.03
423	MM-216	297051.60	6678116.39	-68.49
424	MM-217	297050.96	6678116.39	-67.53
425	MM-218	297050.46	6678116.69	-68.50
426	MM-219	297095.76	6678138.47	-66.57
427	MM-220	297118.48	6678149.18	-66.85
428	MM-221	297118.60	6678148.89	-68.49
429	MM-222	297229.02	6677971.24	-444.33
430	MM-223	297228.90	6677971.58	-445.28
431	MM-224	297229.04	6677971.27	-442.56
432	MM-225	297277.21	6677985.72	-443.93
433	MM-226	297323.98	6678004.76	-443.46
434	MM-227	297347.32	6678014.34	-443.68
435	MM-228	297370.53	6678022.91	-443.50
436	MM-229	297394.53	6678031.05	-443.47
437	MM-230	297370.47	6678023.15	-244.23
438	MM-231	297370.54	6678022.99	-442.77
439	MM-232	297417.79	6678038.85	-443.39
440	MM-233	297417.99	6678038.78	-442.00
441	MM-234	297136.15	6677934.37	-444.61
442	MM-235	297183.57	6677952.01	-443.68
443	MM-236	297135.98	6677935.56	-444.89
444	MM-237	297183.45	6677952.28	-442.37
445	MM-238	297089.83	6677915.80	-444.25
446	MM-239	297136.32	6677933.67	-443.70
447	MM-240	297090.08	6677914.91	-443.32
448	MM-241	297137.39	6677930.38	-441.82
449	MM-242	297090.00	6677915.01	-441.31
450	MM-243	297206.02	6677961.04	-444.06
451	MM-244	297042.94	6677898.02	-442.81
452	MM-245	297206.06	6677960.98	-442.18
453	MM-246	297043.15	6677897.63	-439.57
454	MM-247	297159.89	6677941.90	-443.65
455	MM-248	297040.47	6677902.99	-442.84
456	MM-249	297112.66	6677924.25	-443.28
457	MM-250	297159.83	6677942.07	-441.65
458	MM-251	297370.64	6678026.51	-444.78
459	MM-252	297159.79	6677942.13	-444.46
460	MM-253	297112.43	6677924.75	-441.36
461	MM-254	297112.50	6677924.28	-443.97
462	MM-255	297419.58	6678040.78	-443.43
463	MM-256	297183.32	6677952.79	-444.78
464	MM-257	297206.07	6677961.14	-444.70
465	MM-258	297253.30	6677979.75	-443.88
466	MM-259	297229.00	6677971.27	-444.82
467	MM-260	297347.03	6678014.57	-441.94
468	MM-261	297347.16	6678014.54	-442.37
469	MM-262	297394.40	6678031.36	-442.09
470	MM-263	297226.09	6677900.52	-256.00
471	MM-264	297181.45	6677875.47	-256.01
472	MM-265	297181.39	6677875.71	-256.84
473	MM-266	297181.33	6677875.94	-254.68
474	MM-267	297227.08	6677899.38	-255.45
475	MM-268	297203.29	6677887.40	-255.40
476	MM-269	297203.36	6677887.31	-257.46
477	MM-270	297323.71	6678004.71	-443.00
478	MM-271	297158.37	6677866.46	-255.38
479	MM-272	297158.34	6677866.57	-254.31
480	MM-273	297158.17	6677866.47	-256.10
481	MM-274	297558.50	6678009.92	-254.91
482	MM-275	297582.20	6678018.58	-255.57
483	MM-276	297604.47	6678028.80	-255.18
484	MM-277	297225.64	6677974.79	-447.36
485	MM-279	297626.80	6678042.61	-256.00
486	MM-280	297625.84	6678047.19	-255.90
487	MM-281	297689.23	6678091.71	-255.71
488	MM-282	297690.08	6678093.13	-255.71

Appendix 5. Continues. List of 540 drill holes used to create the models

Count	Hole ID	Easting	Northing	Z
489	MM-283	297370.40	6677937.08	-255.53
490	MM-284	297370.27	6677937.40	-254.92
491	MM-285	297370.37	6677937.14	-257.00
492	MM-287	297370.31	6677937.25	-257.35
493	MM-288	297393.36	6677951.36	-255.64
494	MM-289	297393.24	6677951.83	-255.10
495	MM-290	297393.40	6677951.29	-257.20
496	MM-291	297393.35	6677951.39	-257.45
497	MM-292	297174.97	6677883.21	-312.57
498	MM-293	297153.48	6677880.32	-312.55
499	MM-294	297191.22	6677895.71	-312.78
500	MM-295	297247.51	6677904.84	-445.07
501	MM-296	297136.15	6677929.50	-257.08
502	MM-297	297114.21	6677921.06	-256.25
503	MM-298	297114.25	6677920.92	-257.03
504	MM-299	297301.08	6677993.75	-257.61
505	MM-300	297301.12	6677993.84	-255.76
506	MM-301	297438.40	6678056.37	-254.33
507	MM-302	297438.35	6678056.42	-257.25
508	MM-303	297415.37	6677865.61	-313.17
509	MM-304	297416.09	6677862.02	-312.11
510	MM-305	297414.00	6677865.84	-313.13
511	MM-306	297416.34	6678042.75	-444.54
512	MM-307	297134.65	6677934.44	-444.34
513	MM-308	297158.17	6677942.31	-443.94
514	MM-309	297694.39	6678157.85	-442.73
515	MM-310	297540.46	6678063.62	-443.09
516	MM-311	297730.43	6678210.92	-442.33
517	MM-312	297607.14	6678103.11	-442.83
518	MM-313	297769.65	6678250.25	-442.00
519	MM-314	297809.51	6678290.14	-440.04
520	MM-315	297650.03	6678131.64	-442.80
521	MM-316	297672.35	6678144.11	-442.62
522	MM-317	297628.26	6678118.01	-442.84
523	MM-318	297650.23	6678131.81	-443.70
524	MM-319	297650.21	6678131.77	-438.80
525	MM-320	297628.11	6678118.21	-440.38
526	MM-321	297627.73	6678124.38	-443.70
527	MM-322	297810.05	6678290.26	-441.96
528	MM-323	297849.28	6678331.25	-441.70
529	MM-324	296877.61	6677755.39	-443.02
530	MM-325	296877.71	6677751.71	-442.87
531	MM-326	296925.83	6677772.57	-443.01
532	MM-327	296974.19	6677791.17	-443.23
533	MM-328	296975.70	6677786.22	-443.02
534	MM-329	297019.78	6677807.56	-443.51
535	MM-330	297849.93	6678332.23	-441.75
536	MM-331	297379.65	6677961.88	-473.65
537	MM-332	297382.81	6677961.86	-473.39
538	MM-333	297358.72	6677955.10	-476.23
539	MM-334	297227.97	6677975.77	-445.00
540	MM-335	297324.32	6678002.81	-444.00

Appendix 6. Mine level maps and cross-sections of the Aijala and Metsämonttu deposits.

Count	Mine level maps of the Aijala deposit
1	1950_Taso_51_lansi
2	1950_Taso_54_ita
3	1950_Taso_57_lansi
4	1950_Taso_64_lansi
5	1950_Taso_69_ita_A277
6	1950_Taso_69_lansi
7	1950_Taso_82_ita_2
8	1950_Taso_82_ita_A110
9	1950_Taso_82_lansi
10	1950_Taso_93_ita_2
11	1950_Taso_93_ita_A107
12	1950_Taso_93_lansi
13	1950_Taso_107_ita_2
14	1950_Taso_107_ita_A109_A111_A112
15	1950_Taso_107_lansi
16	1950_Taso_115_ita_A101-A255
17	1950_Taso_115_ita_A237-A263
18	1950_Taso_115_lansi_A122_A128_A222
19	1950_Taso_132_ita
20	1950_Taso_132_ita_2
21	1950_Taso_132_lansi
22	1950_Taso_147_ita
23	1950_Taso_147_ita_2
24	1950_Taso_147_lansi
25	1950_Taso_165_ita
26	1950_Taso_165_ita_2
27	1950_Taso_165_lansi_A157_A158
28	1950_Taso_175_ita_A134-A239
29	1950_Taso_175_ita_A239-A260
30	1950_Taso_175_lansi_A152_A187_A188
31	1950_Taso_190_ita
32	1950_Taso_205_ita
33	1950_Taso_220_ita_A250
34	1950_Taso_223_ita
35	1950_Taso_250_ita_A180-A264
36	1950_Taso_250_lansi_A182_A183
37	1950_Taso_320_ita_A224-A275
38	1950_Taso_320_ita_A228_A258_A261

Appendix 6. Continues. Mine level maps and cross-sections of the Aijala and Metsämonttu deposits.

Count	Cross-sections and profiles of the Aijala deposit
1	1950_Poikkileikkaus_510_A139-222
2	1950_Poikkileikkaus_540_RN12_A133-138
3	1950_Poikkileikkaus_570_RN14_A131-132-187-188
4	1950_Poikkileikkaus_600_RN5-20_A130
5	1950_Poikkileikkaus_630_RN22_A126-A285
6	1950_Poikkileikkaus_660_RN21_A123
7	1950_Poikkileikkaus_690_RN24_A119-A273
8	1950_Poikkileikkaus_720_RN13-23-6_A137-152-154-155
9	1950_Poikkileikkaus_740_RN26_A114-A178
10	1950_Poikkileikkaus_760_RN19_A151-A282
11	1950_Poikkileikkaus_780_RN28_A118-120-197-220
12	1950_Poikkileikkaus_800_R3-25_A106-A290
13	1950_Poikkileikkaus_830_RN16_A103-A283
14	1950_Poikkileikkaus_860_A102-A293
15	1950_Poikkileikkaus_860_RN11-27-30_A102-A293
16	1950_Poikkileikkaus_890_A141-A218
17	1950_Poikkileikkaus_890_RN18-29-32_A105-A249
18	1950_Poikkileikkaus_920_A113-A292
19	1950_Poikkileikkaus_920_RN9-15-31_A113-A292
20	1950_Poikkileikkaus_950_A135-294
21	1950_Poikkileikkaus_950_RN17_A203-A294
22	1950_Poikkileikkaus_980_A228-239-240
23	1950_Poikkileikkaus_980_RN10_A237-A277
24	1950_Poikkileikkaus_1010_A242-245-260
25	1950_Poikkileikkaus_1010_RN66_A238-A260
26	1950_Poikkileikkaus_1040_R8-68-77_A256
27	1950_Poikkileikkaus_1070_A258-261
28	1950_Poikkileikkaus_1100_RN70
29	1950_Poikkileikkaus_1130_RN73
30	1950_Poikkileikkaus_1160_RN34
31	1975_Aijala profiili 10630_AIJALA
32	1975_Aijala profiili 10720_AIJALA
33	1975_Aijala profiili 10800_AIJALA
34	1975_Aijala profiili 10890_AIJALA
35	1975_Aijala profiili 10950_AIJALA
36	1975_Aijala profiili 11010_AIJALA

Appendix 6. Continues. Mine level maps and cross-sections of the Aijala and Metsämonttu deposits.

Count	Mine level maps of the Metsämonttu deposit
1	1951_Taso_22
2	1951_Taso_37
3	1951_Taso_45
4	1951_Taso_57
5	1951_Taso_68
6	1951_Taso_75
7	1951_Taso_85
8	1951_Taso_98
9	1951_Taso_115
10	1951_Taso_128
11	1951_Taso_135
12	1951_Taso_135_lansi
13	1951_Taso_153_lansi
14	1951_Taso_155
15	1951_Taso_190
16	1951_Taso_202
17	1951_Taso_223
18	1967_Metsamonttu_380
19	1969_Kalliomekaniikkaraportti_nro6_Metsamonttu_250_itaperat
20	1969_Kalliomekaniikkaraportti_nro6_Metsamonttu_320
21	1969_Kalliomekaniikkaraportti_nro6_Metsamonttu_380
22	1969_Kalliomekaniikkaraportti_nro6_Metsamonttu_510_itapera
23	Metsamonttu_380_331

Appendix 6. Continues. Mine level maps and cross-sections of the Aijala and Metsämonttu deposits.

Count	Cross-sections and profiles of the Metsämonttu deposit
1	1951_Poikkileikkaus_350
2	1951_Poikkileikkaus_9375_MM214_MM215_MM216
3	1951_Poikkileikkaus_9400_RN004_MM212_MM213
4	1951_Poikkileikkaus_9425_MM211_MM219
5	1951_Poikkileikkaus_9450_RN039_MM220_MM221_MM165
6	1951_Poikkileikkaus_9475_MM118
7	1951_Poikkileikkaus_9500_RN038_RN052_MM114_MM131_MM137
8	1951_Poikkileikkaus_9525_MM156_MM163
9	1951_Poikkileikkaus_9525_RN054_MM112_MM130
10	1951_Poikkileikkaus_9550_RN045_MM108_MM129_MM134_MM135
11	1951_Poikkileikkaus_9575_RN048_RN050_MM119_MM124_MM150
12	1951_Poikkileikkaus_9600_RN007_MM102_MM123_MM128_MM133_MM142
13	1951_Poikkileikkaus_9625_RN049_MM101_MM121_MM122_MM127_MM140_ MM144_MM146_MM147_MM149_MM158_MM159
14	1951_Poikkileikkaus_9650_RN033_RN051_MM103_MM125_MM138_MM139_ MM141
15	1951_Poikkileikkaus_9675_RN053_MM109_MM110
16	1951_Poikkileikkaus_9700_RN041
17	1975_Metsämonttu profiili 9400 (Parkkinen)
18	1975_Metsämonttu profiili 9600 (Parkkinen)
19	1975_Metsämonttu profiili 9700 (Parkkinen)
20	1975_Metsämonttu profiili 9800 (Parkkinen)
21	1975_Metsämonttu profiili 9950 (Parkkinen)
22	MM_Y_9500_RN038_RN052_MM114_MM131_MM137_MM168_MM169_MM175_ MM222_MM223_MM224_MM259_MM277